

# **Design of Symmetric 10 Gbps Bi-Directional Wavelength Reused Optical Access Networks**

By

**(Tanvir Zaman Khan)**

A thesis submitted in partial fulfillment of the requirements for the degree of  
Master of Engineering in Electronics and Communication Engineering (ECE)



Khulna University of Engineering & Technology  
Department of Electronics and Communication Engineering (ECE)  
Khulna 9203, Bangladesh

August 2016

## Declaration

This is to certify that the thesis work entitled “Design of Symmetric 10 Gbps Bi-Directional Wavelength Reused Optical Access Networks” has been carried out by Tanvir Zaman Khan in the Department of Electronics and Communication Engineering (ECE), Khulna University of Engineering & Technology, Khulna, Bangladesh. The above thesis or any part of this work has not been submitted anywhere for the award of any degree or diploma.

---

Signature of Supervisor

---

Signature of Candidate

## Approval

This is to certify that the thesis work submitted by Tanvir Zaman Khan entitled “Design of Symmetric 10 Gbps Bi-Directional Wavelength Reused Optical Access Networks” has been approved by the board of examiners for the partial fulfillment of the requirements for the degree of Master of Engineering in the Department of Electronics and Communication Engineering (ECE), Khulna University of Engineering & Technology, Khulna, Bangladesh in August 2016.

### BOARD OF EXAMINERS

1. \_\_\_\_\_ Chairman  
Dr. Pallab Kumar Choudhury (Supervisor)  
Associate Professor,  
Department of Electronics and communication Engineering  
Khulna University of Engineering & Technology (KUET)
2. \_\_\_\_\_ Member  
Dr. Md. Faruque Hossain  
Professor and Head,  
Department of Electronics and communication Engineering  
Khulna University of Engineering & Technology (KUET)
3. \_\_\_\_\_ Member  
Dr. Md Osman Goni  
Professor  
Department of Electronics and communication Engineering  
Khulna University of Engineering & Technology (KUET)
4. \_\_\_\_\_ Member  
Dr. Monir Hossen  
Associate Professor,  
Department of Electronics and communication Engineering  
Khulna University of Engineering & Technology (KUET)
5. \_\_\_\_\_ Member  
Dr. Md. Sohel Mahmud Sher (External)  
Professor  
Electronics and communication Engineering Discipline  
Khulna University, Khulna

## Acknowledgement

I would like to offer my foremost appreciation to my supervisor Dr. Pallab Kumar Choudhury for his support, encouragement and guidance through the course of this work. He introduced me to the world of optical access networks and integrated photonics. I am so fortunate to have such a great advisor who truly taught me how to identify and solve research problems. His knowledge, passion and excellent personality were inspiring, and his flexibility and accommodating approach paved my way for research.

I gratefully acknowledge Professors Dr. Md. Faruque Hossain for serving as head at department of ECE, KUET and giving valuable feedback during this thesis work.

I would also like to thank the financial support given by HEQEP Project of University Grants Commission (UGC) of Bangladesh and World Bank. (Under the sub-project CP-3470 entitled “Establishment of Virtual Lab for Collaborative Research in the area of Signal Processing and Communication Engineering”). I wish also to express my gratitude to all the present and past members of this project.

Beyond the professional environment, I would like to thank my parents, firstly for trusting me and giving me the opportunity to continue my university studies, and, secondly, for being an example of strength to adversity. My warmest regards to my parents, for their understanding, support and love during all these times. And to all the members of my family and friends, for so many good moments.

## Abstract

This research was conducted to deal with the problem of finding cost-effective solutions for Fiber-to-the-Home (FTTH) network deployment. In the FTTH network, the transceiver at the user premises and the deployment of fiber at the last mile are the major barriers.

A novel approach is demonstrated for reducing the noise of residual modulation and Rayleigh backscattering (RB) in bidirectional single fiber wavelength division multiplexing passive optical network (WDM-PON) with 10 Gb/s symmetric differential phase shift keying (DPSK) signal in downstream (DS) and OFDM re-modulated signal in upstream (US).

Centralized wavelength reused WDM-PON produces re-modulation noise and bidirectional single fiber generates RB noise. For simplicity, first approach only studied the effect of re-modulation noise and the second approach is the final design of this thesis work.

The first approach proposed a 10 Gb/s symmetric bidirectional dual fiber wavelength reuse WDM-PON with DPSK signal in DS and reflective semiconductor optical amplifier (RSOA) re-modulation with orthogonal frequency division multiplexing (OFDM) in US. RSOA is used for its colorless and cost effective property and dual fiber is used to avoid RB noise. Similarly, DPSK is used for its constant envelop (CE) property to reduce re-modulation noise. The results show that the proposed first approach can achieve good performance over 25 km fiber transmission with error free operation in DS and bit error rate (BER) lower than forward error correction (FEC) limit in US.

But the dual fiber approach is not cost effective. It increases the use of optical resources and network size outside of the plan. Therefore, another approach of single fiber is also presented in this thesis.

The second proposed approach is a 10 Gb/s symmetric bidirectional single fiber wavelength reuse WDM-PON with DPSK signal in DS and Mach-zhender modulator (MZM) re-modulation with OFDM signal in US. MZM is used to overcome the bandwidth limitation to reach 10 Gb/s. But this scheme severely affected by RB noise. Because RB noise spectra overlaps with OFDM signal near the DC frequency. This in-band coherent noise severely degrades the system performance. To overcome this limitation, wavelength shifted approach is used to reduce the spectral overlap. It is found that by shifting only 375 MHz, system can achieve a significant improvement.

## Contents

	<b>PAGE</b>
Title Page	i
Declaration	ii
Approval	iii
Acknowledgement	iv
Abstract	v
Contents	vi-viii
List of Tables	ix
List of Figures	ix
Nomenclature	xii
<b>CHAPTER I</b>	
Introduction	
1.1 Introduction	1
1.2 Literature Review	2
1.3 Motivation	3
1.4 Thesis Objectives	4
1.5 Thesis Outline	4
References	6
<b>CHAPTER II</b>	
Optical Access Networks	
2.1 Access Networks: An Overview	7
2.2 FTTx Architectures	9
2.3 Passive Optical Network (PON)	11
2.3.1 TDM-PON	12
2.3.2 WDM-PON	14
2.4 WDM wavelength allocation	15
2.5 Bidirectional Transmission in PONs	16
2.6 WDM PON architectures	18
2.6.1 Tunable laser WDM PON	19
2.6.2 Wavelength reuse WDM PON	20
2.6.3 Coherent injection and seeding WDM PON	21

2.7 RSOA in WDM PON	22
2.8 Impairments	23
2.8.1 Rayleigh Backscattering (RB)	24
2.8.2 Re-modulation Noise	27
2.9 Available Modulation Formats	28
2.9.1 Non Return To Zero (NRZ)	29
2.9.2 Differential Phase Shift Key (DPSK)	30
2.9.3 Orthogonal Frequency Division Multiplexing	31
2.9.3.1 Introduction to OFDM	31
2.9.3.2 Orthogonality	31
2.9.3.3 OFDM Subcarriers	32
2.9.3.4 OFDM spectrum	32
2.9.3.5 Spectrum efficiency of OFDM	33
2.9.3.6 Inter symbol interference (ISI)	34
2.9.3.7 Inter carrier interference (ICI)	35
2.9.3.8 Cyclic prefix (CP)/ Guard interval	35
2.9.4 Discrete Multi Tone (DMT) Modulation	36
References	39
<b>CHAPTER III</b>	<b>Simulation Environment</b>
3.1 Introduction	43
3.2 Transmitter	44
3.2.1 Continuous Wave (CW) laser	44
3.2.2 Mach-Zehnder Modulator	44
3.2.3 Pseudo Random Bit Sequence (PRBS)	48
3.3 Receiver	49
3.3.1 Photo detector (PIN)	49
3.3.2 Low Pass Filter	49
3.3.3 Bit Error Rate Tester (BERT)	50
3.4 Channel	51
3.4.1 Single Mode Fiber (SMF)	51
3.4.2 Bidirectional Fiber	51
3.5 Downstream Modulation	52

	3.6 Upstream Modulation	52
	References	54
<b>CHAPTER IV</b>	<b>10 Gb/s Symmetrical Wavelength Reused Bidirectional WDM-PON</b>	<b>55</b>
	4.1 Introduction	55
	4.2 Two-Fiber Network: High Tolerance against Re-modulation Noise	55
	4.2.1 Proposed Network	56
	4.2.2 Simulation setup	57
	4.2.3 Results and analysis	59
	4.3 Single Fiber Network: Rayleigh Backscattering (RB) Noise analysis	63
	4.3.1 Simulation setup	65
	4.3.2 Results and analysis	68
	4.4 Single Fiber Network: Both Rayleigh Backscattering and Re-modulation Noise Analysis	72
	4.4.1 Simulation setup	74
	4.4.2 Results and analysis	76
	References	79
<b>CHAPTER V</b>	<b>Conclusion and Future Work</b>	<b>81</b>
	5.1 Conclusion	81
	5.2 Future Work	82
	Appendix	82

## LIST OF TABLES

<b>Table No</b>	<b>Description</b>	<b>Page</b>
2.1	TDM-PON comparison	14
4.1	Wavelength shifting parameters for OFDM-QAM signal	66

## LIST OF FIGURES

<b>Figure No</b>	<b>Description</b>	<b>Page</b>
1.1	Information network	1
2.1	Bottleneck of present copper-based access networks	8
2.2	A typical optical networking architecture	8
2.3	Different architectures for fiber-to-the-Home (FTTH)	10
2.4	Typical PON diagram	11
2.5	PON topologies	12
2.6	TDM-PON architecture	13
2.7	WDM-PON architecture.	15
2.8	CWDM and DWDM wavelength grids based on ITU standards	16
2.9	Bidirectional options for PON	17
2.10	Architecture of WDM-PON	18
2.11	Tunable Laser WDM PON	20
2.12	Wavelength Reuse WDM-PON	21
2.13	Coherent-injection and CW-seeding WDM-PON	21
2.14	RSOA operating characteristics (a) Gain vs RSOA input optical power and (b) E/O normalized frequency response.	23
2.15	Schematic of RB effect in bidirectional single fiber Transmission	24
2.16	Fiber model for Rayleigh Backscattering	25
2.17	Normalized Rayleigh Backscattering intensity vs. fiber length	25

<b>Figure No</b>	<b>Description</b>	<b>Page</b>
2.18	Two major impairments of WDM-PON architecture	26
2.19	Representation of the NRZ code	29
2.20	NRZ transmitter diagram	29
2.21	Harmonics which are summed to create sub-carriers.	32
2.22	Understanding orthogonality (OFDM symbol spectrum)	33
2.23	FDM band	33
2.24	Bandwidth comparisons between OFDM and conventional technique	34
2.25	OFDM signal with different cyclic extensions.	35
2.26	Implementation blocks for DMT system	37
2.27	Schematic block diagram showing the principle of DMT over an optical IM/DD channel	38
3.1	Schematic of wavelength reused WDM-PON	43
3.2	(a) CW laser (b) CW laser parameters	44
3.3	(a) Schematic of Mach-Zehnder modulator (b) MZM power transfer function showing a degraded extinction ratio	45
3.4	(a) MZM (b) MZM parameters	47
3.5	(a) Laser Driver (b) Laser Driver parameters for DMT	47
3.6	(a) PRBS (b) PRBS parameters for DMT	48
3.7	(a) PRBS parameters for NRZ (b) PRBS parameters for DPSK	48
3.8	(a) PIN parameters for DPSK (b) PIN parameters for DMT	49
3.9	(a) Electrical Filter (b) Filter parameters for DPSK	50
3.10	(a) BERT (b) BERT parameters for DPSK	50
3.11	(a) SMF (b) SMF parameters	51
3.12	(a) Bidirectional fiber (b) Bidirectional fiber parameters	51
3.13	DPSK modulated signal generation	52
3.14	DMT modulated signal generation using MZM	53
3.15	DMT modulated signal generation using RSOA	53

<b>Figure No</b>	<b>Description</b>	<b>Page</b>
4.1	Proposed architecture for 10 Gb/s symmetric bidirectional wavelength reused WDM-PON.	56
4.2	Simulation setup for 10 Gb/s DPSK signal in downstream and RSOA re-modulation with OFDM signal in upstream.	57
4.3	BER performance of 10 Gb/s downstream DPSK modulated signal for both back to back and over 25 km fiber transmission.	59
4.4	Signal to Noise Ratio (SNR) for each OFDM subcarrier under different seeding power at the input of RSOA.	61
4.5	Measured SNR for each OFDM subcarrier in the case of back-to-back (BB) and with/without dispersion compensated 25 km fiber transmission at the RSOA input power of 6dBm and US received power of 12dBm.	61
4.6	Measured BER for different US received power in the case of back-to-back (BB) and over 25 km dispersion compensated fiber transmission.	62
4.7	Schematic of RF spectra indicating RB of OFDM signal.	64
4.8	Schematic of OFDM spectra shifting to reduce interference with RB spectra (a) small shift (b) large shift (c) No interference with RB	65
4.9	Schematic to analysis the signal to crosstalk ratio performance	66
4.10	Experimental setup of SCR measurement using CW source to generate RB noise (Tx section)	67
4.11	Experimental setup of SCR measurement using DPSK modulated source to generate RB noise (Tx section)	67
4.12	Experimental setup of SCR measurement using NRZ modulated source to generate RB noise (Tx section)	68
4.13	Normalized Optical spectra of CW, 10 Gb/s NRZ and 10 Gb/s DPSK modulated signal	69
4.14	Spectrum of OFDM signal with different frequency shifting	69
4.15	BER performance under different SCR level at different OFDM spectrum shifting while CW source generates the RB noise; constellation diagram at SCR 31 in (a) and SCR 46 in (b)	70

<b>Figure No</b>	<b>Description</b>	<b>Page</b>
4.16	BER performance under different SCR level at different OFDM spectrum shifting while NRZ modulated signal generates the RB noise	71
4.17	BER performance under different SCR level at different OFDM spectrum shifting while DPSK modulated signal generates the RB noise	71
4.18	Measured BER for different sources (CW, DPSK, NRZ)	72
4.19	Proposed architecture for 10 Gb/s symmetric bidirectional single fiber wavelength reused WDM-PON	73
4.20	Simulation setup for single fiber 10 Gb/s DPSK in DS and MZM re-modulation with OFDM-QAM in US	75
4.21	BER performance of 10 Gb/s downstream DPSK modulated signal for both B-B and over 20 km fiber transmission.	76
4.22	Measured BER for different US received power in the case of B-B for CW and DPSK seeded wavelength	76
4.23	Measured BER Vs SCR for CW and DPSK seeding with shifted wavelength	77

### **Nomenclatures**

ASE	Amplified Spontaneous Emission
AWG	Array Waveguide Grating
BER	Bit Error Rate
BLS	Broad-band Light Source
CAPEX	Cost Capital Expenditures
CO	Central Office
CW	Continuous Wave
DFB	Distributed Feedback Laser
DSL	Digital Subscriber Line
EAM	Electro-Absorptive modulator
EDFA	Erbium-Doped Fiber Amplifier
EIN	Excess Intensity Noise
FP-LD	Fabry-Perot Laser Diode

FSR	Free Spectral Range
FTTB	Fiber-to-the-Building
FTTC	Fiber-to-the-Curb
FTTH	Fiber-to-the-Home
FWHM	Full-Width Half-Maximum
ITU	International Telecommunication Union
LD	Laser Diode
MAN	Metro Area Network
NF	Noise Figure
NRZ	Non Return to Zero
ONU	Optical Network Unit
OLT	Optical Line Terminal
OSA	Optical Spectrum Analyzer
PDFA	Praseodymium-Doped Fiber Amplifier
PON	Passive Optical Network
PRBS	Pseudo-Random Bit Sequence
P2MP	Point to Multipoint
P2P	Point to Point
RIN	Relative Intensity Noise
RN	Remote Node
RSOA	Reactive Semiconductor Optical Amplifier
SCH	Separate Con_ nement Heterostructure
SLED	Super Luminescent Light Emitting Diode
SNR	Signal to Noise Ratio
TDM	Time Division Multiplexing
TO	Transistor Outlook
TE	Transverse Electric
TEC	Thermo-Electric Cooler
TM	Transverse Magnetic
VOA	Variable Optical Attenuator
VCSEL	Vertical Cavity Surface-Emitting Laser
WDM	Wavelength Division Multiplexing
WiFi	Wireless Fidelity
WiMAX	Worldwide Interoperability for Microwave Access

## CHAPTER I

### Introduction

#### 1.1 Introduction

After a rapid growth during the late 90s, the optical networking has been experiencing some challenging times over the past several years. Nevertheless, even though the telecoms market is unsettled today, we need to be ready with the appropriate solutions to meet the growing bandwidth needs of our information society.

Telecommunications have become a central element of society's daily life and newly emerged communication services such as video conference, remote medical support, online gaming or social networking are adopted at a rapid speed. These huge bandwidth demanding services require the transport of large information flows from one place to another, passing through different segments of the communication network until reaching the end-users, as illustrated in Fig. 1.1.

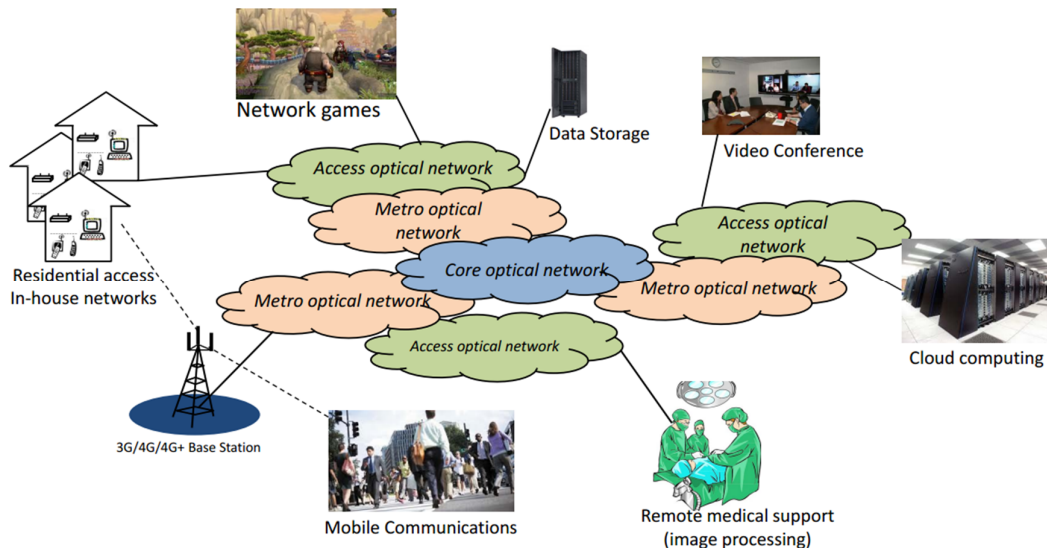


Figure 1.1: Information network

As result, there is a relentless demand for more network capacity, putting a great pressure on the communication network infrastructures at every scale, from core to metro, access networks and in-building or in-house networks. It is most commonly known as Fiber to the home technology in optical fiber communication.

Similar approach also happens in optical communication. Technical advances re brought by research on to have the achievement of higher data rates, longer distances, lower cost and more functionality. To achieve those issues, researchers focused on advanced modulation formats, coherent systems with digital signal processing (DSP), advanced coding, low-loss optical components, low-noise optical amplifiers, passive network, Bi-directional scheme, wavelength reuse approach, passive optical network (PON), wavelength division multiplexing (WDM) and advanced optical fibers. Among these, research on wavelength reused scheme with bi-directional approach and design of colorless optical network unit (ONU) to reach high data rates (~10 Gb/s) are of special importance to understand the motivation of this work.

## 1.2 Literature Review

The passive optical network (PON) is considered to be an ultimate solution in access technology to meet ever increasing bandwidth demand especially for high speed broadband services [1]. Hence, full service access network (FSAN) group has defined the IEEE Std. 802.3av 10 Gigabit Ethernet -PON that support the symmetric 10 Gbps capacity in both downstream (DS) and upstream (US) transmission [2]. The potential architecture that can effectively support the above standardization in cost effective manner is WDM PONs [3]. The WDM-PONs supporting bi-directional 10 Gbps capacity has been studied by several research groups. In [4], reflective semiconductor optical amplifier (RSOA) is used as a “Colorless” source in ONU side of WDM-PON. To overcome the limited bandwidth (<1GHz) response of RSOA, detuned optical filter and electrical equalization are utilized to operate the RSOA based WDM-PON system towards 10 Gbps capacity in [4]. However, the proposed method is highly dependent on optimum filter position and tab setting of equalizer and thus, increases the implementation complexity in practical deployment. A bi-directional 10Gbps cross-wavelength reused approach is presented in [5], where the Differential Phase Shift Keying (DPSK) modulated signal is used in DS as a seeding wavelength for Reflective Electro-absorption Modulator (R-EAM) placed in the ONU side. However, the proposed architecture is based on two transmission fibers, which eventually increases the deployment cost. A

symmetric rate of 10 Gbps WDM-PON with directly modulated laser in DS and wavelength reused orthogonal frequency division multiplexing (OFDM) signal in US has been proposed in [6]. The proposed architecture is severely limited by the residual DS modulation in US and thus an optimum DS extinction ratio (ER) is needed to be maintained for acceptable performance in bidirectional transmission.

In this thesis work, 10 Gbps wavelength reused bidirectional WDM-PON is designed based on RSOA as a colorless modulator in ONU with OFDM modulation to overcome the limited bandwidth response of RSOA to reach 10 Gbps. Moreover, the proposed system can be effectively improved the resilience against fundamental noises such as re-modulation and Rayleigh backscattering [7].

### **1.3 Motivation**

Bidirectional fiber strategy seems to be the most interesting architecture in terms of reducing the cost capital expenditures (CAPEX) per customer. It requires new ONU designs hence the ONU becomes a key element in access networks and an interesting area of investigation. For a total successful Fiber to the Home deployment, the network unit model should be simple, robust, flexible and cost-available for the final customer.

There are some technical specifications and design guidelines need to be considered are following:

- Single-Fiber Solution Design to reduce network size.
- Wavelength Independency (Colorless) to allow transparent in WDM operation.
- Without Active Light Source to prevent stabilization and provisioning at the customer premises.
- Amplification to increase the number of users and achieve longer distances.
- Designing the architecture for bidirectional connection with a centralized light source.

These are the fundamental drivers of this thesis work.

## 1.4 Thesis Objectives

The key objectives of this thesis work are as follows:

a) To develop simulation model for bi-directional 10Gbps wavelength reused WDM-PON and analyze the impact of re-modulation and Rayleigh backscattering noise on system performance.

b) To propose new architectures for 10Gb/s RSOA based WDM-PON that can work effectively for bi-directional transmission.

c) Based on the propose methods, different performance metrics will be measured that have the significant influence on practical deployment of such optical system.

d) Compare the advantages and complexity of propose methods to the existing 10 Gb/s wavelength re-used WDM-PON system.

## 1.5 Thesis Outline

In chapter I, the basic background information is described followed by motivation and thesis objectives.

Chapter II focuses necessary theoretical information towards our architecture. These include optical access networks and methods to deploy FTTH in user premises. The advantages of PON, WDM and their scope in future research field. It also includes advantages and disadvantages of different modulation formats to design cost sensitive ONU to reach high data rates with less components.

Chapter III demonstrates the simulation environment that carried out optical system design simulation tool VPITransmissionMaker-9.1<sup>®</sup>. System setup schematics are illustrated with necessary parameters.

In IV chapter, a 10 Gb/s symmetric bidirectional dual fiber wavelength reuse WDM- PON is proposed with DPSK signal in DS and RSOA remodulation with OFDM-QAM signal in US. DPSK is used due to its resilience against re-modulation noise. OFDM signal is used due to overcome the limited bandwidth response of RSOA. Dual fiber is used due to avoid RB reflection. Further study on RB is carried out using three different setups. The effect of 10 Gb/s NRZ induced RB as well as DPSK induced RB in OFDM-QAM modulated signal is investigated for further analysis of RB effect in single fiber network. System performance is measured in terms of BER Vs. SCR. Finally, a 10 Gb/s symmetric Bidirectional Single Fiber

Single Wavelength (BSFSW) transmission system is proposed with DPSK in DS and MZM remodulation with OFDM-QAM in US. BSFSW is more cost effective comparing to dual fiber implementation. The main concern of single fiber deployment is RB noise which severely degrades the US performance. To overcome this limitation, wavelength shifted approach is used. Hence it requires additional bandwidth. Therefore, MZM is used due to overcome the limited bandwidth response of RSOA.

Finally chapter V includes the summary of this thesis work and also proposes some topics for future work.

## REFERENCES

- [1].K. Grobe, and J. P. Elbers, "PON in adolescence: from TDMA to WDM-PON," IEEE Commun. Mag. vol.46, no. 1, pp.26-34, 2008.
- [2].N. Derek, "NG-PON2 technology and standards," J. Lightw. Technol., vol. 33, no. 5, pp. 1136-1143, 2015.
- [3].E. Wong, "Next-generation broadband access networks and technologies," J. Lightw. Technol., vol. 30, no. 4, pp. 597-608, 2012.
- [4].M. Omella, I. Papagiannakis, B. Schrenk, D. Klionidis, A. N. Birbas, J. Kikidis, J. Prat, and I. Tomkos, "Full-duplex bidirectional transmission at 10 Gbps in WDM PONs with RSOA-based ONU using offset optical filtering and electronic equalization". Proc. OFC, paper: OThA7, SanDiego, CA, USA, 2009
- [5].A. Chiuchiarelli, R. Proietti, M. Presi, P. Choudhury, G. Contestabile, and E. Ciaramella, "Symmetric 10 Gbit/s WDM-PON based on cross-wavelength reuse to avoid Rayleigh backscattering and maximise band usage," Electron. Lett., vol. 45, pp. 1343-1344, 2009.
- [6].Ming-Fang Huang, et. al. "Lightwave centralized WDM-PON system at symmetric rate of 10Gbit/s employing cost-effective directly modulated laser." ECOC 2009.
- [7].C. Arellano, K. Langer, J. Prat, "Reflections and multiple Rayleigh backscattering in WDM single-fiber loopback access networks," J. Lightwave Technol., vol. 27, no. 1, pp.12-18, 2009.

## CHAPTER II

### Optical Access Networks

#### 2.1 Access Networks: An Overview

An access network is the network between Central Office (CO) and end users and is traditionally called last-mile networks. They are also called first-mile networks in recent years as they are the first segment of the broader network seen by users of telecom services [1]. The "last mile" is the most expensive part of the network because there are far more end users than backbone nodes [2]. Example of access networks are i) twisted copper pairs connecting to each individual household ii) residential coaxial cable drops from community antenna TV (CATV) service providers. Wi-Max is another type of access technology which uses radio waves for last-mile connectivity. Traditionally, optical fibers have been widely used in backbone networks because of their huge available bandwidth and very low loss. However, until the beginning of this century, fiber has not been used as the technology of last-mile connection.

The most widely deployed "broadband" solutions today are Digital Subscriber Line (DSL) and Cable Modem networks. Although broadband copper-based access networks provide much higher data rate than 56 Kbps dial-up lines, they are unable to provide enough bandwidth for the tremendous growth of Internet traffic, emerging services such as Video-On-Demand, High Definition Television and interactive gaming, or two-way video conferencing. These Copper-based access technologies are close to their bandwidth limit, and provide only few Mb/s per user over a short distance. These technologies generate a bottleneck at the gateway of the backbone to the access networks, shown schematically in Figure 2.1. In this place there is often a lot of traffic causing to slow down or stop.

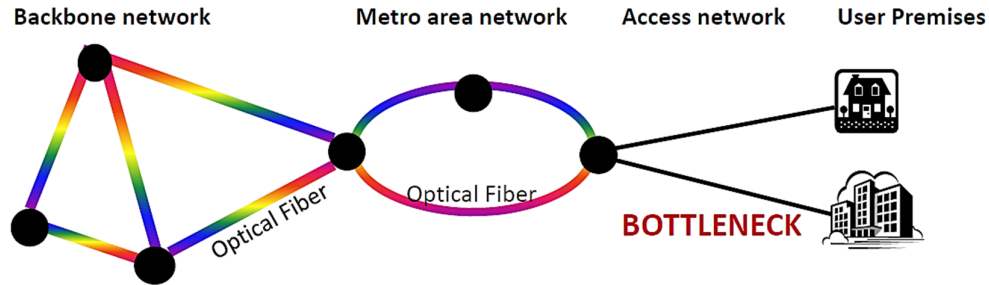


Figure 2.1: Bottleneck of present copper-based access networks

Access network contrasted with the core network, (for example the Network Switching Subsystem in GSM) which connects local providers to each other. The access network may be further divided between feeder plant or distribution network, and drop plant or edge network. When the architecture of access network is based on wireless or wired (optical fiber) optical link is called optical access network and also shown below in Figure 2.2

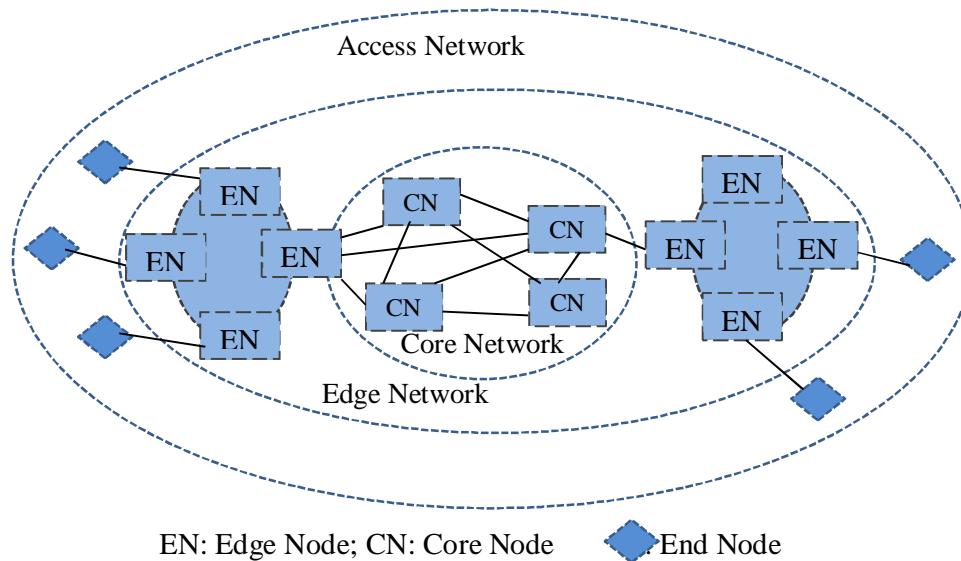


Figure 2.2: A typical optical networking architecture [3]

We can identify three ellipses representing the core network, the edge network, and the access network. The long-haul core network interconnects big cities, major communications hubs, and even different continents by means of submarine transmission systems. The core networks are often called the wide area networks (WANs) or interchange carrier networks. The edge optical networks are deployed within smaller geographical areas and are commonly recognized as metropolitan area networks (MANs) or local exchange carrier networks. The

access networks represent peripheral part of optical network and provide the last-mile access or the bandwidth distribution to the individual end-users. The common access networks are local area networks (LANs) and distribution networks. The common physical network topologies are mesh network (often present in core networks), ring network (in edge networks), and star networks (commonly used in access networks).

## **2.2 FTTx Architectures**

Optical technology is a promising candidate for solving the bandwidth problem in access networks because it can provide at least 10 to 100 times more bandwidth over a large coverage area. In the last decades, optical networks have experienced substantial growth with the deployment of optical fiber in metro and core network segments. It is essential to use single-mode fiber (SMF) as the transmission media in future access networks. SMF provides essentially unlimited transmission bandwidth over extremely long distances. The end goal is to provide an optical fiber to each customer premise or home.

This type of network is commonly referred to as Fiber to the Home/Premise (FTTH/P) or more generally fiber-to-the-x (FTTx) system, where “x” can be “home,” “building,” “curb,” “premises,” etc., depending on how deep in the field fiber is deployed or how close it is to the user. In a fiber-to-the-home (FTTH) system, fiber is connected all the way from the service provider to household users. In an FTTC system, fiber is connected to the curb of a community where the optical signal is converted into the electrical domain and distributed to end users through twisted pairs. Therefore, an FTTC system can also be regarded as a hybrid fiber twisted pair system. FTTx which brings high-capacity optical fiber networks closer to the end users, appears to be the best candidate for the next-generation access network. FTTx is considered an ideal solution for access networks because of the inherent advantages of optical fiber in terms of low cost, huge capacity, small size and weight, and its immunity to electromagnetic interference and crosstalk.

There are two important types of systems that make FTTH broadband connections possible. The straightforward way perhaps the most expensive one, is with active point-to-point (P2P) Ethernet technologies. Active optical networks rely on some sort of electrically powered equipment to distribute the signal, such as a switch, router, or multiplexer. Such networks are identical to the Ethernet computer networks used in businesses and academic institutions, except that their purpose is to connect homes and buildings to a central office (CO) rather than to connect computers and printers within a campus.

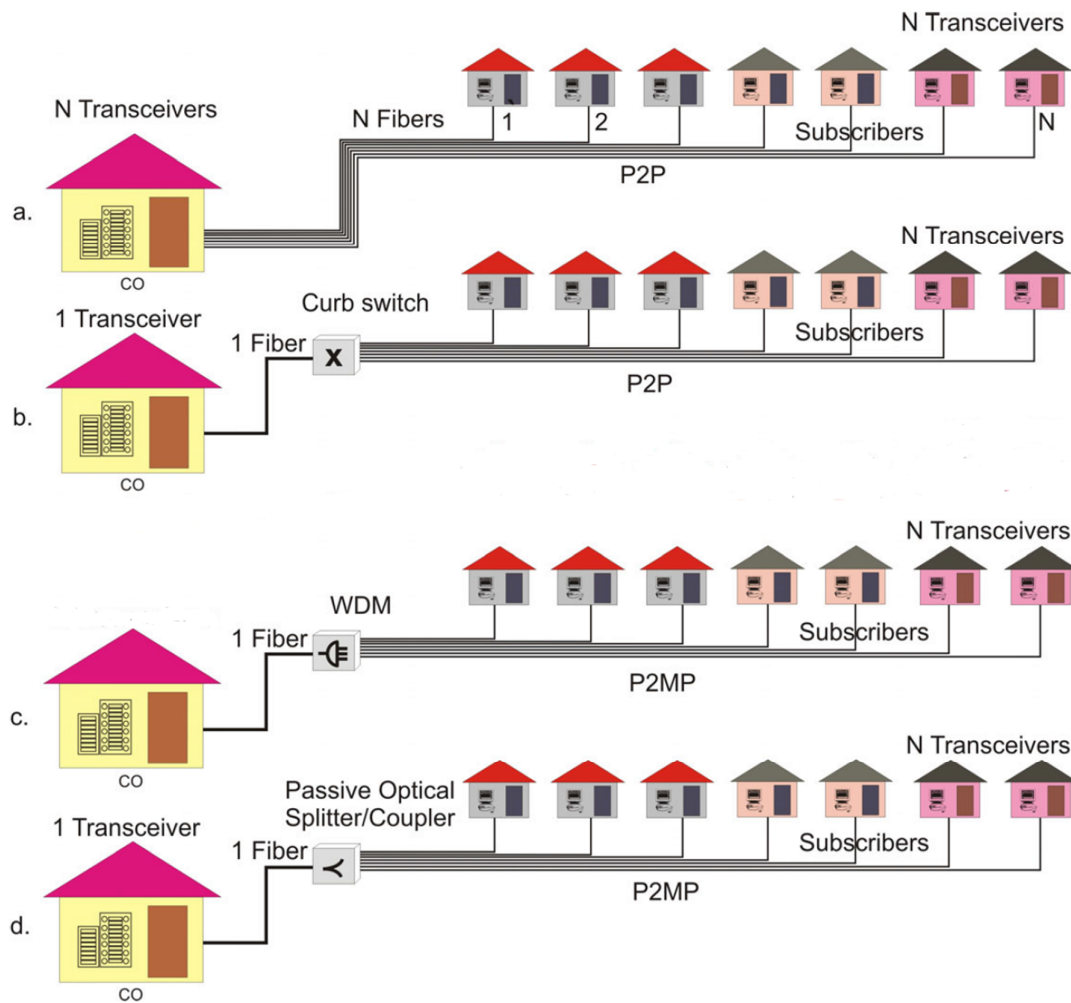


Figure 2.3: Different architectures for fiber-to-the-Home (FTTH)

Figure 2.3 (a) depicts direct P2P architecture which is simple but expensive due to its extensive fiber deployments. The second architecture in Figure 2.3 (b) uses a curb switch which reduces the deployed fiber but the curb switch is an active component that requires electrical power as well backup power.

The network topology of the last two architectures Figures 2.3 (c), (d) are normally referred as passive optical network, where only passive optical devices are used, namely fibers and splitters/couplers or combiners or wavelength multiplexer/de-multiplexer.

## 2.3 Passive Optical Network (PON)

The key feature of a PON is the presence of only passive components in the field, i.e. elements that operate without any electrical power. PON are point-to-multipoint (P2MP) networks. Typically, a PON configuration reduces the required amount of fiber and CO equipment compared with active architectures. PON architectures offer great advantages like low cost, high reliability and easy maintenance for network operators. Most FTTx models are based on the PON due to its cost effectiveness and low energy consumption per bit.

A typical PON topology with terminology is shown in Figure 2.4. Fiber connectivity is established from the optical line terminal (OLT) at CO to the ONU at customer premises. The passive elements are placed at the remote node (RN), which sits close to ONU. The data traveling from user-end towards OLT is known as US traffic, and the data traveling to the user-end nodes is known as DS traffic.

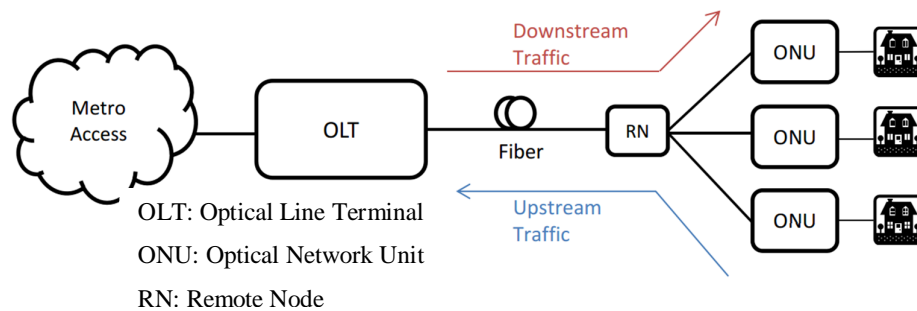


Figure 2.4: Typical PON diagram

There are several possible topologies suitable for PONs, like tree, ring or bus as shown in Figure 2.5. Different topologies have different advantages based on system requirements and implementation complexity.

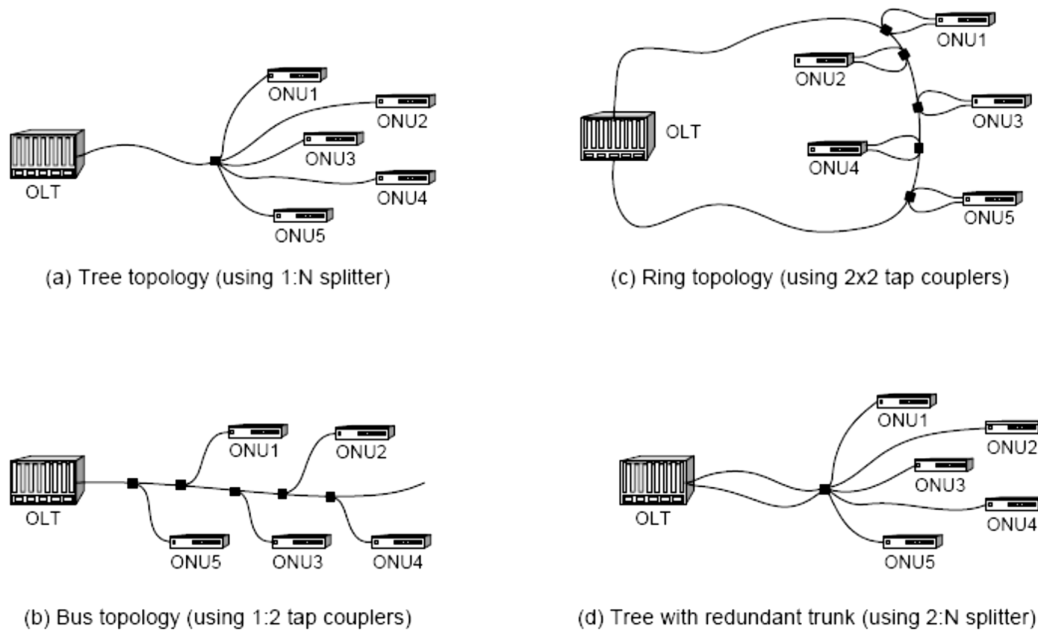


Figure 2.5: PON topologies [4]

Because of its point-to-multipoint (P2MP) architecture, multiplexing techniques are required in a PON to multiple access capability. These multiplexing schemes can be generally categorized as time-division multiple access (TDMA), wavelength-division multiple access (WDMA), subcarrier-division multiple access (SCMA), and code-division multiple access (CDMA). Among them, the TDM-PON and WDM-PON systems are expected to be most promising candidates for widespread use [4, 5]. Most of research work and standardization towards next-generation optical access networks have focused on these two PON systems.

### 2.3.1 TDM-PON

TDM-PON is currently the most popular FTTP approach and is starting to see significant deployments in various regions of the world [6]. A typical TDM-PON system is shown in Figure 2.6. In a TDM-PON, a passive optical splitter is deployed at the RN as a cost effective and simple device for splitting the incoming optical power into equal output power. The down-stream traffic from OLT is distributed to ONUs through the passive splitter by broadcasting.

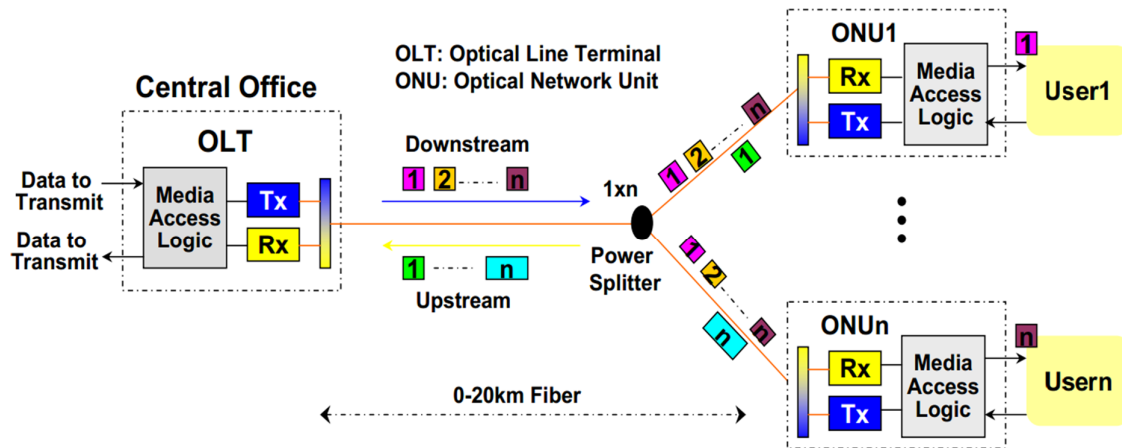


Figure 2.6: TDM-PON architecture

The broadcast data is encrypted properly, so each ONU can only access its own data. The upstream traffic from all ONUs to OLT is multiplexed in the time-domain. This is shown in Figure 2.6 where the bandwidth of a single wavelength is time-shared between different users using various protocols. To separate the upstream and downstream traffic, a wavelength duplexing scheme is used. As an example, for downstream data, 1490 nm wavelength region is used while for upstream data 1310 nm region is deployed. The user-end at the ONU can compose of a single home, a building with many users or it can alternatively be a wireless access point.

To make a TDM-PON cost effective and practical for widespread deployment, standardization of the algorithms and protocols must be established. Broadband PON (BPON) uses the ATM protocol [7]. Ethernet PON (EPON) deploys the Ethernet protocol [8]. Gigabit PONs (GPON) carries ATM as well as Ethernet traffic [9]. GPON nicely combines the quality-of-service advantages of ATM with the efficiency of Ethernet. A more recent standard for data links covering shared data rates of up to 1-10 Gb/s has been standardized and named 10-GPON [10]. Depending on each protocol, aggregate data rates can range from 1-10 Gb/s, shared between 32-128 user nodes, and covering ranges up to 30 km. Table 2.1 compares these technologies based on bitrate, distance covered and number of power splitting nodes.

Table 2.1: TDM-PON comparison

Technology	Standard	Downstream Rate	Upstream Rate	Reach	Nodes
BPON	ITU G.98	622 Mb/s	155 Mb/s	20 km	32
EPON	IEEE 802.3ah	1.25 Gb/s	1.25 Gb/s	20 km	64
GPON	ITU G.984	2.5Gb/s	1.25 Gb/s	20 Km	64
10 GPON	ITU G.987	10 Gb/s	2.5 Gb/s	25 km	128

However TDM-PONs have some drawbacks which hinder their future-proof application. These shortcomings can be outlined as follows:

- Security issues due to broadcasting nature of downstream traffic.
- Bandwidth sharing of upstream traffic which diminishes the maximum bandwidth offered by a single wavelength.
- Short coverage reach due to the power split losses associated with the optical splitter.
- Complicated bandwidth allocation protocols.
- Requirement for ranging protocols and timely synchronization between nodes.

### 2.3.2 WDM-PON

Wavelength division multiplexing is the ultimate solution for fast, efficient and secure bandwidth allocation in passive optical networks, and the subject of research proposals for next generation broadband access. WDM-PON was first proposed in [11]. WDM-PON systems can eliminate the complicated time-sharing issues in TDM-PON systems by providing virtual point-to-point (P2P) optical connectivity to multiple end users through a dedicated pair of wavelengths. In addition to the advantages of high scalability and flexibility, longer transmission distance can be achieved because of the efficient use of optical power at the remote node. The architecture of a WDM-PON system is shown in Fig. 2.7. The big difference in the outside fiber plant is replacing the optical-power splitter in a TDM-PON with an array waveguide Grating (AWG) to de-multiplex the downstream wavelengths and multiplex the upstream wavelengths. In the downstream direction of a WDM-PON, the wavelength channels are transmitted from the OLT to the ONUs on a single fiber using an array of tunable lasers located at the OLT. The wavelength channels are then de-multiplexed by an AWG router located at the passive RN, and a unique wavelength is assigned to each ONU port.

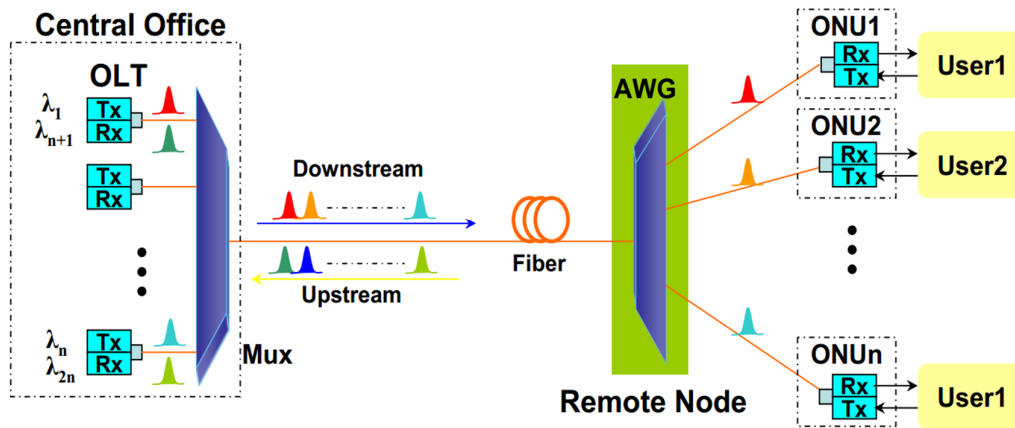


Figure 2.7: WDM-PON architecture.

The AWG ports are periodic in nature, where multiple spectral orders of input wavelength channels are routed to the same output port. This cyclic feature of the AWG allows for downstream and upstream transmission to occur in different wavelength windows. Within each wavelength window, the wavelengths are separated with wavelength spacing's determined by AWG ports. The Wavelength spacing's and wavelength bands are further discussed in the next section.

Cost is the final factor to limit the commercial deployment of WDM-PON systems. To reduce the cost, many research have been conducted on colorless ONUs based on centralized light sources using amplified spontaneous emission (ASE)-injected Fabry-Perot laser diodes (FPLDs), ASE-seeded RSOAs, and spectrum sliced RSOAs [12, 13]. Other efforts have been carried out on the reduction of Rayleigh noise or re-modulation noise for longer transmission distance, protection and restoration scheme, architecture design, and wavelength management.

## 2.4 WDM Wavelength Allocation

It is very important to allocate upstream and downstream wavelength channels with maintaining standards. The downstream and upstream wavelengths allocated to each ONU are intentionally spaced at a multiple of the free spectral range (FSR) of the AWG, allowing both wavelengths to be directed in and out of the same AWG port that is connected to the destination ONU. WDM allocates operational wavelengths to users in a systematic manner.

The wavelength spacing for WDM networks can be categorized as either Coarse WDM (CWDM) with around 20 nm spacing or dense WDM (DWDM) with less than 1 nm spacing.

The spectral grid for CWDM is defined in ITU G.694.2, with a wavelength spacing of 20 nm [14]. If the full wavelength band from 1270-1610 nm is used, it can house 18 individual wavelength channels seen in Figure 2.8. CWDM networks have less stringent operational requirements for temperature-controlled environments due to larger spectral range. However, using a conventional single-mode optical fiber for these systems limits the number of available channels due to the presence of water peak attenuation in the 1370-1410 nm range.

The wavelength spacing in a CWDM for all wavelength bands is shown in Figure 2.8. In DWDM, on the other hand, the wavelength spacing can be as narrow as 0.2 nm (25 GHz) [15]. Because DWDM can allocate many wavelength channels within a narrow range, it is considered the ultimate solution for WDM-PON. The devices used for DWDM applications need to be controlled for cross talk between adjacent channels and also temperature controlled. Therefore, the DWDM scheme introduces more cost than CWDM. The multiplexing devices must also support the requirements for dense channel spacing with low channel cross-talk. The standardized wavelength spacing for 0.8 nm (100 GHz) channel spacing is shown in Figure 2.8.

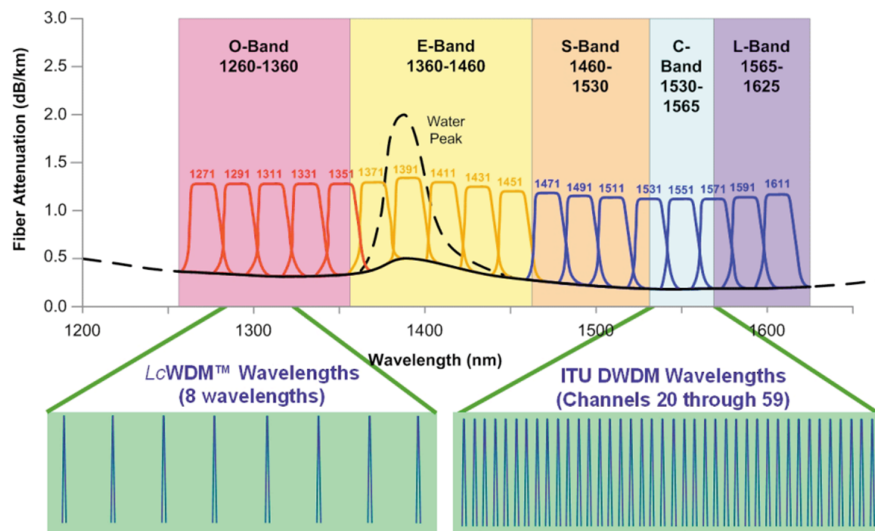


Figure 2.8: CWDM and DWDM wavelength grids based on ITU standards [15]

## 2.5 Bidirectional Transmission in PONs

WDM allows bidirectional communication over a single fiber since it is a method of combining multiple laser wavelengths for transmission along a fiber media. This method also increases signal capacity. Bidirectional single-wavelength single-fiber transmission (BSFSW)

is the most interesting scheme for application in the access network domain, mainly because of its cost-efficiency in terms of CAPEX. The share of cost per subscriber for the needed infrastructure and scalability in terms of both number of users and bit rate are fundamental constraints for the development of novel designs.

One of the major barriers of FTTH technologies is the deployment of new fiber infrastructure. The size of the outside plant is then a critical constraint when deploying the access network. The number of kilometers of fiber required and the number of optical fusions needed to connect the ONUs to the OLT depends not only on the network topology but also on the number of fibers used for the transmission. In Figure 2.9 there are represented the basic options for bidirectional transmission. To deploy compact architecture in both directions, it is necessary to deal with general aspects of bidirectional transmission.

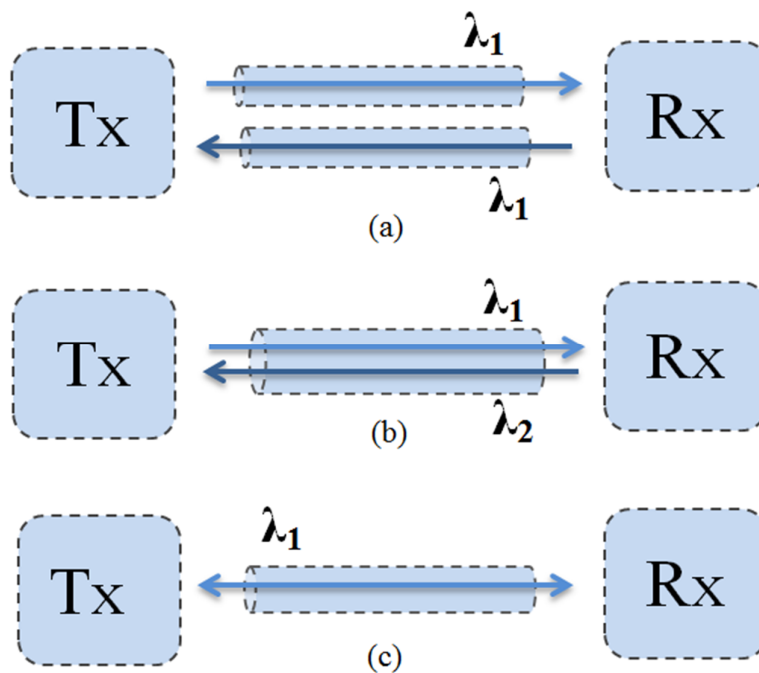


Figure 2.9: Bidirectional options for PON

A plain option is the two-fiber solution, consisting in one fiber for each direction, Figure 2.9 (a). Even if this is not a cost-effective design, most of the actual commercial technologies for PONs are based on this architecture. The main reason is that optical components employed are less restrictive and inexpensive laser or even Light Emitting Diode (LED) sources can be employed achieving correct transmission results. Single fiber transmission presents a more efficient solution because only half of the amount of fibers is necessary; as well, the cost for connectors, splices and other network components decrease. Transmission over a single fiber

can be implemented using two strategies. The simplest way is to transmit down and uplink data using different wavelength in Figure 2.9 (b). Thus, the signals do not interfere with each other, as they are carried in separated frequencies. This option requires sources of different wavelength as well as and optical filters to divide up- and down-link channels. The second alternative consists in using the same wavelength in both directions, Figure 2.9 (c).

The last strategy presents a clear advantage for WDM networks, as wavelengths for both directions are now available especially for CWDM networks where the number of wavelength is limited.

## 2.6 WDM PON Architectures

Figure 2.10 illustrates a typical WDM PON architecture comprising a CO, two cyclic AWGs, a trunk or feeder fiber, a series of distributions fibers, and ONUs at the subscriber premises. The first cyclic AWG located at the CO multiplexes DS wavelengths to the ONUs and demultiplexes US wavelengths from the ONUs.

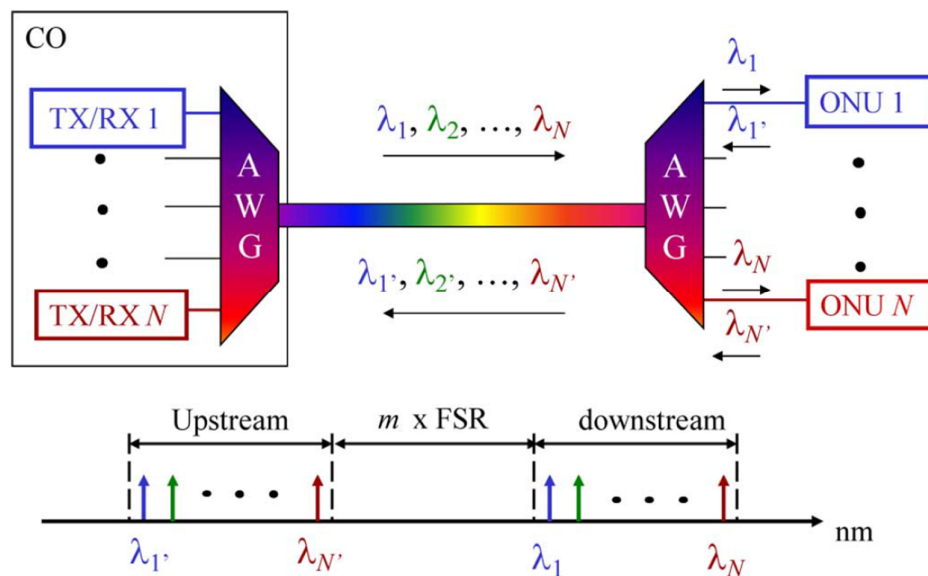


Figure 2.10: Architecture of a WDM-PON. Inset: Allocation of upstream and downstream wavelength channels into two separate wavebands.

The trunk fiber carries the multiplexed downstream wavelengths to a second cyclic AWG located at a remote node. The second AWG demultiplexes the downstream wavelengths and

directs each into a distribution fiber for transmission to the ONUs. The downstream and upstream wavelengths allocated to each ONU are intentionally spaced at a multiple of the free spectral range (FSR) of the AWG, allowing both wavelengths to be directed in and out of the same AWG port that is connected to the destination ONU. In Figure 2.10, the DS wavelengths destined for ONU 1, ONU 2..., and ONU N, are denoted by  $\lambda_1$ ,  $\lambda_2$  and  $\lambda_N$  respectively. Likewise, US wavelengths from ONU 1, ONU 2..., and ONU N, that are destined for the CO are denoted  $\lambda'_1$ ,  $\lambda'_2$  ..., and  $\lambda'_N$  respectively. In a typical WDM PON, wavelength channels are spaced 100 GHz (0.8 nm) apart. In systems classified as DWDM-PON, a channel spacing of 50 GHz or less is deployed. Although a WDM PON has a physical P2MP topology, logical P2P connections are facilitated between the CO and each ONU. In the example shown in Figure 2.10, ONU N receives downstream signals on  $\lambda_N$  and transmits upstream signals on  $\lambda'_N$ . The capacity on these wavelengths is solely dedicated to that ONU. Commonly cited benefits of WDM PON resulting from this unique feature include protocol and bit-rate transparency, security and privacy, and ease of upgradeability and network management.

### 2.6.1 Tunable Laser WDM PON

Fast tunable lasers are widely deployed in WDM-PON. Tunable lasers can also be considered for generating an upstream signal at the ONU. The concept is shown in Figure 2.11. A dedicated tunable laser along with an external modulator is deployed at every ONU node. The laser spectral width is narrower than AWG spacing. Such deployment offers great optical performance and flexibility in terms of wavelength. The number of ONUs supported will be determined by the channel spacing of the AWGs, and the tuning range of the laser. The problem with this scheme is the high cost of a much more sophisticated laser at the source, need for maintenance, and an internal wavelength locker to ensure the laser operates at the correct wavelength channel. It has the benefits of long transmission distances & high bandwidth and Easy scaling of bandwidth, end users & reach.

Since each ONU is assigned a unique upstream wavelength, distinct wavelength transmitters must be deployed at the subscriber premises. The simplest solution is to utilize fixed wavelength transmitters. Long transmission distances and high speed transmission can be achieved with this solution.



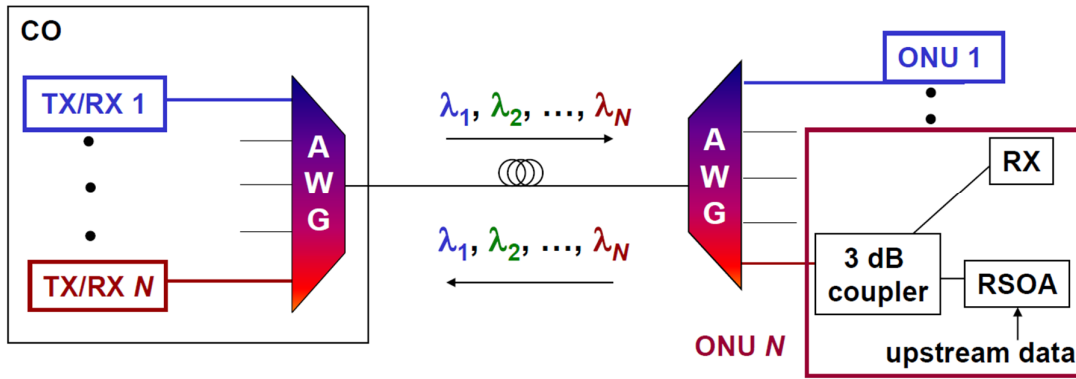


Figure 2.12: Wavelength Reuse WDM-PON

As illustrated in Figure. 2.12, the DS and US wavelengths designated to and from an ONU are identical. The benefits of the wavelength reuse scheme includes the re-modulation of the DS wavelength channel, thereby eliminating the need for seeding sources, is less costly than using tunable lasers, and direct modulation of the RSOA.

### 2.6.3 Coherent injection and seeding WDM PON

In addressing the potential large inventory and cost of wavelength specific sources, researchers have been concentrating on developing cost-efficient and wavelength independent sources termed “colorless” sources. Optical light originating from the CO is fed into the ONUs to injection- lock Fabry–Perot laser diodes (FP LDs) [28, 29] or to wavelength-seed reflective semiconductor optical amplifiers (RSOAs) [30-33].

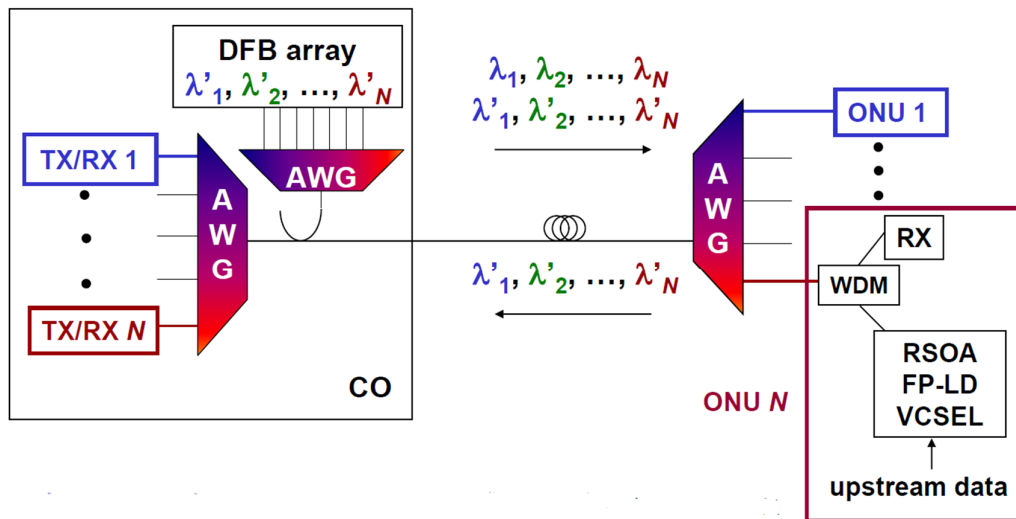


Figure 2.13: Coherent-injection and CW-seeding WDM-PON

As illustrated in Figure 2.13, the injection- locking or wavelength seeding light may be furnished by CW light from a centralized light source located at the CO. The wavelength seeding scheme is identical to the injection-locking scheme except for the use of an RSOA which amplifies and modulates the incoming CW light.

As the transmitting wavelength of a colorless ONU is determined externally by the wavelength of the incoming light, all ONUs may be implemented with identical FP-LDs or RSOAs. Figure 2.13 uses DFB laser array that is placed in CO where ONU  $N$  receives downstream signals on  $\lambda_N$  and transmits upstream signals on  $\lambda'_N$ .  $\lambda'_N$  transmits from CO towards ONU  $N$  and an reflective modulator use it to modulate the upstream data and sent back to CO.

## 2.7 RSOA in WDM PON

RSOA is the perfect candidate for WDM-PON because of its wide optical bandwidth, large gain and low cost, therefore fulfilling most of the requirements. For instance, its moderate optical bandwidth makes it a colorless cost-effective modulator for WDM-PON. The same type of device can be used in different ONUs, which reduces the network cost. Moreover, the large gain provided by an RSOA can compensate link losses without using an extra amplifier, which simplifies the overall solution. RSOA devices faced fast growing interest in US channels transmission based on reflective ONU for WDM-PON applications.

Since, as a modulator, the RSOA is mainly illuminated by a CW optical source, the material gain is assumed to vary linearly, shown in Figure 2.14 (a) with the carrier density but with no wavelength dependence. Figure 2.14 (b) illustrates the frequency response of RSOA. The 3-dB bandwidth for the device is measured to be  $\sim 1.3$  GHz. As such the device should be suitable for 1.25 Gbps modulation and may even be suitable up to 2.5 Gbps modulation depending on the modulation format. However the modulation bandwidth of RSOA is limited to approximately 2 GHz and increasing the modulation bandwidth of RSOA is still a challenge. One way to overcome this bandwidth limitation is to use multi-carrier modulation (MCM) format such OFDM-QAM. Colorless ONU does not require any wavelength specific optical source, which helps to deploy an identical module in each access unit and also reduces the system implementation complexity. A promising candidate for the design of colorless PONs is the RSOA based single fiber loop back network.

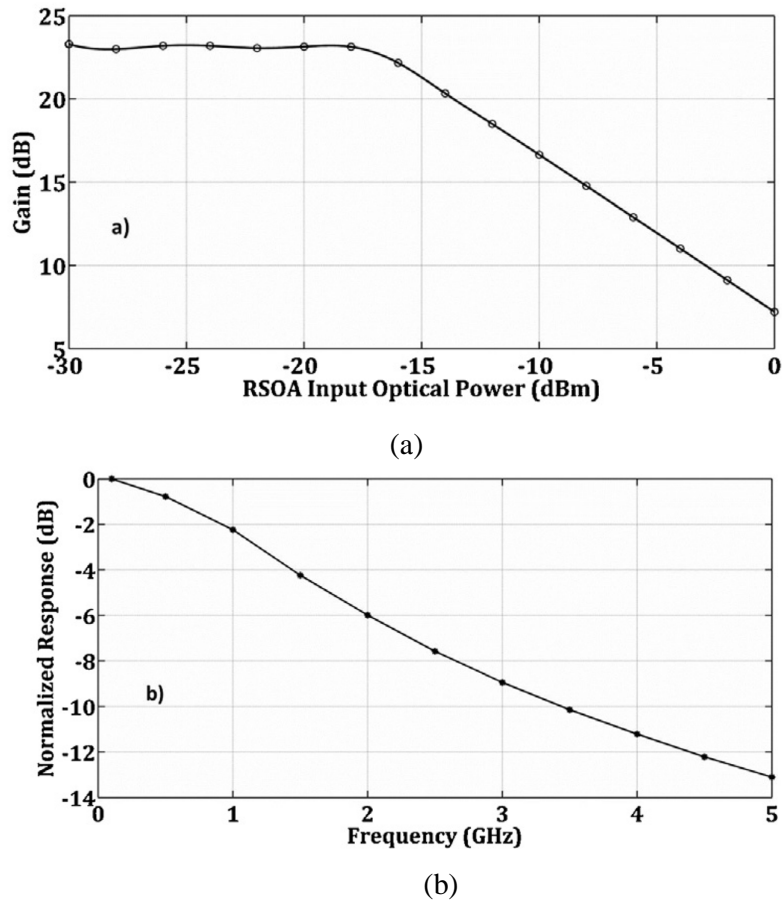


Figure 2.14: RSOA operating characteristics (a) Gain vs RSOA input optical power and (b) E/O normalized frequency response.

In a bidirectional single fiber system, CW light transmits from the CO, propagates over the fiber, modulated and reflected by ONU and finally sends back to the CO. Moreover, RSOA itself is a key device in this reflective ONU architecture due to its properties of optical gain, wide optical band-width, and integration capability. However, as the DS CW signal and US modulated data share the same fiber, the system performance is inherently limited by RB noise.

## 2.8 Impairments

Definitely, bidirectional wavelength reuse architecture is the most interesting scheme to be developed in the access network. The problem of RB and other reflections in single fiber wavelength reuse scheme can overcome by using dual fiber transmission as the signals do not interfere with each other, as they are carried in separate fiber. At the same time, dual fiber

topology can also be severely degraded by the interference between the residual DS and US data at the CO. This is commonly known as re-modulation noise. A solution to minimize residual DS modulation is to ensure that the US and DS modulation formats are orthogonal. However, there is a need of new solutions to deal with potential coherent crosstalk as well as of novel ONU designs. Figure 2.15 shows a schematic of RB effect in bidirectional communication.

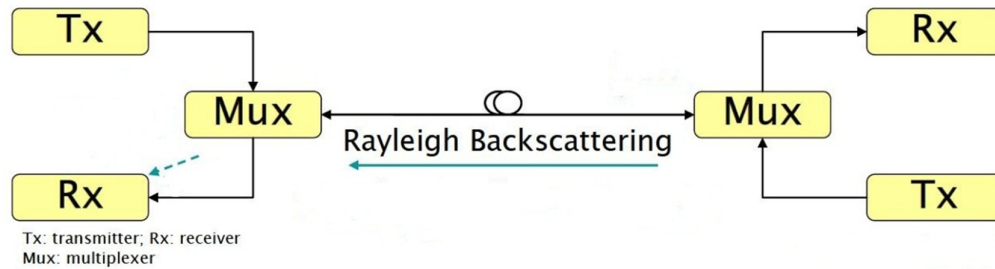


Figure 2.15: Schematic of RB effect in bidirectional single fiber transmission

### 2.8.1 Rayleigh Backscattering (RB)

Rayleigh scattering losses in fiber optics are caused by material density imperfections occurring during the fiber manufacture. The light is scattered in all directions, also in the back direction, which is denoted as RB. The backscattered signal will then overlap with the counter-propagating signal. RB is the most degrading effect in a bidirectional single-fiber single-wavelength system. In order to prevent from this effect, it is required an analysis of its behavior. In this section, the statistical properties of the backscattered signal are presented and also the effect on the transmission of a counter-propagating signal is studied.

As RB loss in fiber is caused by material density imperfections, so it becomes an unavoidable effect inner at the fiber. It is determined by the Rayleigh attenuation coefficient  $\alpha_s$ , which is proportional to  $\lambda^{-4}$ . In a system with two signals at the same  $\lambda$  simultaneously in opposite directions, a beam travelling through the fiber from 'A' to 'B' (see Figure 2.16), causes the light scatter in all directions. The fraction scattered in the back direction, which is given by the recapture coefficient  $S$ , is known as the RB. Whenever a signal is sent from 'B' to 'A', it would be interfered by the RB noise. For the deduction of the statistical properties of the RB signal, we use a two dimensional model for the fiber represented in Figure 2.16. Where,  $L$  is the fiber length and it is divided by  $N$  scatter sections of length  $\Delta L=L/N$ .

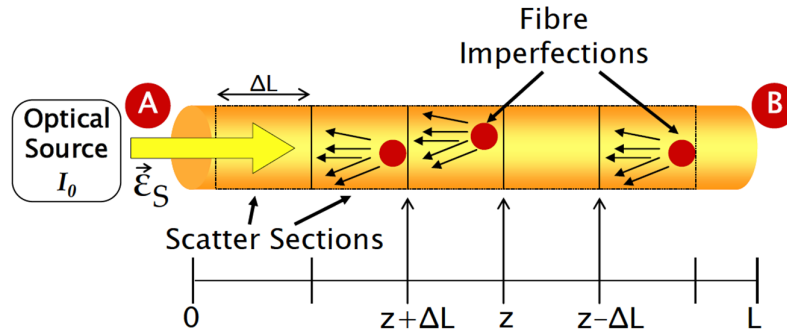


Figure 2.16: Fiber model for Rayleigh Backscattering

Considering the coherence of the source is larger than  $\Delta L$ , the scattered field vectors are statistically independent. From [34] the average intensity noise of Rayleigh Backscattering (RB) can be expressed as

$$\langle I_b \rangle = \alpha_s S I_0 \frac{(1 - e^{-2\alpha L})}{2\alpha} \quad (2.1)$$

Where  $\alpha_s S$  is the average intensity,  $I_0$  is the amplitude of the field and  $L$  is the total backscattered field. Figure 2.17 depicts a graphical exemplification of the averaged intensity normalized. The backscattered intensity increases with the fiber length and converges after 20km approximately, depending of the fiber parameters. The convergence value is usually between -36dB and -32dB below the input power. In the represented example the normalized power achieves -35dB.

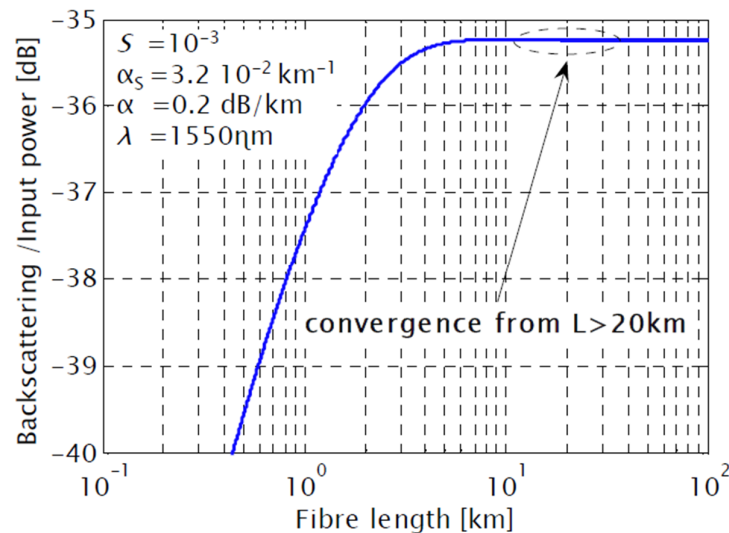
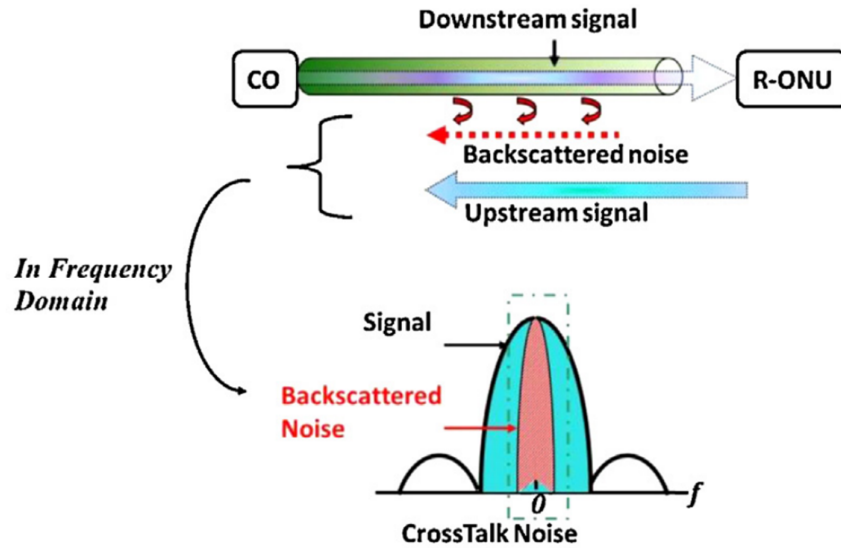


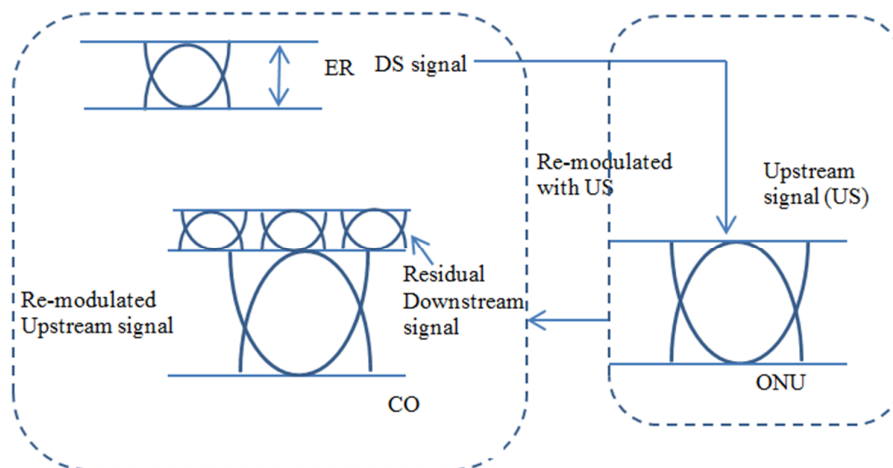
Figure 2.17: Normalized Rayleigh Backscattering intensity vs. fiber length

The interference between US data signal and RB components produce the optical beating noise in CO which is highly coherent near the DC frequency as also shows in Figure 2.18 (.a) Particularly in BSFSW transmission system, the DS signal and US modulated data share the

same fiber, thus system performance is inherently limited by RB noise [35]. This in-band coherent noise severely degrades the system performance if the signal to crosstalk ratio (SCR) goes below the acceptable label. Coherent crosstalk occurs when the signals are phase-correlated. In other words, the phase difference between them is either constant, or changes on a much slower time scale than the coherence time of the optical sources. This condition only happens if the fields are generated by the same optical source. Therefore coherently interfering fields must have identical optical frequencies.



(a) Spectral shape of crosstalk noise i.e RB noise



(b) Remodulation Noise

Figure 2.18: Two major impairments of WDM-PON architecture.

## 2.8.2 Remodulation Noise

Bidirectional wavelength reuse WDM-PONs also introduces re-modulation noise as DS signal is used to re-modulate the US signal. Therefore, some part of DS signal presents in re-modulated US signal which is mainly known as residual DS signal or re-modulation noise as illustrated in Figure 2.18 (b). However, US performance can be severely degraded by the interference between the residual DS and US data at the CO. A solution to minimize residual DS modulation is to ensure that the US and DS modulation formats are orthogonal.

In [24], phase modulation and frequency shift keying modulation are used for the DS modulation with US being modulated with the on-off keying (OOK) format. In another solution reported in [25], data Radio Frequency (RF) subcarrier is modulated onto a carrier and sent DS towards the ONU. At the ONU, the carrier is filtered and then modulated with US data. Therefore, to minimize residual DS signal, unconventional modulation formats and thereby unconventional transceivers must be used. Recently, line coding approaches such as Manchester coding [26] and DC balanced line coding [27] have been demonstrated to eliminate the DC component on the DS data to improve US performance in a WDM PON.

However, the splitting or accumulation of signals at the RN is done by multiplexer (MUX) and de-multiplexer (DEMUX). AWG is such kind of splitter/combiner to exploit its free spectral range by choosing the matching US and DS wavelengths. There are several options of DS and US modulation in wavelength reuse WDM-PONs.

Traditionally, the preferred modulation format for optical signals is intensity modulation (IM). Although it is not the best in terms of sensibility or robustness against noise, it is the simplest and the most cost effective to implement. However, as in the electric world, there are other ways of transmitting data, which offer better performance, but require more complex receiver schemes.

This thesis work demonstrates a symmetrical 10 Gb/s WDM-PON with RSOA based ONU realizing DPSK in DS and OFDM-QAM in US transmission for further investigating the effect of re-modulation noise. Thanks to the constant envelop (CE) property of DPSK format for DS transmission and ONU seeding, thus making the re-modulation stage at the ONU by far more practical. Hence, modulation formats becomes a key element for the network design.

## 2.9 Available Modulation Formats

In optical access networks, different modulation formats may be selectively employed depending on the network size and the system settings. To improve the transmission performance of WDM systems, a wide variety of techniques have been proposed. The use of advanced modulation formats is the most effective solution in managing transmission impairments. In general, different data formats lead to different signal quality at the receiver end for a given transmission link, because they exhibit different waveforms and spectra. The important and most used modulation formats such as Non Return To Zero (NRZ), Return To Zero (RZ), DPSK and DMT etc.

The modulation format describes how the data is coded onto the optical signal. The amplitude, phase, frequency and state of polarization (SOP) of optical signal can be modulated. The variety of modulation formats can be classified into the following four categories:

- Amplitude Shift Keying (ASK) or OOK
- Phase Shift Keying (PSK)
- Frequency Shift Keying (FSK)
- Polarization Shift Keying (PolSK)

ASK encodes data by turning on or off the amplitude of light, depending on whether the symbol to be transmitted is a mark (“1”) or a space (“0”), at a rate equal to the information frequency. In this modulation format, each binary symbol (“1” or “0”) is represented by the presence or the absence of light. It includes NRZ, RZ, and duobinary formats. There are also a number of variations of the RZ format. It includes simple RZ, carrier suppressed RZ (CSRZ), chirped RZ (CRZ), vestigial sideband RZ (VSB-RZ), and dispersion-managed soliton-based RZ (DMS-RZ).

PSK encodes data by modulating the phase of light. In this modulation format, each binary symbol (“1” or “0”) is represented by light phase of “0” or “ $\pi$ ”. It includes DPSK, RZ-DPSK, CSRZ-DPSK, and differential quaternary PSK (DQPSK) and its pulse-carved forms.

FSK encodes data via the modulation of the frequency of light, and includes FSK, continuous phase FSK (CPFSK), and minimum shift keying (MSK) [14-17]. PolSK encodes data by the modulating the polarization of light. In polarization shift keying, the modulator generates two orthogonal polarization states, which correspond to “1” and “0” bits.

PolSK encodes data by the modulating the polarization of light. In polarization shift keying, the modulator generates two orthogonal polarization states, which correspond to “1” and “0” bits.

There is variety of factors that should be considered for the right choice of modulation format: spectral efficiency, power margin, and tolerance against group velocity dispersion (GVD) and against fiber nonlinear effects like self-phase modulation (SPM), cross-phase modulation (XPM), four-wave mixing (FWM), and stimulated Raman scattering (SRS).

### 2.9.1 Non Return To Zero (NRZ)

NRZ has been the dominant modulation format in intensity modulated-direct detection (IM/DD) fiber-optical communication systems for the last years because it is easy to generate, detect and process presented in Figure 2.19.

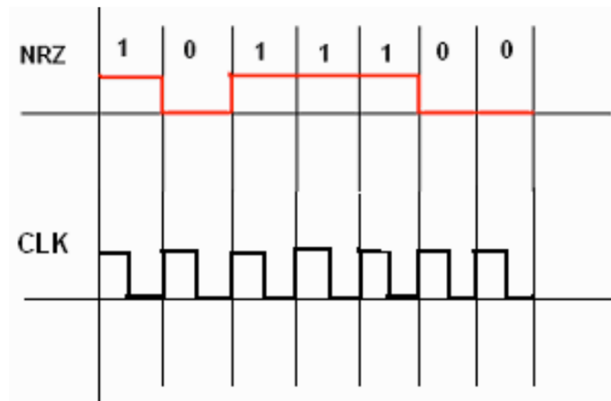


Figure 2.19 Representation of the NRZ code [36].

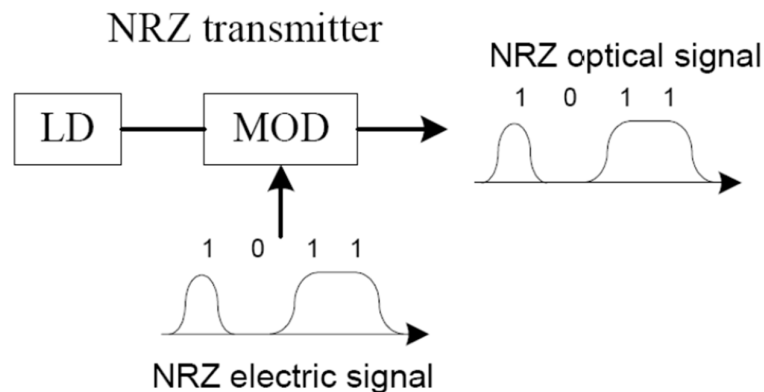


Figure 2.20 NRZ transmitter diagram [37].

Figure 2.20 shows the diagram of the NRZ transmitter. The intensity of the carrier light wave is modulated by the applied electric field which voltage varies with a determined function. The Mach-Zehnder modulator (MZM) is driven at the quadrature point of the modulator power transfer function with an electrical NRZ signal.

The NRZ pulses possess a narrow optical spectrum due to the lower on-off transitions. The reduced spectral width improves the dispersion tolerance and enables higher spectral efficiency, but on the other hand it affects the inter-symbol interference (ISI) between the pulses. NRZ modulated optical signal is less resistive to fiber nonlinear effect compared to its NR counterpart. It requires a relatively low electrical bandwidth for transmitters and receivers compared with RZ. NRZ requires roughly half the bandwidth of RZ, and is thus easier to implement, and is less costly [38].

### **2.9.2 Differential Phase Shift Key (DPSK)**

Digital signal can be represented by instantaneous optical power levels with optical intensity modulation. Similarly, digital signal can also be represented by the phase of an optical carrier and this is commonly referred to as optical phase shift key (PSK). In the early days of optical communications, the optical phase was not stable enough for phase based modulation schemes, because of the immaturity of semiconductor laser sources. In recent years, with the rapid improvement of single frequency laser sources and the application of active optical phase locking, PSK becomes feasible in practical optical systems. More specifically, DPSK is the most often used format [38].

DPSK modulation is an encoding format which records changes in the binary stream. DPSK encodes information on the binary phase change between adjacent bits: a 1-bit is encoded onto a  $\pi$  phase change, whereas a 0-bit is represented by the absence of a phase change. Like intensity modulation, DPSK can be implemented in RZ and NRZ format. The main advantage of using DPSK with compared to intensity modulation is a 3-dB receiver sensitivity improvement [39]. DPSK is also more tolerant to nonlinear effects. It has better resilience to XPM and FWM, as compared with intensity modulation formats. It has also been demonstrated that RZ-DPSK and CSRZ-DPSK exhibit superior transmission performance than simple DPSK [40].

### 2.9.3 Orthogonal Frequency Division Multiplexing

WDM PONs make the best use of OFDM due to its high spectral efficiency of the Quadrature amplitude modulation (QAM) in each subcarrier of the OFDM signal, low-bandwidth optical components can still be used. This means we can directly increase the data rate of the system while using the existing optical components developed for GPONs. Besides, the inherent advantage of OFDM frequency diversity transmission allows simple equalization of frequency response by baseband DSP. These characteristics can be used to mitigate fiber chromatic dispersion which is one of the major impairments in WDM PONs.

#### 2.9.3.1 Introduction to OFDM

OFDM is a multicarrier transmission Technique. The basic principle of OFDM is to split a high-rate data stream into a number of lower rate streams that are transmitted simultaneously over a number of subcarriers. The relative amount of dispersion in time caused by multipath delay spread is decreased because the symbol duration increases for lower rate parallel subcarriers. OFDM makes all the carriers orthogonal to one another, preventing interference between the closely spaced carriers.

For fixed-wired applications OFDM served as the core technology for the Asynchronous Digital Subscriber Line (ADSL) and High-Bit-Rate Digital Subscriber Line (HDSL) systems. In these standards OFDM is better known as DMT.

#### 2.9.3.2 Orthogonality

The word “orthogonal” means “statistically unrelated”. Two periodic signals are orthogonal when the integral of their product over one period is equal to zero. For the case of continuous time:

$$\int_0^T \cos(2\pi n f_0 t) \cos(2\pi m f_0 t) = 0, m \neq n \quad (2.2)$$

For the case of discrete time:

$$\sum_0^{N-1} \cos\left(\frac{2\pi nk}{N}\right) \cos\left(\frac{2\pi mk}{N}\right) = 0, m \neq n \quad (2.3)$$

In the case of OFDM, the sinusoids of our sub-carriers will satisfy this requirement since each is a multiple of a fundamental frequency. Due to this, the spectrum of each carrier has a

null at the center frequency of each of the other carriers in the system. This results in no interference between the carriers, allowing them to be spaced as close as theoretically possible. This overcomes the problem of overhead carrier spacing required in other techniques.

### 2.9.3.3 OFDM Subcarriers

Each sub-carrier in an OFDM system is a sinusoid with a frequency that is an integer multiple of a fundamental frequency  $f_0$ . Each sub-carrier is like a Fourier series component of the composite signal, an OFDM symbol. In Figure 2.21, all the sub-carriers have the same amplitude and phase, but in practice these will be modulated separately through the use of QAM. The sub-carrier waveform can be expressed as the following equation:

$$\begin{aligned} s(t) &= \cos(2\pi f_c t + \theta_k) \\ &= a_n \cos(2\pi n f_0 t) + b_n \sin(2\pi n f_0 t) \\ &= \sqrt{a_n^2 + b_n^2} \cos(2\pi f_0 t + \varphi_n), \text{ where } \varphi_n = \tan^{-1}\left(\frac{b_n}{a_n}\right) \end{aligned} \quad (2.4)$$

The sum of the sub-carriers is then the baseband OFDM signal:

$$S_B(t) = \frac{1}{\sqrt{2N}} \sum_{n=0}^{N-1} \{c_n \exp(j2\pi n \frac{k}{2N})\} \quad (2.5)$$

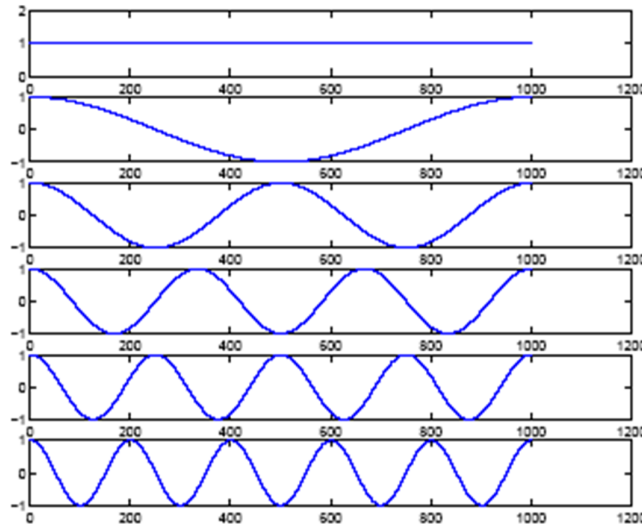


Figure 2.21 Harmonics which are summed to create sub-carriers.

### 2.9.3.4 OFDM Spectrum

Our OFDM symbol is a sum of sinusoids of a fundamental frequency and its harmonics in the time domain. The rectangular windowing of the transmitted OFDM symbol results in a sinc function at each sub-carrier frequency in the frequency response. Thus, the frequency spectrum of an OFDM symbol is as shown below in Figure 2.22. The spectrum of each sub-carrier has been superimposed to illustrate the orthogonality of the sub-carriers. Although overlapping, the sub-carriers do not interfere with each other since each sub-carrier peak corresponds to a zero crossing for all other sub-carriers.

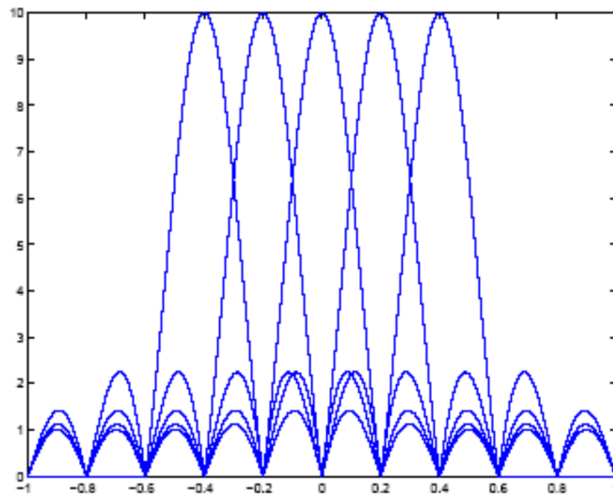


Figure 2.22 Understanding orthogonality (OFDM symbol spectrum)

### 2.9.3.5 Spectrum efficiency of OFDM

Let's first look at what a Frequency Division Multiplexing (FDM) is. If we have a bandwidth that goes from frequency  $a$  to  $b$ , we can subdivide this into a frequency space of four equal spaces. In frequency space the modulated carriers would look like this in Figure 2.23.

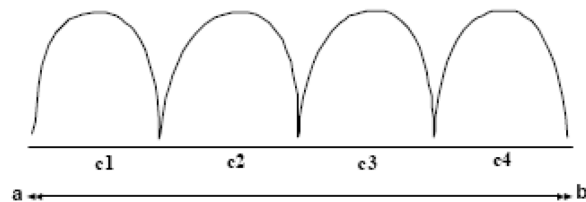


Figure 2.23 FDM band

The frequencies between a and b can be anything, integer or non-integer. Since no relationship exists between them. But, what if frequency  $C_1$  and  $C_n$  were such that for any  $n$  (integer) the following holds.

$$C_n = n * C_1 \quad (2.6)$$

So that

$$C_2 = 2C_1$$

$$C_3 = 3C_1$$

$$C_4 = 4C_1$$

All these frequencies are harmonics to  $C_1$ . In this case since these carriers are orthogonal to each other, when added together, they do not interfere with each other. In other conventional case like in FDM we do not generally have frequency that follows the above relationship. It can be seen from Figure 2.24, in order to implement the conventional parallel data transmission by FDM, a guard band must be introduced between the different carriers to eliminate the inter channel interference. This leads to an inefficient use of the rare and expensive spectrum resource.

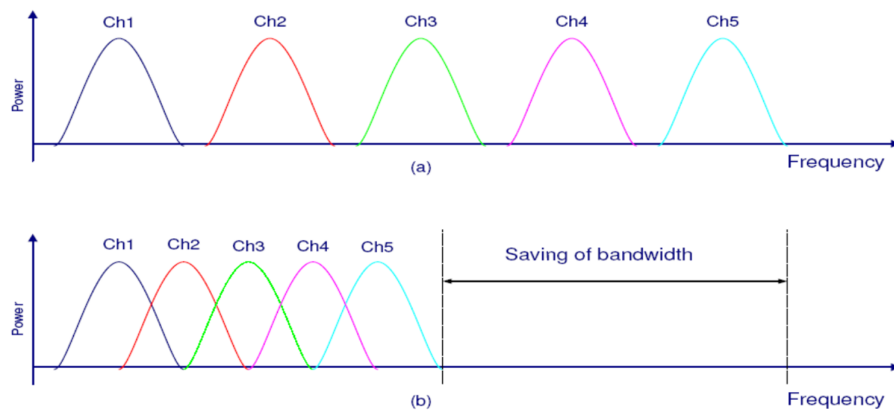


Figure 2.24 Bandwidth comparisons between OFDM and conventional technique

### 2.9.3.6 Inter symbol interference (ISI)

ISI is when energy from one symbol spills over to the next symbol. This is usually caused by time dispersion in multi-path when reflections of the previous symbol interfere with the

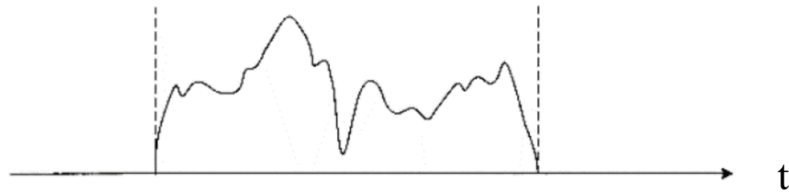
current symbol. In OFDM, because each sub-carrier is transmitting at a lower data rate (longer symbol duration), this will negate the effects of time dispersion, which results in ISI.

### 2.9.3.7 Inter carrier interference (ICI)

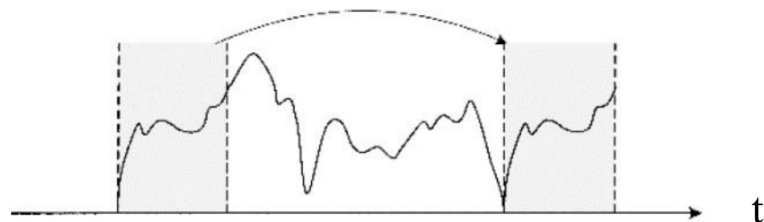
ICI occurs when the sub carriers lose their orthogonality, causing the sub carriers to interfere with each other. This can arise due to Doppler shifts and frequency and phase offsets.

### 2.9.3.8 Cyclic prefix (CP)/ Guard interval

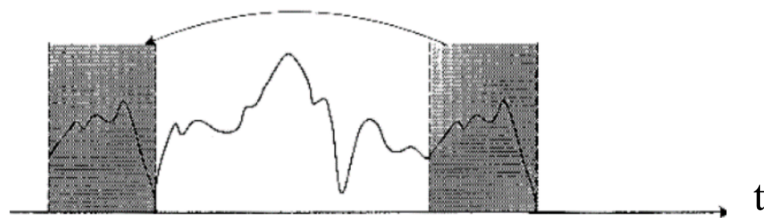
To deal with delay spread of wireless channels, a cyclic extension is usually used in OFDM systems. There are two different types of cyclic extensions which have been shown in Figure 2.25 serially.



(a) OFDM signal



(b) OFDM signal with cyclic



(c) OFDM signal with cyclic prefix

Figure 2.25: OFDM signal with different cyclic extensions.

The CP is a periodic extension of the last part of an OFDM symbol that is added to the front of the symbol in the transmitter, and is removed at the receiver before demodulation. Other variations of guard periods are possible. One possible variation is to have half the guard period a cyclic extension of the symbol, as above, another half a zero amplitude signal. Using this method the symbols can be easily identified. This possibly allows for symbol timing to be recovered from the signal, simply by applying envelop detection. The disadvantage of using this guard period method is that the zero period does not give any multipath tolerance, thus the effective active guard period is halved in length.

The CP has two important benefits:

- The CP acts as a guard space between successive OFDM symbols and therefore prevent ISI, as long as the length of the CP is longer than the impulse response of the channel.
- The CP ensures orthogonality between the sub-carriers by keeping the OFDM symbol periodic over the extended symbol duration, and therefore avoiding ICI.

Mathematically, the CP / Guard Interval convert the linear convolution with the channel impulse response into a cyclic convolution. This results in a diagonalised channel, which is free of ISI and ICI interference.

The disadvantage of the CP is that there is a reduction in the SNR due to a lower efficiency by duplicating the symbol. This SNR loss is given by

$$SNR_{LOSS} = -10 * \log_{10}(1 - T_{CP}/T) \quad (2.7)$$

Where  $T_{cp}$  is the length of the Cyclic Prefix and  $T = T_{cp} + T_s$  is the length of the transmitted symbol. To minimize the loss of SNR, the CP should not be made longer than necessary to avoid ISI and ICI.

#### **2.9.4 Discrete Multi Tone (Modulation)**

OFDM is now being considered widely in optical access network due to its enormous advantages. OFDM enables multilevel modulation and efficient dispersion compensation to achieve spectrally efficient, high-speed, long reach access over a legacy PON fiber plant. There are different forms normal OFDM systems are used in optical solutions for different applications. Besides this, to understand these different techniques, it is useful to realize the fundamentals in each domain. One of these techniques is DMT modulation. DMT is widely employed in copper-based DSL for providing high-speed Internet access via ADSL and very high speed DSL (VDSL).

DMT modulation is a baseband multicarrier modulation technique of the better-known OFDM. The basic idea of DMT is to split the available bandwidth into a large number of sub channels. DMT is able to allocate data so that the throughput of every single sub channel is maximized. If some sub channel cannot carry any data, it can be turned off and the use of available bandwidth is optimized. The transmitter and receiver block diagram are shown in Figure 2.26. [41]

In DMT, a high-speed binary serial input data sequence is divided into  $N/2$  parallel lower-speed binary streams. For each stream indexed by  $n$ , where  $n = 0, 1, \dots, N/2 - 1$ , every  $M$  number of bits are grouped together and mapped onto complex values  $C_n = A_n + jB_n$  according to a QAM constellation mapping consisting of  $2^M$  states. Usually, the IFFT is used in the DMT transmitter to efficiently modulate the complex values  $C_n$  onto  $N/2$  different subcarrier frequencies, which, as a result, are mutually orthogonal.

In order to achieve a real-valued, baseband DMT transmission sequence consisting of  $N/2$  subcarriers, an  $N$ -point IFFT is needed. For the  $N$  inputs of the IFFT, indexed by  $n = 0, 1, \dots, N - 1$  the first half are assigned the values  $C_n$  and the second half have to be assigned the complex conjugate values of  $C_n$ , following the Hermitian symmetry property given by

$$C_{N-n} = C_n^* \quad (2.8)$$

for  $n = 0, 1, \dots, N/2 - 1$ . Generally,  $C_0 = C_n = 0$  so that the resulting DMT sequence does not contain any direct current (DC) value at all.

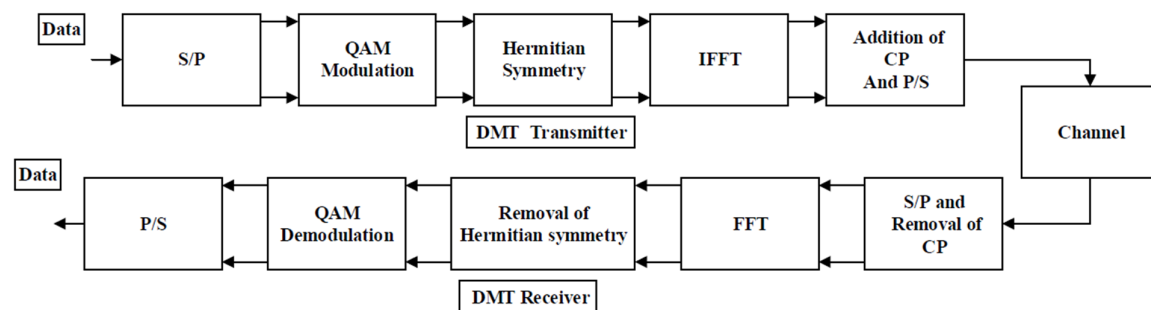


Figure 2.26: Implementation blocks for DMT system

Figure 2.27 illustrates the DMT transmitter and receiver block diagram over an optical intensity modulation/ direct detection system.

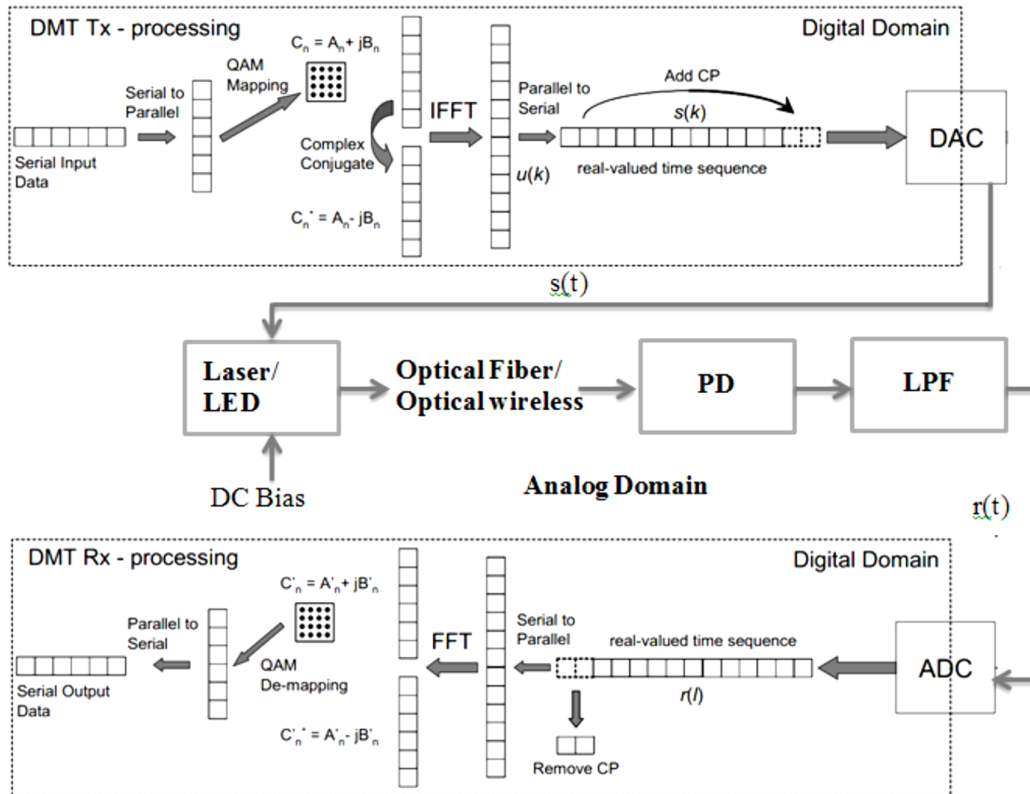


Figure 2.27: Schematic block diagram showing the principle of DMT over an optical IM/DD channel. DAC: digital-to-analog converter, ADC: analog-to-digital converter, LED: light-emitting diode, PD: photo detector, LPF: low-pass anti-aliasing filter, CP: cyclic prefix

Following this, the output  $u(k)$  of the  $N$ -point IFFT is always real-valued, which is as follows,

$$U_k(t) = \frac{1}{\sqrt{2N}} \sum_{n=0}^{N-1} \{c_n \exp(j2\pi n \frac{k}{2N})\} \quad (2.9)$$

$$\text{where } k = 0, 1, \dots, N - 1$$

After adding cyclic prefix of length  $N_{CP}$  with this real valued signal the  $(N + N_{CP})$  samples of the multicarrier DMT time-discrete sequence are finally transmitted. The length of cyclic prefix  $N_{CP}$  is chosen so that it is longer or equal to the channel impulse response. On the other hand in the receiver, inverse actions of transmission processes are performed on the received DMT signal in order to recover the original information bits.

## REFERENCES

- [1]. Cedric F. Lam, "Passive Optical Networks Principles and Practice", Ch. 1, pp. 1-17, 2007
- [2]. James F. Mollenauer, "Functional Requirements for Broadband Wireless Access Network", IEEE 802 Broadband Wireless, Access Study Group, March 5, 1999.
- [3]. I. Djordjevic, W. Ryan, B. Vasic, "Coding for Optical Channels", Springer Science & Business Media, Apr 5, 2010 - Technology & Engineering - 460 page.
- [4]. R. Bavey, J. Kani, F. Bourgart, K. Mc Cammon, "Options for future optical access networks," IEEE Commun. Mag., vol.44, no.10, pp.50-56, Oct. 2006.
- [5]. C. Bock, J. Prat, S. D. Walker, "Hybrid WDM/TDM PON using the AWG FSR and featuring centralized light generation and dynamic bandwidth allocation," J. Lightw. Technol., vol. 23, no. 12, pp. 3981-3988, Dec. 2005
- [6]. C. Lin, "Broadband Optical Access Networks and Fiber-to-the-Home, Systems Technologies and Deployment Strategies," John Wiley and Sons, Ltd., 2006.
- [7]. F.J. Effenberg, H. Ichibangase, and H. Yamashita. "Advances in broadband passive optical networking technologies," IEEE Communications Magazine, 39(12):118-124, Dec 2001
- [8]. G. Kramer and G. Pesavento. "Ethernet passive optical network (EPON): building a next-generation optical access network," IEEE Communications Magazine, 40(2):66-73, Feb 2002.
- [9]. J.D. Angelopoulos, H.C. Leligou, T. Argyriou, S. Zontos, E. Ringoot, and T. Van Caenegem. "Efficient transport of packets with QoS in an FSN-aligned GPON," IEEE Communications Magazine, 42(2):92-98, Feb 2004.
- [10]. J. Kani and N. Yoshimoto. "Next generation PONs: an operator's view," 35th European Conference on Optical Communication (ECOC), 2009.
- [11]. N.J. Frigo, P.P. Iannone, P.D. Magill, T.E. Darcie, M.M. Downs, B.N. Desai, U. Koren, T.L. Koch, C. Dragone, H.M. Presby, and G.E. Bodeep. "A wavelength-division multiplexed passive optical network with cost-shared components", IEEE Photonics Technology Letters, 6(11):1365-1367, Nov 1994.
- [12]. R. Sananes, C. Bock, J. Prat, "Techno-Economic Comparison of Optical Access Networks", Proc. ICTON'05, Th.A1.8, Barcelona (Spain), July 2005

- [13]. K.Iwatsuki, J.Kani, H. Suyuki, M. Fujiwara, "Access and Metro Networks Based on WDM technologies", *IEEE J. Lightwave Technol.*, vol.22, no.11, pp.2623-2630, November 2004
- [14]. ITU-T Recommendation: "G.694.2. Spectral Grids for WDM Applications: CWDM wavelength grid," March 2002.
- [15]. H. Toda, T. Yamashita, K. Kitayama, and T. Kuri. "DWDM demultiplexing with 25-Ghz channel spacing for 60-Ghz band radio-On-fiber systems," In 28th European Conference on Optical Communication (ECOC), volume 3, pages 1-2, Sep 2002.
- [16]. G. Jeong, J. H. Lee, M. Y. Park, C. Y. Kim, S.-H. Cho, W. Lee, and B. W. Kim, "Over 26-nm wavelength tunable external cavity laser based on polymer waveguide platforms for WDM access networks," *IEEE Photon. Technol. Lett.* , vol. 18, no. 20, pp. 2102–2104, Oct. 2006.
- [17]. H.Suzuki, M.Fujiwara, T.Suzuki,N. Yoshimoto,H. Kimura, and M.Tsubokawa, "Wavelength-tunable DWDM-SFP transceiver with a signal monitoring interface and its application to coexistence-type colorless WDM-PON," in *Proc. Eur. Conf. Opt. Commun.*,Sep.2007, paper PD3.4.
- [18]. C. Chang-Hasnain, "Optically-injection locked tunable multimode VCSEL for WDM passive optical networks," in *Proc. Int. Nano-Opto-electron. Workshop (i-NOW)* , 2008, pp. 98–99.
- [19]. Y.-L. Hsueh, M. S. Rogge, S. Yamamoto, and L. G. Kazovsky, "A highly flexible and efficient passive optical network employing dynamic wavelength allocation," *J. Lightw. Technol.*, vol.23, no.1, pp. 277–286, Jan. 2005.
- [20]. J.-I. Kani, "Enabling technologies for future scalable and flexible WDM-PON and WDM/TDM-PON systems," *IEEE J. Sel. Topics Quantum Electron.*, vol. 16, no. 5, pp. 1290–1297, Sep.–Oct. 2010
- [21]. N. Deng, C. K. Chan, L. K. Chen, and F. Tong, "Data re-modulation on downstream OFSK signal for upstream transmission in WDM passive optical network," *Electron. Lett.* , vol. 39, pp. 1741–1743, 2003.
- [22]. L. Xu and H. K. Tsang, "Colorless WDM-PON optical network unit (ONU) based on integrated nonreciprocal optical phase modulator and optical loop mirror," *IEEE Photon. Technol. Lett.* , vol. 20, no. 10, pp. 863–865, May 2008.
- [23]. Y. Katagiri, K. Suzuki, and K. Aida, "Intensity stabilisation of spectrum-sliced Gaussian radiation based on amplitude squeezing using semiconductor optical amplifiers with gain saturation," *Electron. Lett.* ,vol. 35, no. 16, pp. 1362–1364, 1999.

- [24]. I. Garces et al., "Analysis of narrow-FSK downstream modulation in colorless WDM PONs," *Electron. Lett.*, vol. 43, pp. 471–472, 2007.
- [25]. M. Attygalle, N. Nadarajah, and A. Nirmalathas, "Wavelength reused upstream transmission scheme for WDM passive optical networks," *Electron. Lett.*, vol. 41, no. 18, pp. 1025–1027, 2005.
- [26]. S. Y. Kim, S. B. Jun, Y. Takushima, E. S. Son, and Y. C. Chung, "Enhanced performance of RSOA based WDM PON by using Manchester coding," *J. Opt. Netw.*, vol. 6, pp. 624–430, 2007.
- [27]. Z. Al-Qazwini and H. Kim, "Line coding for downlink DML modulation in lambda-shared, RSOA-based asymmetric bidirectional WDM PONs," in *Proc. Opt. Fiber Comm. Conf. Nat. Fiber Optic Eng. Conf.*, Mar. 2011, paper OMP5.
- [28]. H. D. Kim, S.-G. Kang, and C.-H. Lee, "A low-cost WDM source with an ASE injected Fabry–Perot semiconductor laser," *IEEE Photon. Technol. Lett.*, vol. 12, no. 8, pp. 1067–1069, Aug. 2000.
- [29]. D.J. Shin, D.K. Jung, J.K. Lee, J.H. Lee, Y.H. Choi, Y. C. Bang, H.S. Shin, J. Lee, S.T. Hwang, and Y.J. Oh, "155 Mbit/s transmission using ASE-injection Fabry–Perot laser diode in WDM-PON over 70 C temperature range," *Electron. Lett.*, vol. 39, pp. 1331–1332, 2003.
- [30]. D.J. Shin, Y.C. Keh, J.W. Kwon, E.H. Lee, J.K. Lee, M.K. Park, J.W. Park, K.Y. Oh, S.W. Kim, I.K. Yun, H.C. Shin, D. Heo, J. S. Lee, H.S. Shin, H.S. Kim, S.B. Park, D.K. Jung, S. Hwang, Y. J. Oh, D. H. Jang, and C. S. Shim, "Low-cost WDM-PON with colorless bidirectional transceivers," *J. Light wave Technol.*, vol. 24, no. 1, pp. 158–165, Jan. 2006.
- [31]. M. D. Feuer, J. M. Wiesenfeld, J. S. Perino, C. A. Burrus, G. Raybon, S. C. Shunk, and N. K. Dutta, "Single-port laser-amplifier modulators for local access," *IEEE Photon. Technol. Lett.*, vol.8, no.9, pp.1175–1177, Sep. 1996.
- [32]. P. Healey, P. Townsend, C. Ford, L. Johnston, P. Townley, I. Lealman, L.Rivers, S.Perrin, and R.Moore,"Spectral slicing WDM-PON using wavelength-seeded reflective SOAs," *Electron. Lett.*, vol.37, pp. 1181–1182, 2001.
- [33]. F. Payoux, P. Chanclou, M. Moignard, and R. Brenot, "Gigabit optical access using WDM PON based on spectrum slicing and reflective SOA," in *Proc. Eur. Conf. Opt. Comm.*, Sep. 2005, vol. 3, pp. 455–456.
- [34]. P.Gysel, R.K. Staubli, "Statistical Properties of Rayleigh Backscattering in Single Mode Fibers", *IEEE J. Light wave Technol.*, vol.8, no.4, pp.561-567, April 1990

- [35]. C. Arellano, K. Langer, J.Pratt, "Reflections and multiple Rayleigh backscattering in WDM single fiber loopback access networks," *J. Lightwave Technol.* 27 (1)(2009)12–18.
- [36]. L.N. Binh and D. Wong, "DWDM Optically Amplified Transmission Systems-Simulink Models and Test-Bed: PART III –DPSK Modulation Format", Monash University, Department of Electrical and Computer Systems Engineering, Technical Report, 2005
- [37]. Sen Zhang, "Advanced Optical Modulation Formats in High-speed Lightwave System", Thesis (M.S.), Department of Electrical Engineering and Computer Science and the Faculty of the Graduate School of the University of Kansas, 2004
- [38]. A. Garcia Perez, J.A. Andrade Lucio, O.G. Ibarra Manzano, M. Trejo Duran, H.Gutierrez Martin, "Efficient Modulation Formats for High Bit-Rate Fiber Transmission", *Acta Universitaria*, mayoagosto, anovol. 16, numero 002, Universidad de Guanajuato, Mexico, pp. 17-26, 2006.
- [39]. Peter J. Winzer, Rene-Jean Essiambre, "Advanced Optical Modulation Formats", *Proceedings of the IEEE*, Vol. 94, No. 5, May 2006, 952-985.
- [40]. Yang Jing Wen, Jinyu Mo, and Yixin Wang, "Advanced Data Modulation Techniques for WDM Transmission", *IEEE Communications Magazine*, August 2006, 58-65
- [41]. C. Sramek, "DMT: Implementation", <http://cnx.org/content/m11721/1.3>

## CHAPTER III

### Simulation Environment

#### 3.1 Introduction

The transmission system design and analysis are carried out by optical system design simulation tool VPITransmissionMaker-9.1<sup>®</sup> [1]. The general schematic of propose simulation model is shown in Fig.3.1.

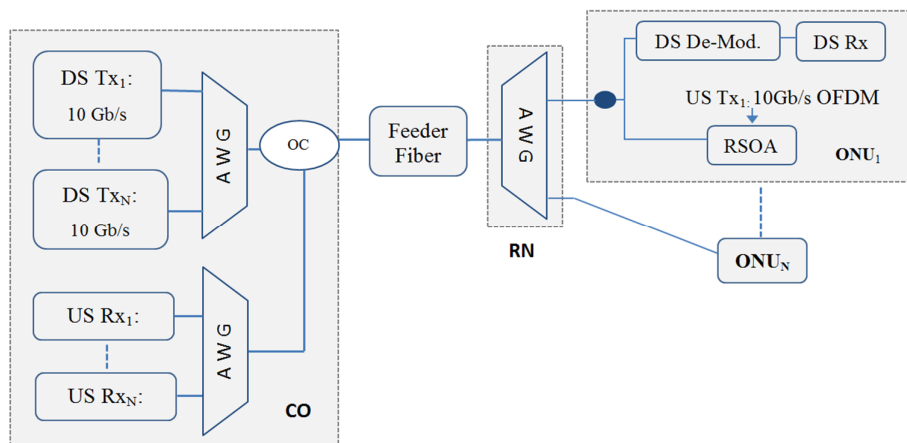


Figure 3.1: Schematic of wavelength reused WDM-PON

AWG: Array Waveguide Grating; RN: Remote Node; CO: Central Office; OC: Optical Circulator; ONU: Optical Network Unit; DS: Downstream; US: Upstream

The CO consists of 10 Gb/s modulated signal for each wavelength channel, which are multiplexed by AWG before propagating over the feeder fiber. In ONU, the DS signal splits by two portions; one portion is received by DS receiver, whereas the other portion further re-modulated with US data in US modulator such as RSOA or MZM. To operate the system with 10 Gb/s, spectrally efficient modulation format such as OFDM is utilized in RSOA modulation. The US modulated data finally received by the receiver placed in CO.

### 3.2 Transmitter

The CO acts as a transmitter which mainly consists of Pseudo Random Bit Sequence (PRBS) generator, CW laser, MZM etc. PRBS generates random bit sequence. A DFB laser produces a CW optical signal for modulation electrical data where MZM acts as an external modulator.

#### 3.2.1 Continuous Wave (CW) laser

This CW module models a DFB laser producing a CW optical signal. All the parameters are set to default values. The schematic symbol of CW laser in VPI is given in Figure 3.2 (a) and the default parameter of CW laser is shown in Figure 3.2 (b).

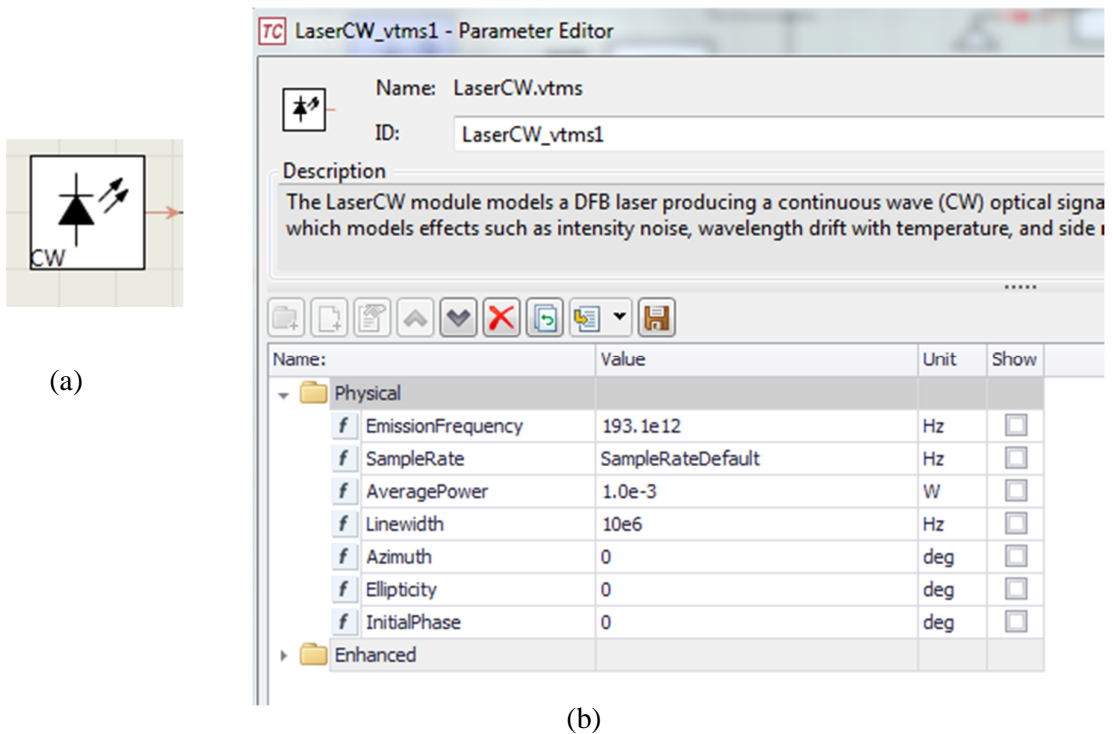


Figure 3.2 (a) CW laser (b) CW laser parameters

#### 3.2.2 Mach-Zehnder Modulator (MZM)

The direct modulation of a laser is cheap and also easy to adapt to low cost applications for moderated distances or transmission rates. However, for advanced applications involving high data rates or long distance links, resorting to external modulation is a good solution.

The most typical external modulator is the Mach-Zehnder modulator (MZM), which modulates the light generated in a laser operating in continuous wave mode. A typical MZM modulator is shown in Figure 3.3 (a).

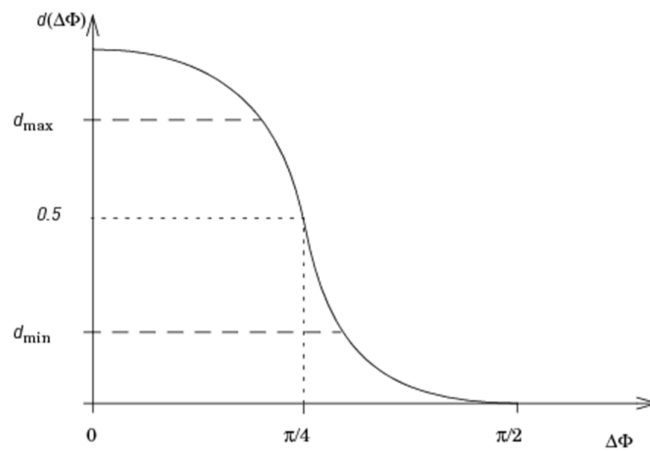
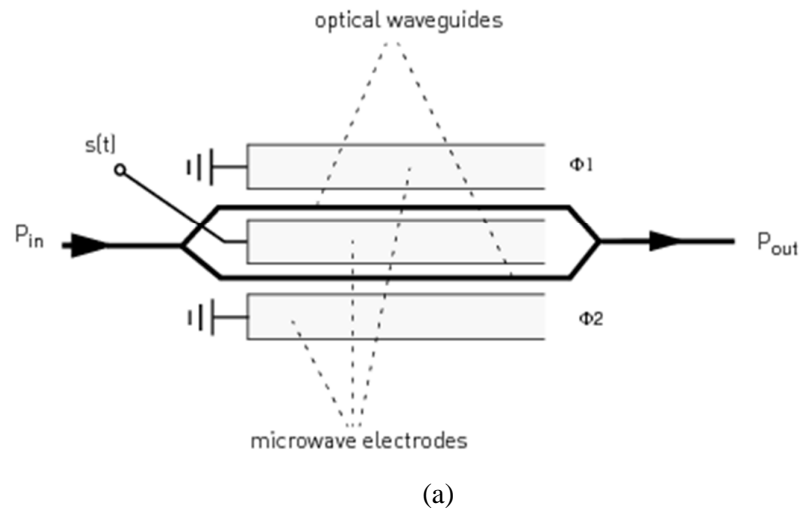


Figure 3.3 (a) Schematic of MZM (b) MZM power transfer function showing a degraded extinction ratio

The MZM is an intensity modulator based on an interferometric principle. It consists of two 3 dB couplers which are connected by two waveguides of equal length. By means of an electro-optic effect, an externally applied voltage can be used to vary the refractive indices in the waveguide branches. The different paths can lead to constructive and destructive interference at the output, depending on the applied voltage. Then the output intensity can be modulated according to the voltage.

For intensity modulation applications the MZM should be biased at quadrature bias point while for linear field modulation application MZM should be biased at null bias point [1]. MZM can be biased at quadrature bias point. In this case, a bipolar electrical signal should be applied to its input. If MZM is biased at null bias point, where MZM acts as a linear field modulator, the applied electrical signal to its input should be a unipolar signal.

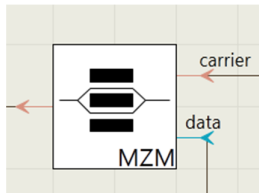
The optical power  $P_{out}$  at the output of MZM depends on the phase difference  $\Delta\Phi$  between the two modulator branches.

$$P_{out}(t) = P_{in}(t) \cdot d(t) = P_{in}(t) \cos^2[\Delta\phi(t)] \quad (3.1)$$

With

$$\Delta\phi(t) = \frac{\Delta\phi_1(t) - \Delta\phi_2(t)}{2}$$

Where  $d(t)$  is the power transfer function and  $\Delta\phi_1(t)$  and  $\Delta\phi_2(t)$  are the phase changes in each branch caused by the applied modulation signal data (t). The phase changes take place due to the electro-optical effect. Requiring a power ER of  $f_{extinc} = \frac{d_{max}}{d_{min}}$  (see Figure 3.3 (b)) and assuming a “quadrature” operating point. The schematic symbol of MZM in VPI is given in Figure 3.4 (a) and the default parameter of MZM is shown in Figure 3.4 (b).



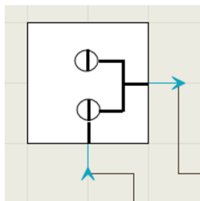
(a)

Name:	Value	Unit	Show
Physical			
f Extinction	30.0	dB	<input type="checkbox"/>
ChirpDefinition	SymmetryFactor		<input type="checkbox"/>
f SymmetryFactor	-1.0		<input type="checkbox"/>
ChirpSign	Positive		<input type="checkbox"/>
f AlphaFactor	0.0		<input type="checkbox"/>
Enhanced			

(b)

Figure 3.4 (a) MZM (b) MZM parameters

As DMT is a bipolar electrical signal so quadrature bias point is preferred for its modulation onto optical carrier. In order to obtain this bias point the following approximation are considered. The schematic symbol of laser driver in VPI is given in Figure 3.5 (a) and taken drive amplitude and bias voltage to drive OFDM signal are shown in Figure 3.5 (b).



(a)

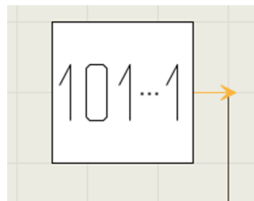
Name:	Value	Unit	Show
Physical			
f DriveAmplitude	0.1	A, V	<input type="checkbox"/>
f Bias	2.5	A, V	<input type="checkbox"/>

(b)

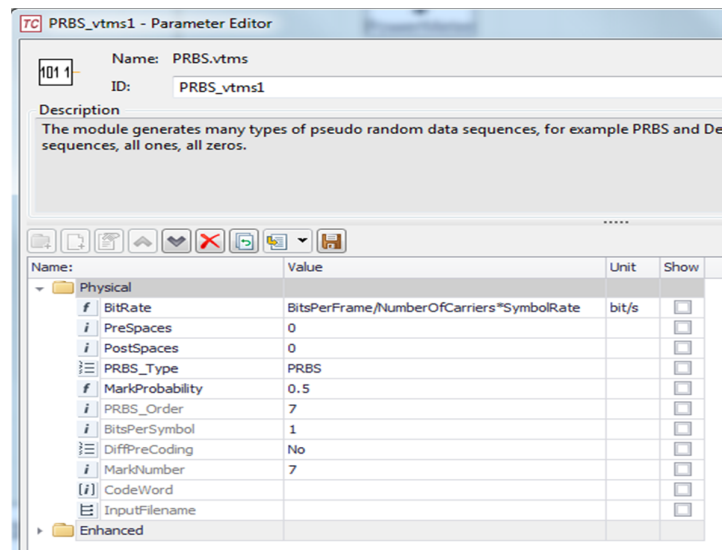
Figure 3.5 (a) Laser Driver (b) Laser Driver parameters for DMT

### 3.2.3 Pseudo Random Bit Sequence (PRBS)

The module generates many types of pseudo random data sequences, for example PRBS of order  $N$ , alternate ones and zeros, predefined sequences, all ones, all zeros. The PRBS is usually required when modeling the information source in simulations of digital communication systems. The schematic symbol of PRBS in VPI is given in Figure 3.6 (a) and the PRBS parameter for DMT, NRZ and DPSK signal generation are shown in Figures 3.6 (b), 3.7 (a) and 3.7 (b) respectively.

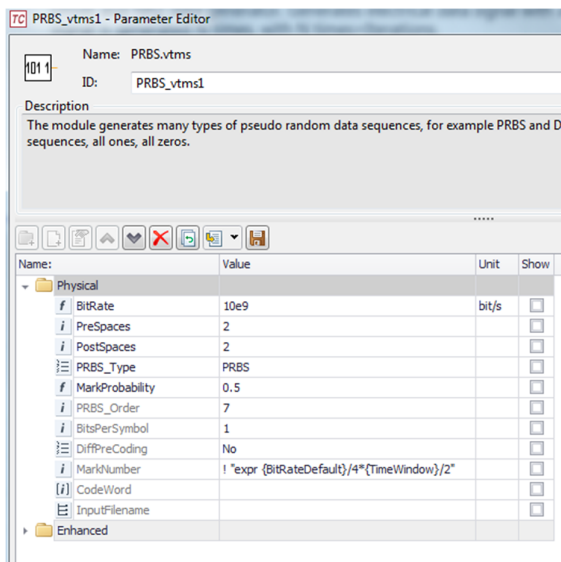


(a)

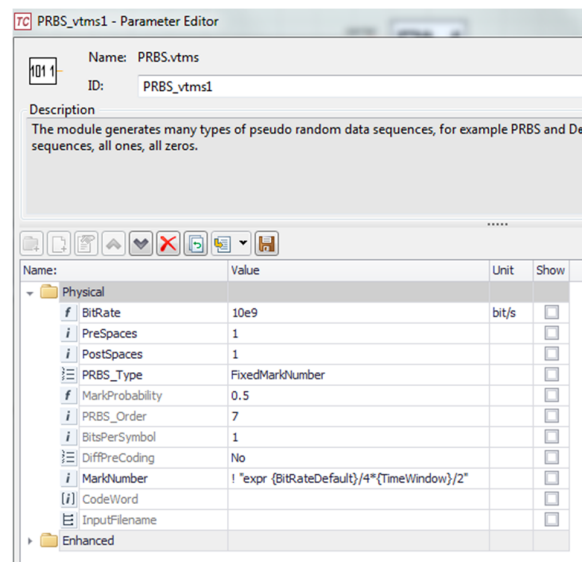


(b)

Figure 3.6 (a) PRBS (b) PRBS parameters for DMT



(a)



(b)

Figure 3.7 (a) PRBS parameters for NRZ (b) PRBS parameters for DPSK

### 3.3 Receiver

Receiver consists of photodiode, low pass filter, and bit error rate taster.

#### 3.3.1 Photo Detector (PIN)

Photo-detector is usually used to recover electrical signal from Optical carrier. This module is a model of PIN and Avalanche Photodiodes (APD). These can be simulated on base of predefined responsivity, avalanche multiplication, dark current and noise. The PIN receiver parameters for DPSK and DMT are illustrated in Figures 3.8 (a) and 3.8 (b) respectively.

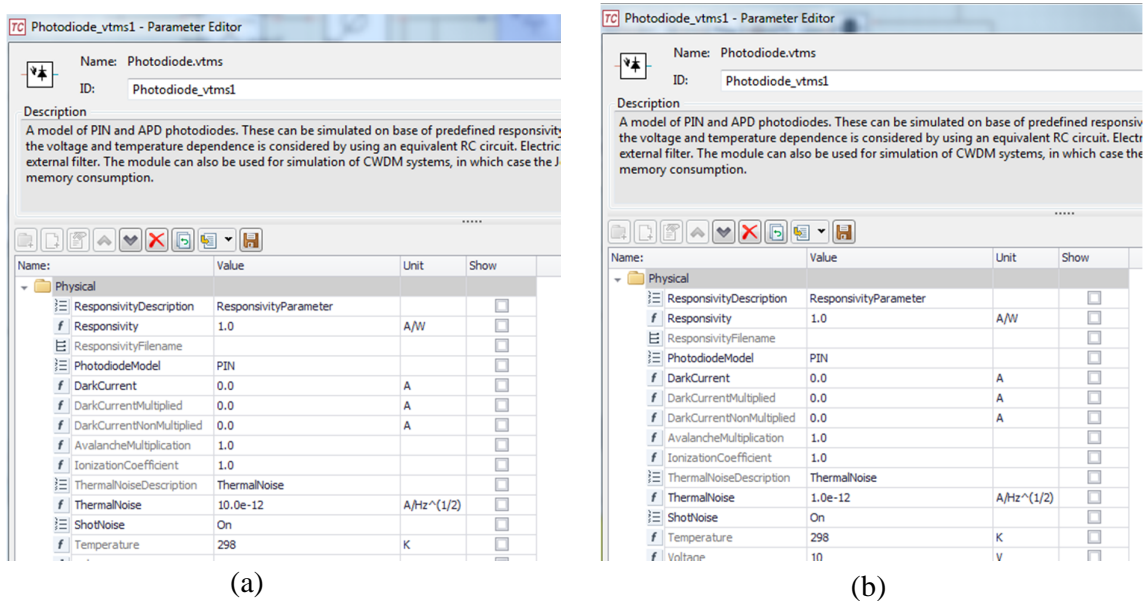
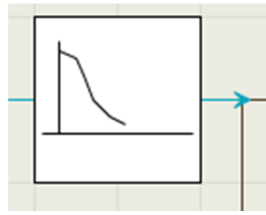


Figure 3.8 (a) PIN parameters for DPSK (b) PIN parameters for DMT

#### 3.3.2 Low Pass Filter (LPF)

The FilterEl module is a universal electric filter model for simulations of low pass, high pass, band pass, band stop and comb filters with the standard transfer functions: Butterworth, Bessel, Chebyshev, Elliptic, Gaussian, Rectangular, Trapezoid and Integrator. The schematic symbol of LPF in VPI is given in Figure 3.9 (a) and the LPF parameter for DPSK receiver is shown in Figures 3.9 (b).



(a)

TC FilterEl\_vtms1 - Parameter Editor

Name: FilterEl.vtms  
ID: FilterEl\_vtms1

Description  
The FilterEl module is a universal electric filter model for simulations of low pass, high pass, band pass, and band stop functions: Butterworth, Bessel, Chebyshev, Elliptic, Gaussian, Rectangular, Trapezoid and Integrator whose transfer function is supplied in an input file.

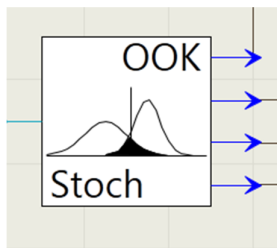
Name:	Value	Unit	Show
Physical			
FilterType	LowPass		<input type="checkbox"/>
A			<input type="checkbox"/>
B	1.0		<input type="checkbox"/>
TransferFunction	Bessel		<input type="checkbox"/>
Bandwidth	0.75* BitRateDefault	Hz	<input type="checkbox"/>
CenterFrequency	40e9	Hz	<input type="checkbox"/>
PassBandRipple	0.5	dB	<input type="checkbox"/>
FilterOrderDefinition	FilterOrder		<input type="checkbox"/>
FilterOrder	4		<input type="checkbox"/>
GaussianOrder	1		<input type="checkbox"/>
StopBandwidth	2*BitRateDefault	Hz	<input type="checkbox"/>
StopbandAttenuation	40	dB	<input type="checkbox"/>

(b)

Figure 3.9 (a) Electrical Filter (b) Filter parameters for DPSK

### 3.3.3 Bit Error Rate Tester (BERT)

This module estimates the error probability, or bit error ratio (BER) in digital direct detection optical transmission systems. The schematic symbol of BERT is shown in Figure 3.10 (a) and the BERT parameter for DPSK receiver is shown in Figures 3.10 (b).



(a)

TC BER\_OOK\_Stoch\_vtms1 - Parameter Editor

Name: BER\_OOK\_Stoch.vtms  
ID: BER\_OOK\_Stoch\_vtms1

Description  
This module estimates the error probability, or bit error ratio (BER) in digital direct detection optical transmission systems. The estimation and absolute decision threshold used to perform the calculations are also output. The estimation statistics for the optical beat noise. Post-detection thermal noise, shot noise, and intersymbol interference are included in this module.

Name:	Value	Unit	Show
Physical			
EstimationMethod	Gauss		<input type="checkbox"/>
ISI_Prebites	1		<input type="checkbox"/>
ISI_Postbites	1		<input type="checkbox"/>
SampleType	Optimum		<input type="checkbox"/>
SampleTime	0.5		<input type="checkbox"/>
SampleRange	0		<input type="checkbox"/>
ThresholdType	Optimum		<input type="checkbox"/>
Threshold	1.0e-3		<input type="checkbox"/>
DetectorType	PIN		<input type="checkbox"/>
DarkCurrent	0.0	A	<input type="checkbox"/>
DarkCurrentMult	0.0	A	<input type="checkbox"/>
DarkCurrentNonMult	0.0	A	<input type="checkbox"/>
AvalancheMult	1.0		<input type="checkbox"/>
IonizationCoefficient	1.0		<input type="checkbox"/>
IncludeShotNoise	Yes		<input type="checkbox"/>
ThermalNoise	10.0e-12*0	A/Hz^(1/2)	<input type="checkbox"/>
ElectNoiseBandwidth	10.0e9	Hz	<input type="checkbox"/>
Enhanced			

(b)

Figure 3.10 (a) BERT (b) BERT parameters for DPSK

### 3.4 Channel

In our system design, we used optical fiber as a channel to propagate signal. It can be either SMF or bidirectional fiber.

#### 3.4.1 Single Mode Fiber (SMF)

The optical fiber component simulates the propagation of an optical field in a SMF with the dispersive and nonlinear effects taken into account. The schematic symbol of SMF is shown in Figure 3.11 (a) and the SMF parameter is shown in Figure 3.11 (b).



(a)

FiberNLS\_vtms1 - Parameter Editor

Name: FiberNLS.vtms  
ID: FiberNLS\_vtms1

Description  
When used with sampled-mode signals, this module solves the nonlinear Schroedinger (NLS) e optical waves in fibers using the split-step Fourier method. Depending on the signal represent a Single Frequency Band (SFB), or JoinSampledBands = ON, the model takes into account stim self-phase modulation (SPM), cross-phase modulation (XPM), first order group-velocity dispers fiber. If the signals are in a Multiple Frequency Band (MFB), the above effects are calculated with the use of the split-step Fourier method. The model also includes interactions between MCDs and between MCDs and Raman effects.

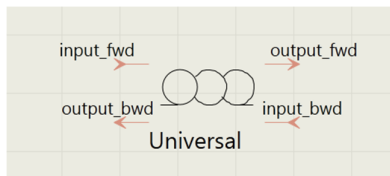
Name	Value	Unit	Show
Physical			
f ReferenceFrequency	193.1e12	Hz	<input type="checkbox"/>
f Length	25e3	m	<input type="checkbox"/>
f GroupRefractiveIndex	1.47		<input type="checkbox"/>
f Attenuation	0.2e-3	dB/m	<input type="checkbox"/>
AttFileName			<input type="checkbox"/>
f Dispersion	16e-6	s/m <sup>2</sup>	<input type="checkbox"/>
f DispersionSlope	0.08e3	s/m <sup>3</sup>	<input type="checkbox"/>
f NonLinearIndex	0 #2.6e-20	m <sup>2</sup> /W	<input type="checkbox"/>
f CoreArea	80.0e-12	m <sup>2</sup>	<input type="checkbox"/>
f Tau1	12.2e-15	s	<input type="checkbox"/>
f Tau2	32.0e-15	s	<input type="checkbox"/>
f RamanCoefficient	0.0		<input type="checkbox"/>
Numerical			
Enhanced			

(b)

Figure 3.11 (a) SMF (b) SMF parameters

#### 3.4.2 Bidirectional Fiber

The most effective way is to use a single fiber for bidirectional transmission. The schematic symbol of bidirectional fiber in VPI is shown in Figure 3.12 (a) and the parameter is shown in Figure 3.12 (b).



(a)

UniversalFiber\_vtms1 - Parameter Editor

Name: UniversalFiber.vtms  
ID: UniversalFiber\_vtms1

Description  
The Universal Fiber model simulates a wideband nonlinear signal transmission in optical fiber span individually, taking into account bidirectional signal flow, stimulated and spontaneous Kerr nonlinearity, dispersion, PMD effects, local insertion loss and reflectance at each joint pumped Raman amplifiers, which often form part of the transmission fiber itself. Fiber cha module as industry-standard data files.

Name	Value	Unit	Show
Physical			
i NumberOfFiberSpans	1		<input type="checkbox"/>
f Length	20.0e3	m	<input type="checkbox"/>
f GroupRefractiveIndex	1.47		<input type="checkbox"/>
AttenuationDescription	AttenuationParameter		<input type="checkbox"/>
f Attenuation	0.2e-3	dB/m	<input type="checkbox"/>
AttFilename			<input type="checkbox"/>
f ReferenceFrequency	193.1e12	Hz	<input type="checkbox"/>
DispersionDescription	DispersionParameters		<input type="checkbox"/>
f Dispersion	16e-6	s/m <sup>2</sup>	<input type="checkbox"/>
f DispersionSlope	0.08e3	s/m <sup>3</sup>	<input type="checkbox"/>
DispersionFilename			<input type="checkbox"/>
f PMDCoefficient	0.1e-12/31.62	s/sqrt(m)	<input type="checkbox"/>
f CorrelationLength	50.0	m	<input type="checkbox"/>
Nonlinear Effects			
RayleighScattering	Yes		<input type="checkbox"/>
Rayleigh Scattering Para...			
Event Loss and Reflecta...			
UseOTDRdata	No		<input type="checkbox"/>
OTDR File			

(b)

Figure 3.12 (a) Bidirectional fiber (b) Bidirectional fiber parameters

### 3.5 Downstream Modulation

In DS 10 Gb/s DPSK is experimented. The following schematic shown in Figure 3.13 generates DPSK modulated signal. DPSK encodes the information on the binary phase change between adjacent bits: a “1” bit is encoded onto a  $\pi$  phase change, whereas a “0” bit is represented by no phase change. Thus, the optical signal intensity is maintained constant.

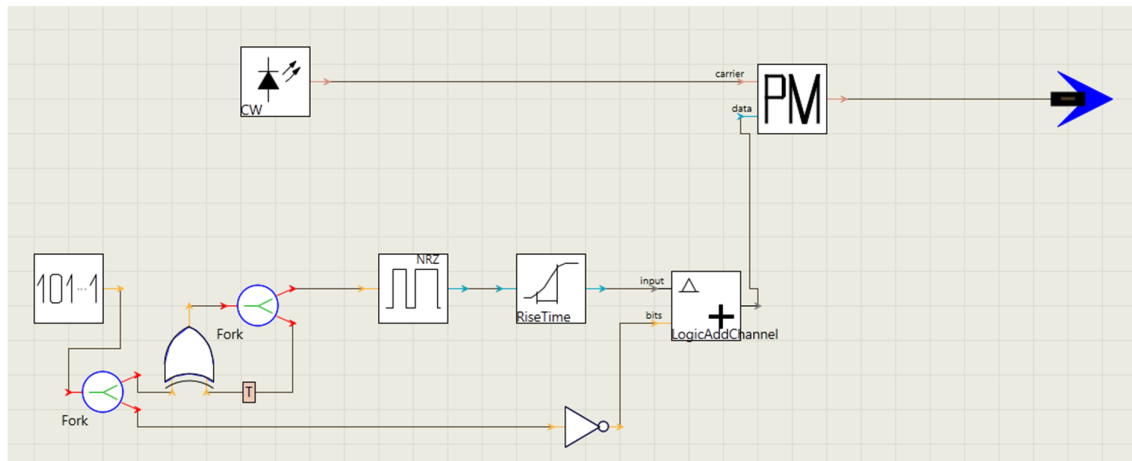


Figure 3.13 DPSK modulated signal generation

### 3.6 Upstream Modulation

In US, a real valued baseband OFDM is generated with the signal processing of serial-to-parallel conversion, QAM symbol encoding, mirroring, inverse Fast Fourier transform (IFFT), cyclic prefix insertion and finally parallel-to-serial (P2S) transmission. Each OFDM symbol consists of 64 subcarriers of which 31 subcarriers carry real data, and one (1) carrier has no power. The remaining 32 subcarriers are the complex conjugate of the aforementioned 32 subcarriers. Figure 3.14 is the schematic that generates DMT signal using MZM.

In upstream RSOA is used due to its colorless property and high optical gain. Typically the bandwidth of RSOA is ( $\sim 1$ GHz). OFDM signal is used to overcome the limited bandwidth response of RSOA to reach 10 Gbps. Besides, OFDM has high spectral efficiency and inherent tolerance against chromatic dispersion. Figure 3.15 shows the DMT modulated signal generation using RSOA.

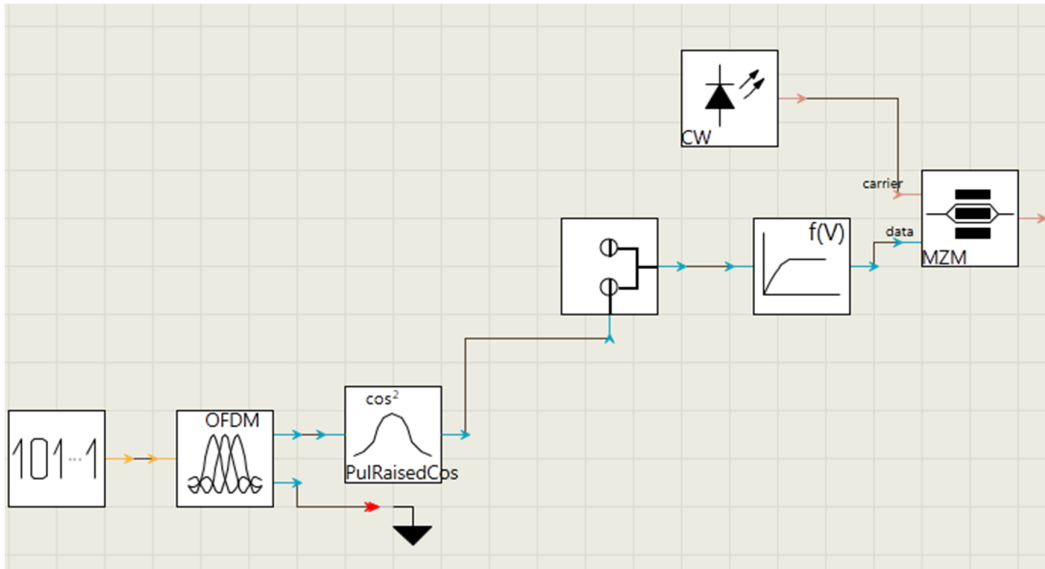


Figure 3.14 DMT modulated signal generation using MZM

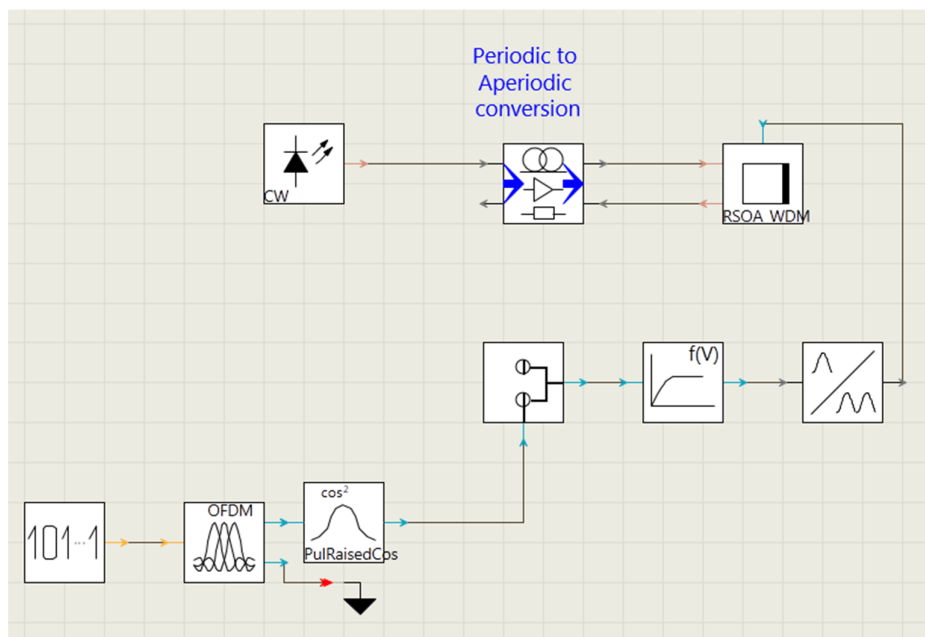


Figure 3.15 DMT modulated signal generation using RSOA

### 3.7 Summary

This chapter mainly describes the simulation environment that carried out in VPITransmissionMaker-9.1<sup>®</sup> i.e. a powerful simulation tool for optical system design. System setup schematics are illustrated with necessary parameters. Different modules for transmitter, channel and receiver for signal generation and reception are explained with parameters.

## REFERENCES

- [1]. VPITrans-missionMaker9.1<sup>®</sup> (<http://www.vpiphotonics.com> )
- [2]. A. Mirbadin, AB. Mohammad, "Performance analysis of DCO OFDM and DCO WOFDM systems in MMF optical links," Communications, Computers and Signal Processing (PacRim), 2011 IEEE Pacific Rim Conference on , vol., no., pp.388,393, 23-26 Aug. 2011.

## CHAPTER IV

### 10 Gb/s Symmetrical Wavelength Reused Bidirectional WDM-PON

#### 4.1 Introduction

Bidirectional systems are of great interest, particularly in optical links where physical constraints or cost can prevent installing system equipment. Transparent and flexible architecture based on WDM technology is necessary thus colorless ONU needs to be available. High gain should be provided by the transmitter to reach the necessary optical budget and high modulation speed is needed. Bidirectional single wavelength transmission can either be single fiber or dual fiber network. BSFSW transmission performance is mainly limited by RB reflections. One way to overcome this problem is to use dual fiber transmission. Bidirectional Dual Fiber Single Wavelength (BDFSW) does not suffer from RB reflections because it uses separate fiber for DS and US transmission. On the other hand, remodulation noise degrades the system performance. Remodulation noise can be bypassed by using different modulation formats in DS and US transmission which must be orthogonal. However, BSFSW transmission performance is restricted by both RB reflections and remodulation noise. This chapter studies on both BDFSW and BSFSW transmission system in order to separately analyze these two major impairments.

#### 4.2 Two-Fiber Network: High Tolerance against Re-modulation Noise

A 10 Gb/s symmetrical wavelength reuse WDM-PON is proposed with RSOA in ONU side. Beside 'colorless' intensity modulator, RSOA has the properties of optical gain, wide optical bandwidth and integration capability. A 10 Gb/s DPSK modulated signal is used in DS that act as a seeding wavelength for US transmission. Thanks for the constant amplitude property of DPSK signal that is considered to be the most desirable DS seeding signal in wavelength reused WDM-PON to improve the resilience against remodulation noise [1, 2]. For 10 Gb/s wavelength reuse US transmission, OFDM signal is used to overcome the limited bandwidth response of RSOA. Recently, OFDM signaling technique has received much attention in fiber

optic transmission system for its high spectral efficiency and inherent tolerance against chromatic dispersion [3 –7]. The symmetric 10 Gb/s wavelength reuse access system with DPSK in DS and OFDM in US is analyzed over 25 km single mode fiber. The system performance is measured in terms of BER and error vector magnitude (EVM) for DPSK modulated and OFDM signals respectively. Error free operation as well as low value of EVM per subcarrier is simultaneously achieved in acceptable receiver sensitivity.

#### 4.2.1 Proposed Network

Figure 4.1 shows the proposed architecture for symmetric 10 Gb/s wavelength reuse WDM-PON. The CO consists of 10 Gb/s DPSK signal for each WDM wavelengths, which are multiplexed before transmission over the optical distribution network of SMF. At RN, DEMUX distributes the DS signal to each ONU. The DS DPSK modulated signal is split into two portions in each ONU. One portion is used for DS receiver with narrow band optical filter as a DPSK de-modulator that converts phase information to amplitude variation and finally, reaches to conventional direct detection photodiode. The other portion is used for generating the US modulated signal, where DPSK modulated DS optical signal is used as a seed wavelength for RSOA re-modulation. Note that DPSK encodes the information on the binary phase change between adjacent bits: a “1” bit is encoded onto a  $\pi$  phase change, whereas a “0” bit is represented by no phase change. Thus, the optical signal intensity is maintained constant, which is useful as a re-modulation wavelength in ONU side.

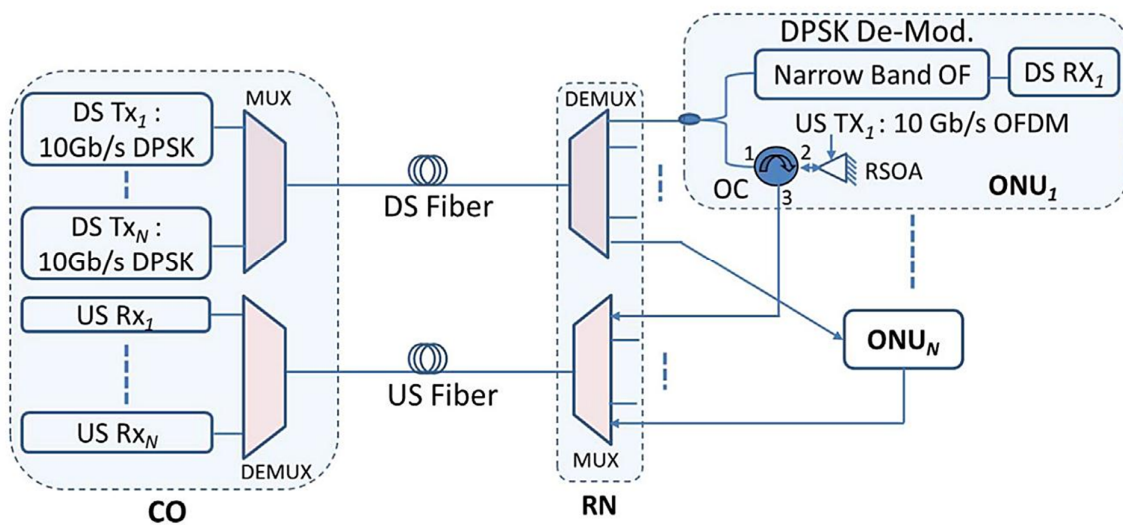


Figure 4.1: Proposed architecture for 10 Gb/s symmetric bidirectional wavelength reused WDM-PON.

As the RSOA poses a very limited bandwidth ( $\sim 1$  GHz), a spectrally efficient modulation format like OFDM is used to achieve 10 Gb/s US data transmission. The 10 Gb/s OFDM signals of each ONU are further multiplexed at RN and transmitted over the US feeder fiber to reach in the US receiver at CO for data recovery. The proposed bidirectional WDM-PON offers the following advantages: (1) due to the constant envelope property of DPSK seed signal, the re-modulation noise can be effectively minimized in US receiver. (2) Instead of using costly delay Mach-Zehnder interferometer (MZI), narrow band optical filter is used as a DPSK demodulator in each ONU [8], which eventually makes the DS receiver just a simple photodiode. (3) Narrow band optical filter also significantly improves the system tolerance against dispersion accumulated by high data rate transmission system [8] and thus, avoids the extra loss introduced by dispersion compensation fiber (DCF). (4) Moreover, OFDM signal with high order data format is used for limited bandwidth RSOA modulation to operate the device in 10 Gb/s, which effectively improves the spectral efficiency of the proposed system.

#### 4.2.2 Simulation setup

Figure 4.2 shows the simulation setup to evaluate the performance of proposed bi-directional 10 Gb/s wavelength reuse WDM-PON. The transmission system design and analysis are carried out by optical system design simulation tool VPITransmissionMaker-9.1<sup>®</sup>. At the CO, a DFB laser operating at 1550 nm is externally modulated by a phase modulator (PM) with a 10 Gb/s NRZ  $2^{31} - 1$  PRBS sequence to generate the DPSK signal. The DS signal is then transmitted to the ONU over the 25 km standard SMF (chromatic dispersion  $D=16$  ps/nm/km, 5 dB propagation loss). At the ONU, the DS DPSK signal is divided by a 50:50 optical coupler, where part of the signal is detected by a DPSK demodulator followed by direct detection optical receiver. As a DPSK demodulator, a narrow optical filter [Gaussian profile, full width half maximum (FWHM) is 60% of data rate] is used to convert phase information to intensity [1]. Note that identical fiber bragg grating (FBG) with required bandwidth can also be used in each ONU for WDM operation as a colorless module of phase to intensity converter. Finally, the DS signal is received by a direct detection optical receiver consists of variable optical attenuator (VOA), PIN photodiode and electrical low pass Bessel filter (bandwidth is 75% of data rate).

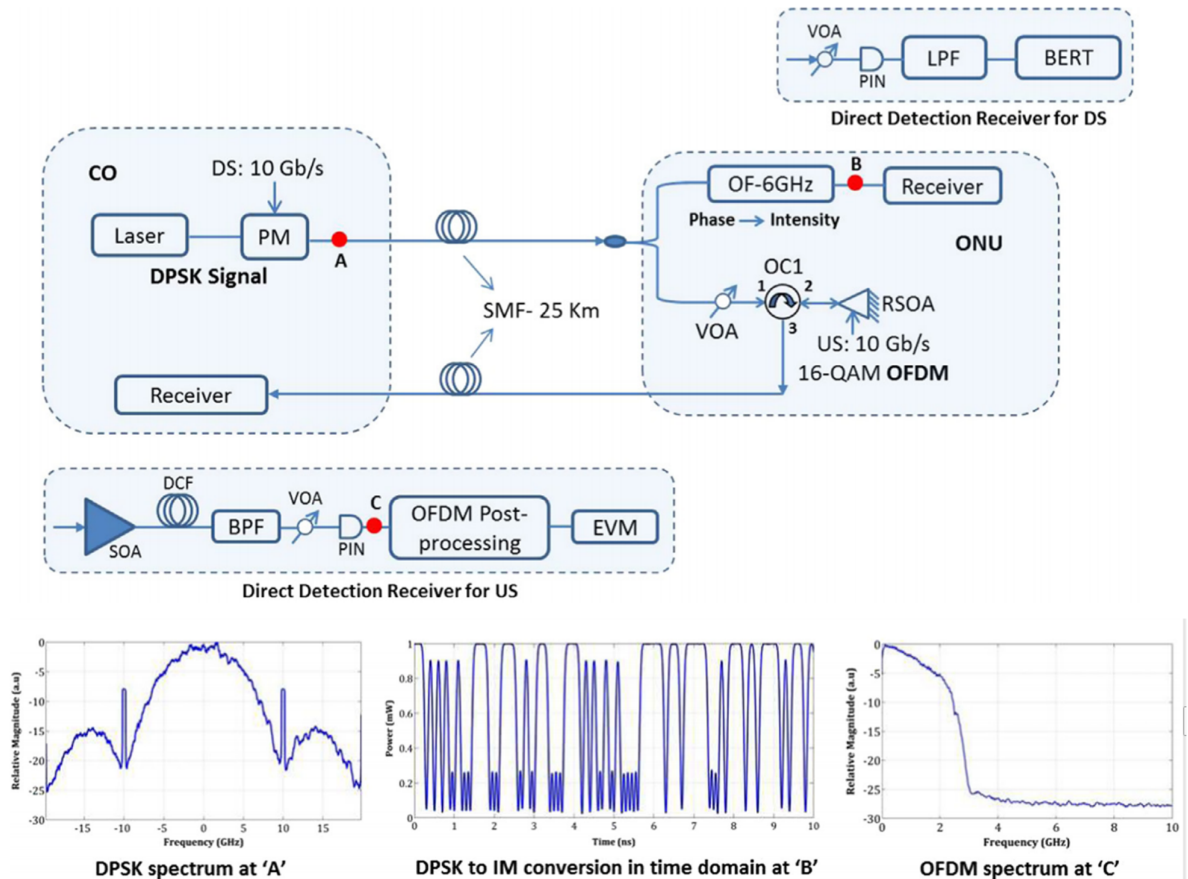


Figure 4.2: Simulation setup for 10 Gb/s DPSK signal in downstream and RSOA re-modulation with OFDM signal in upstream.

Another part of the DPSK modulated DS optical signal is seeded to RSOA for the re-modulation with 10 Gb/s OFDM signal. As the seeding power of RSOA has a significant effect on US signal to noise ratio (SNR) performance, a VOA is used to maintain an acceptable optical power at the input of RSOA. The optical circulator (OC) is used to separate the DS seeding signal and US modulated signal of RSOA. RSOA input saturation power and gain are approximately 15 dBm and 21 dB respectively. In addition, electrical/optical modulation bandwidth of RSOA is around 1 GHz. A real valued baseband OFDM is generated with the signal processing of serial-to-parallel conversion, QAM symbol encoding, mirroring, inverse Fast Fourier transform (IFFT), cyclic prefix insertion and finally parallel-to-serial (P2S) transmission.

Each OFDM symbol consists of 64 subcarriers of which 31 subcarriers carry real data, and one (1) carrier has no power. The remaining 32 subcarriers are the complex conjugate of the aforementioned 32 subcarriers to maintain Hermitian symmetry in the input of IFFT processing block. The IFFT and FFT size is 64 and the cyclic prefix (CP) length is 1/32. The total number of 1000 OFDM symbols are utilized in the simulation. The bandwidth of OFDM signal is set to 2.5 GHz, where the subcarriers are modulated with 16-QAM format and thus provides a data rate of 10 Gb/s. The modulated OFDM signal is transmitted over the US feeder fiber and pre-amplified by a semiconductor optical amplifier (SOA) with specification of 15 dB small signal gain and 12 dBm output saturation power. A dispersion compensation fiber (DCF) (compensating 400 ps/nm) is used to overcome the effect of chromatic dispersion in US performance. An optical bandpass filter (OTF, Gaussian shape, 25 GHz bandwidth) that tuned to center frequency of laser is useful to avoid the out of band amplified spontaneous emission (ASE) noise as generated by SOA. Finally, the US OFDM is received by PIN photodiode for post signal processing and EVM measurement.

#### 4.2.3 Results and analysis

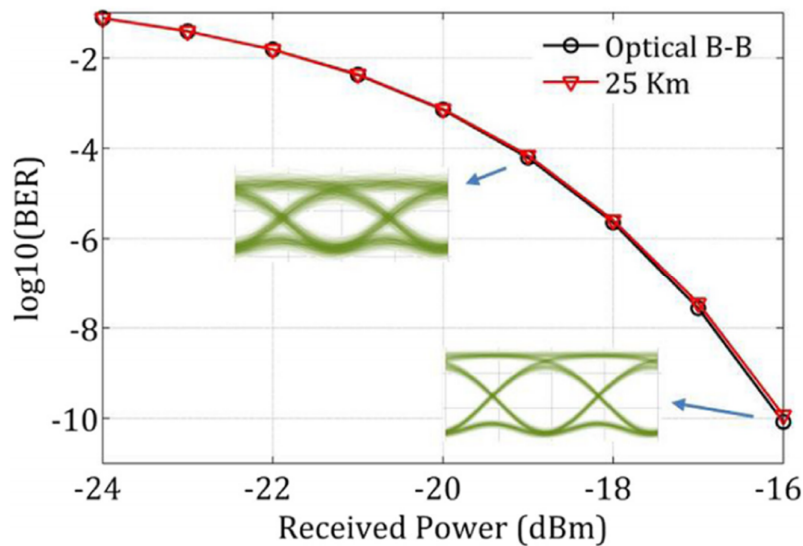


Figure 4.3: BER performance of 10 Gb/s downstream DPSK modulated signal for both back to back and over 25 km fiber transmission.

Figure 4.2 also shows the measured signals at different positions of the proposed system. The DPSK modulated optical spectrum is illustrated in Figure 4.2. Moreover, Figure 4.2 shows

the effect of narrow band optical filter that successfully converts the phase information to amplitude variation making the DPSK de-modulator and DS receiver simple. The received OFDM signal is also shown in Figure 4.2 indicating the limited modulation response in high frequency region due to the low bandwidth of RSOA. The performance of DPSK modulated signal in DS is measured through BER against photodiode received power as shown in Figure 4.3. Figure 4.3 represents the negligible power penalty in DPSK transmitted signal over 25 km fiber in compared to back-to-back transmission. The received signal shows a clear eye opening as also illustrated in Figure 4.3. The aforementioned performance confirms that the fiber chromatic dispersion does not have significant impact on DPSK modulated signal, especially for this short transmission distance. As the modulation characteristic of RSOA is significantly affected by its seeding power, the Figure 4.4 illustrates the OFDM subcarrier SNR performance for different RSOA input power. The SNR is calculated for each subcarrier from the EVM) of received and transmitted constellations with 16-QAM modulation by using the following formula [9]:

$$EVM_{RMS} = \sqrt{\frac{\sum_{i=1}^{S_T} [\sum_{j=1}^{S_C} |\tilde{x}_{ij} - \bar{x}_{ij}|^2]}{S_T S_C P_{Avg}}} = \sqrt{\frac{1}{SNR}} \quad (4.1)$$

where  $\bar{x}_{ij}$  is the normalized ideal constellation symbol in the complex plain corresponding to the estimated symbol  $\tilde{x}_{ij}$ ,  $|\tilde{x}_{ij} - \bar{x}_{ij}|$  denotes the magnitude of the error vector,  $S_C$  denotes the total number of data-carrying subcarriers in each OFDM symbol,  $S_T$  denotes total number of OFDM Symbols, and  $P_{Avg}$  is the average power of the constellation which is 1 (one) since normalization is applied. Due to the limited bandwidth response of RSOA, the high frequency subcarriers show low SNR performance compare to low frequency subcarriers as shown in Figure 4.4. However, the overall SNR performance can be improved with high seeding power at RSOA input. In particular, over 15 dB subcarrier SNR can be maintained with RSOA input power of  $-10$  dBm. Note that minimum 15 dB SNR is required for OFDM subcarriers to reach target BER of FEC Limit  $3.8 \times 10^{-3}$  [3]. Moreover, Figure 4.4 shows the comparison result of experimental [10, 11] and simulated SNR, indicating an excellent agreement across the entire OFDM subcarrier region. Based on the above SNR performance, RSOA input power is fixed to  $-6$  dBm for maintaining the BER in FEC limit for rest of the US performance measurement.

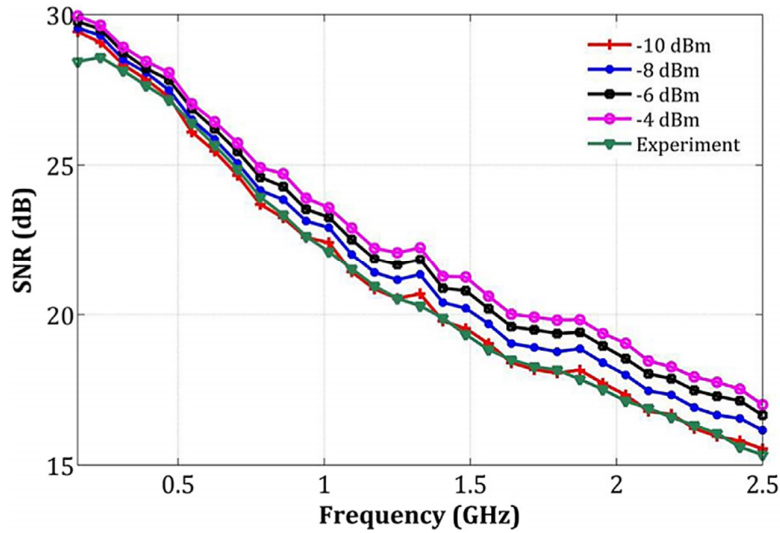


Figure 4.4: Signal to Noise Ratio (SNR) for each OFDM subcarrier under different seeding power at the input of RSOA.

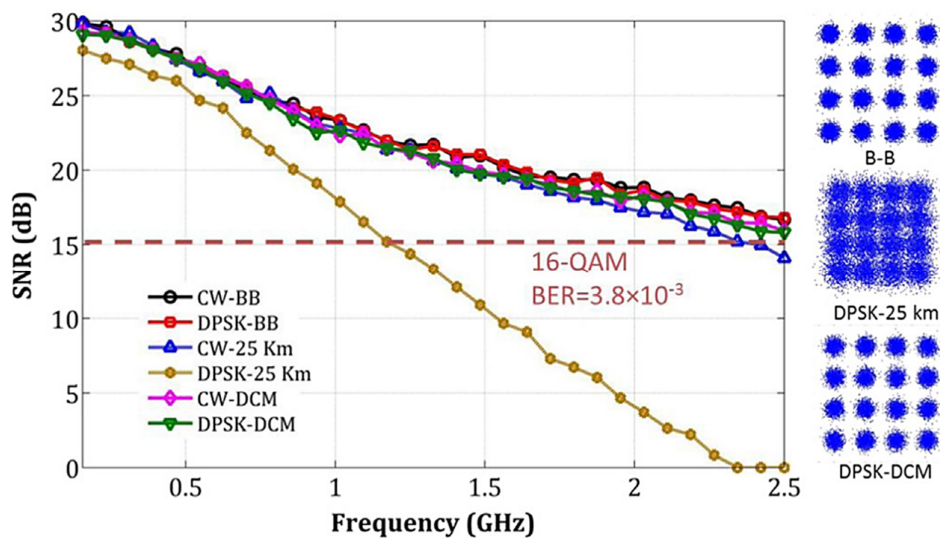


Figure 4.5: Measured SNR for each OFDM subcarrier in the case of back-to-back (BB) and with/without dispersion compensated 25 km fiber transmission at the RSOA input power of 6dBm and US received power of 12dBm.

Figure 4.5 shows the subcarrier SNR performance for 10 Gb/s OFDM modulated signal at US receiver with fixed photodiode input power of  $-12$  dBm. The US performance is measured for different cases; Firstly, with and without feeder fiber in US link called as 25 km transmission and back-to-back (BB) respectively, Secondly, with the presence of dispersion compensation module (DCM) (SOA+DCF). Each of the cases is further analyzed for both CW and DPSK modulated DS signal as a seeding source for US remodulation. Figure 4.5

shows that the received OFDM subcarrier SNRs in BB transmission are very similar for both CW and DPSK seed signal. With 25 km fiber propagation, the CW seed OFDM modulated signal shows around 1.3 dB SNR degradation in high frequency region mainly due to chromatic dispersion effect in US transmission. When the DPSK seed OFDM modulated signal is transmitted over 25 km fiber, the subcarrier SNRs are degraded significantly as can be seen from Figure 4.5. The reason is that the detected OFDM signal has still some residual phase modulation, which is strongly affected by the chromatic dispersion, accumulated over the double-pass path. This results into a distorted signal. To avoid this SNR degradation, a preamplifier and a DCF are inserted in CO at US receiver side. The system SNR can be improved close to the back to back transmission with this addition of DCF as also shown in Figure 4.5. Note that the loss introduced by the DCF is not so critical as it is placed in CO and also the system has additional power gain from both the RSOA and pre-amplifier in US data transmission. The inset of Figure 4.5 shows the constellation for 16-QAM data format for both BB and 25 km fiber transmission with/without DCF. The noise introduced by chromatic dispersion is clearly seen, which can be minimized by the compensated fiber link.

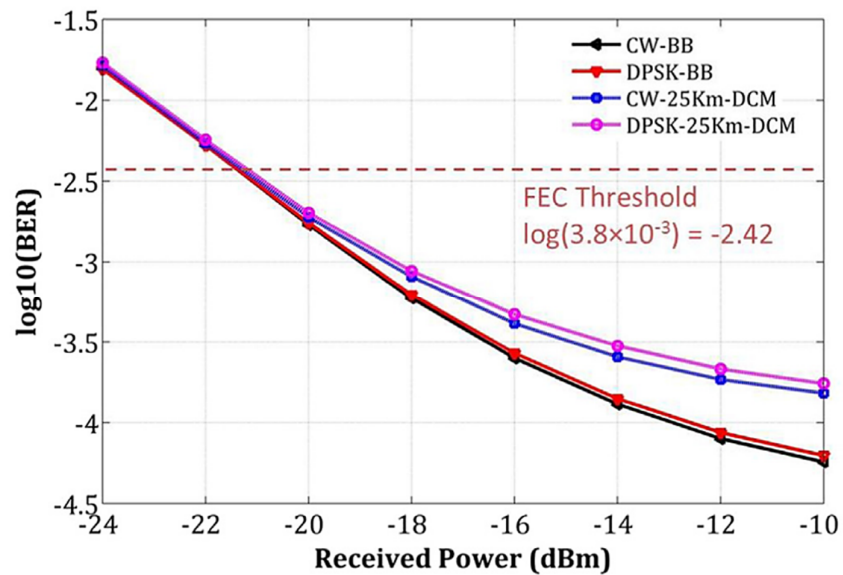


Figure 4.6: Measured BER for different US received power in the case of back-to-back (BB) and over 25 km dispersion compensated fiber transmission.

Finally, Figure 4.6 shows the BER for different US received power in both back-to-back (BB) and 25 km fiber transmission with dispersion compensation technique. The BER is calculated based on the subcarrier SNRs by using the following formula [9]:

$$BER = \frac{2\left(1-\frac{1}{L}\right)}{\log_2 L} Q \left( \sqrt{\left(\frac{3\log_2 L}{L^2-1}\right) \left(\frac{2SNR}{\log_2 M}\right)} \right) \quad (4.2)$$

Here,  $L$  is the number of levels in each dimension of the  $M$ -ary modulation system (i.e.,  $L$  is 4 for 16-QAM),  $M$  is the number of constellation points of the modulation format (i.e.,  $M$  is 16 for 16-QAM). The function is evaluated by  $0.5 \times \text{erfc}(x/\sqrt{2})$ , where  $\text{erfc}(\cdot)$  is the complementary error function. Figure 4.6 shows the negligible power penalty for US data transmission over dispersion compensated 25 km fiber compared to BB to maintain the BER better than FEC threshold ( $3.8 \times 10^{-3}$ ). In particular, 10 Gb/s OFDM signal with 16-QAM modulated data has the BER of  $3.8 \times 10^{-3}$  at the received power of  $-21.7$  dBm.

#### 4.3 Single Fiber Network: Rayleigh Backscattering (RB) Noise analysis

In BSFSW transmission system CW light transmits from CO, propagates over the fiber, modulated and reflected by ONU and finally sends back to the CO. However, as the DS CW signal and US modulated data share the same fiber, the system performance is inherently limited by RB noise. The RB noise is partially polarize in nature, with a colored power spectral density (PSD) proportional to the PSD of the generating input signal [12].

Therefore, the spectral shape of the noise shows a narrow line width with high amount of low frequency components when it is generated from CW seeding source. These frequency components are mainly responsible to generate a concentrated noise near DC (see Figure 4.7). Figure 4.7 clearly illustrates the source of RB generation. As CW light travels through the fiber, RB is generated which is mainly a back reflection due to the fiber material density imperfection. The PSD of RB is also identical with the CW source. This RB noise is different form ASE, which is typically assumed to be white noise. RB induced signal degradation can be mitigated by using proper network architecture and advanced modulation formats [13, 14]. Centralized carrier distribution with colorless reflective ONU (RONU) is attractive since wavelength seed is provide in CO. PON with OFDM is also attractive due to its high spectral efficiency of  $M$ -QAM where low bandwidth optical components can be used.

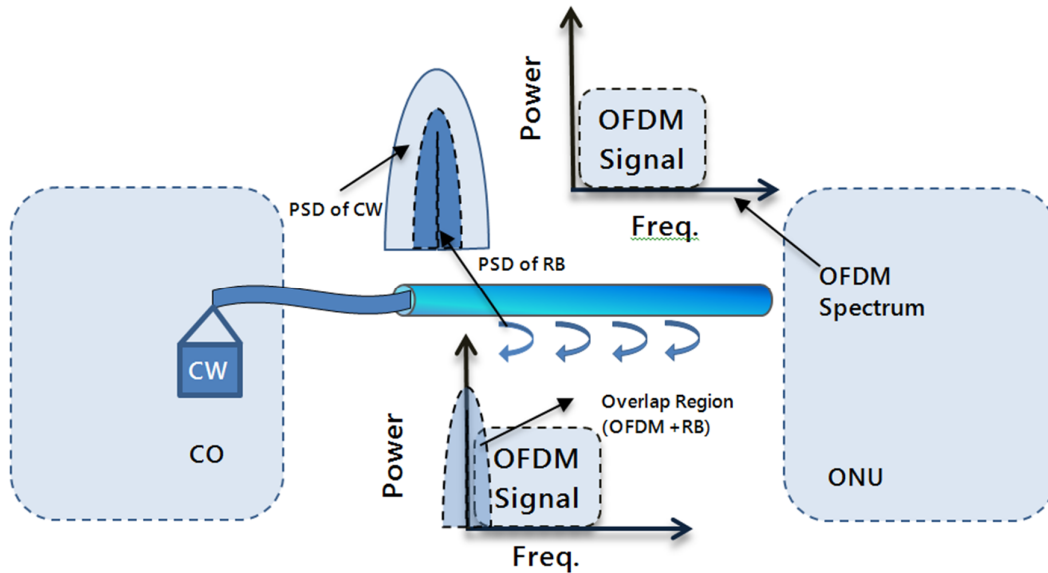


Fig. 4.7: Schematic of RF spectra indicating RB of OFDM signal

Equalization of frequency response by DSP can also be possible in OFDM. The OFDM signal has high tolerance to chromatic dispersion (CD). This high tolerance is essential in WDM-PON since the distance between CO and ONU is a main factor which cannot be fully dispersion compensated.

Previous works show that carrier-distributed OFDM-PON suffers from interferometric beat noise generated by RB [15]. Another work investigated the performance of OFDM-QAM signal when subjected to RB where CW carrier sent from CO [16]. The effect of 10 Gb/s NRZ induced RB as well as DPSK induced RB in OFDM-QAM modulated signal is investigated for further analysis of RB effect in single fiber network. Moreover, the analysis of RB noise generated by NRZ and DPSK modulated carrier are investigated for further comparing with unmodulated CW carrier. Besides realizing RSOA, MZM is used as an external modulator in US. RSOA has some limitation in E/O modulation bandwidth and distance by the fiber dispersion can dramatically increase depending on the spectral width of the source. We also proposed a RB mitigation scheme in the carrier distributed OFDM-PON without using the dual-feeder architecture. Figure 4.8 shows the schematic of the carrier distributed OFDM-PON, where wavelength-shifting is used to mitigate RB. The carrier is generally launched towards the colorless ONU. US OFDM-QAM is generated and modulated by the CW carrier and finally sent back to transmitter at OLT. Here, the interference between US data signal and RB components produce the optical beating noise in CO which is highly coherent and overlaps the signal spectra near the DC frequency as shown in Figure 4.7.

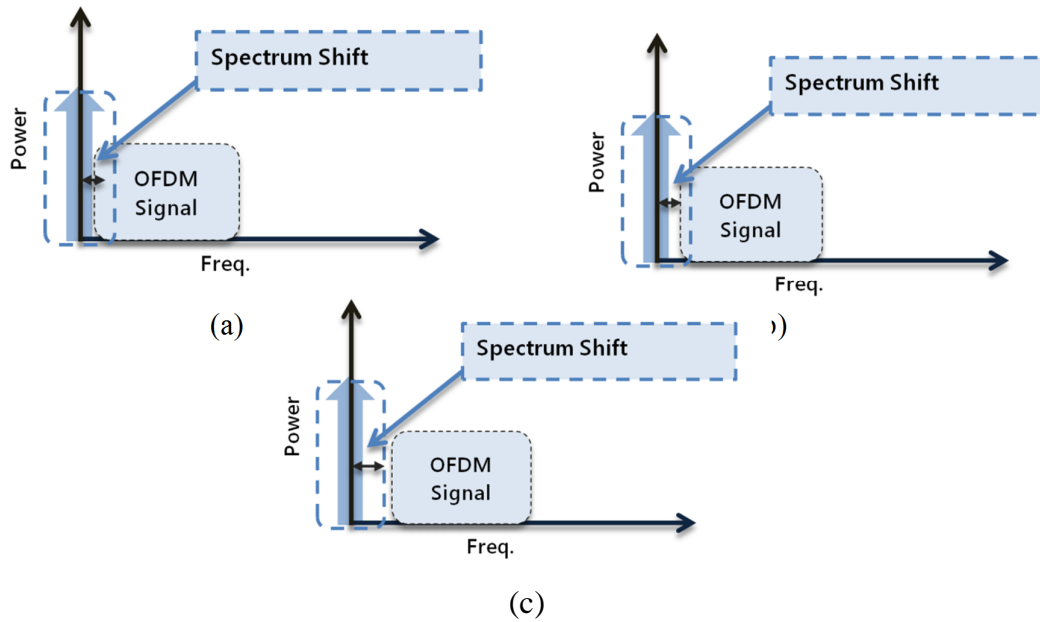


Figure 4.8: Schematic of OFDM spectra shifting to reduce interference with RB spectra (a) small shift (b) large shift (c) No interference with RB

This inband coherent noise severely degrades the system performance if the SCR goes below the acceptable label. So, it needs to separate the noise from information contents to minimize the crosstalk effect as illustrated in Figure 4.8. This wavelength shifting technique separates the concentrated DC noise from US data. Thus the system performance can be improved.

### 4.3.1 Simulation setup

Figure 4.9 shows the schematic used for the measurement of system's SCR against different bit error rate in the presence of RB noise from CW source, DPSK modulated source and finally NRZ modulated source. A real valued baseband OFDM is generated with the signal processing of serial-to-parallel conversion, QAM symbol encoding, mirroring, inverse Fast Fourier transform (IFFT), cyclic prefix insertion and finally parallel-to-serial (P2S) transmission. Each OFDM symbol consists of 32 subcarriers of which 15 subcarriers carry real data, and one (1) carrier has no power. The remaining 16 subcarriers are the complex conjugate of the aforementioned 16 subcarriers to maintain Hermitian symmetry in the input of IFFT processing block. The IFFT and FFT size is 32 and the CP length is 1/16. The total number of 1000 OFDM symbols are utilized in the simulation. The bandwidth of OFDM signal is set to 2.5 GHz, where the subcarriers are modulated with 16-QAM format and thus provides a data rate of 10 Gb/s.

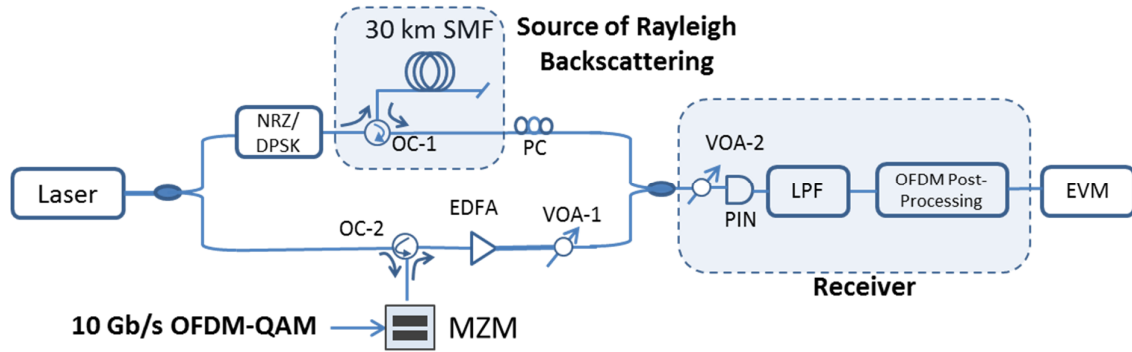


Figure 4.9: Schematic to analysis the signal to crosstalk ratio performance

There are three different noise source are investigated. The more general one is CW light (center frequency = 193.1 THz, 10 MHz line-width), the next one is 10Gbps NRZ and the final one is 10Gbps DPSK signal. The CW light from DFB laser was divided into two paths, firstly the path (top) for RB noise and secondly, the path (bottom) for modulate the US data signal. The RB noise was extracted from optical circulator (OC-1) when the source light including modulated signal, passed through 30 km of fiber span. Since the optical power at fiber input was fixed to 0 dBm, the RB noise label was found to a value of  $-33$  dBm. Changing signal to crosstalk ratio, the EVM value of OFDM was recorded [9]. By using formula (4.2), the final BER was measured. Further measurement was done by shifting the OFDM signal while maintaining gross data rate of approximately 10 Gbps. Table 4.1 shows the wavelength shifting parameters of OFDM-QAM signal.

Table 4.1: Wavelength shifting parameters for OFDM-QAM signal

SL. No	Wavelength shift	Carrier taken	Gross data rate	Actual Bandwidth	Symbol rate
1	No shift	2 ~16	9.3748 Gb/s	2.3437 GHz	5GHz
2	375 MHz	3 ~ 16	10.5 Gb/s	2.625 GHz	6 GHz
3	600 MHz	4 ~ 16	10.4 Gb/s	2.6 GHz	6.4 GHz
4	1.125 GHz	6 ~ 16	9.9036 Gb/s	2.475 GHz	7.2 GHz

The following figures are the schematics, analyzed in VPI. Figure 4.10, 4.11 and 4.12 illustrate three different sources to generate RB noise i.e. CW, DPSK and NRZ modulated signal respectively. Insets are the modulated signal with RB noise taken at SCR of 40.

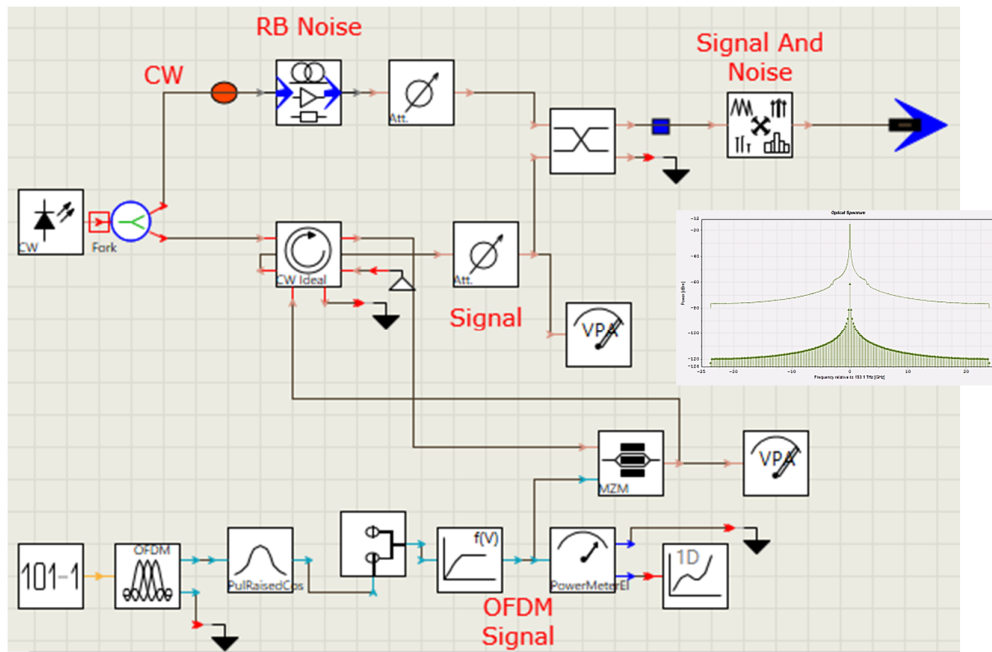


Figure 4.10: Experimental setup of SCR measurement using CW source to generate RB noise (Tx section)

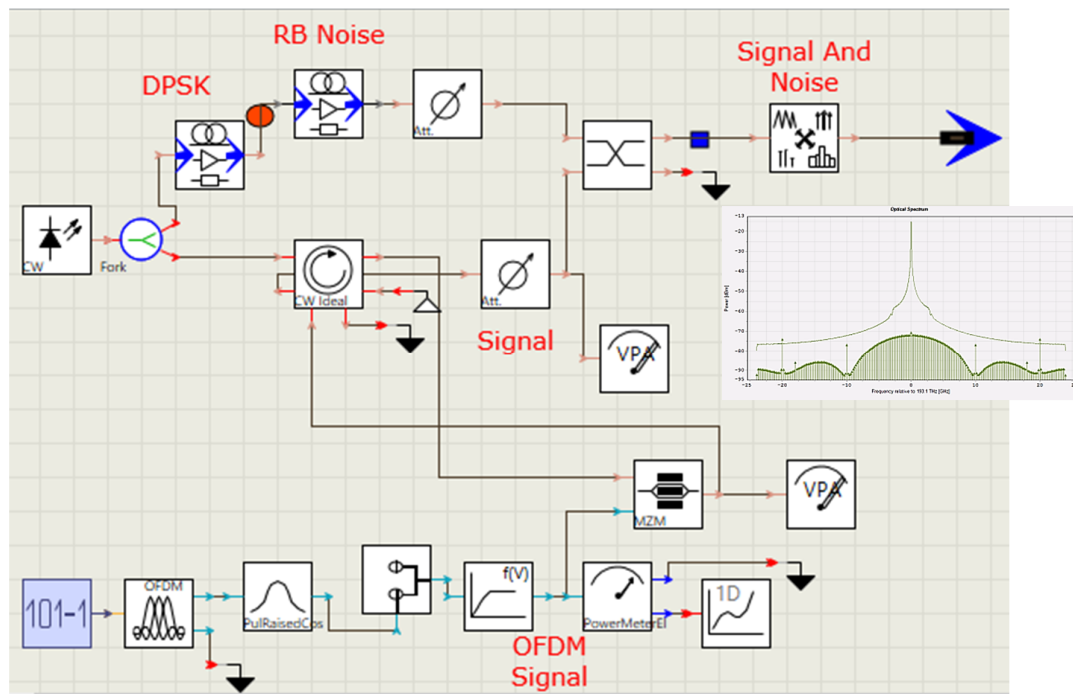


Figure 4.11: Experimental setup of SCR measurement using DPSK modulated source to generate RB noise (Tx section)

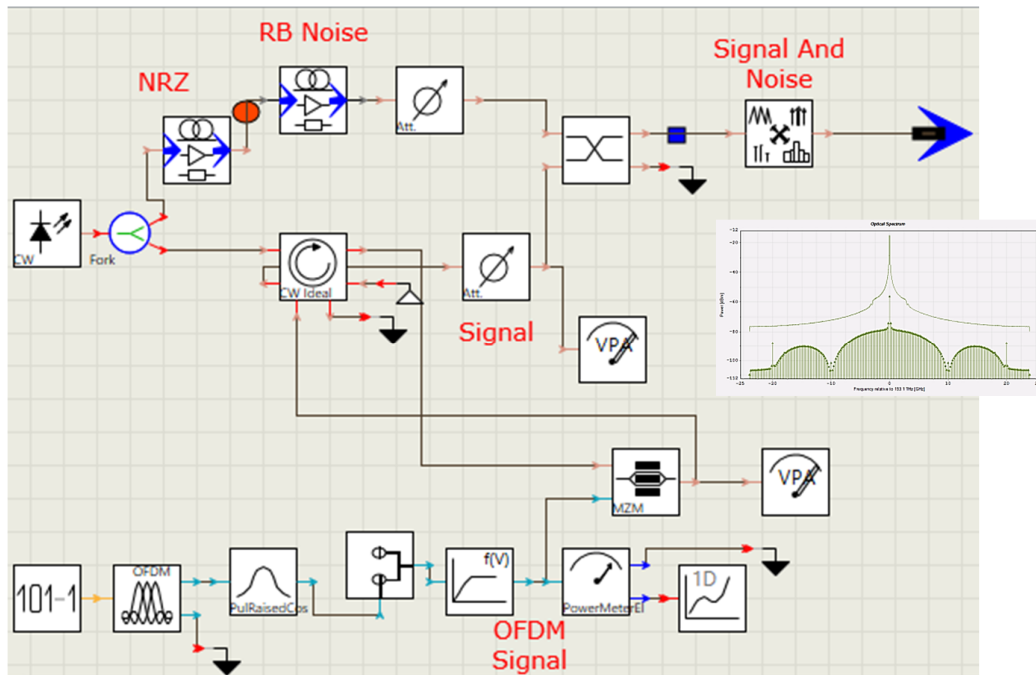


Figure 4.12: Experimental setup of SCR measurement using NRZ modulated source to generate RB noise (Tx section)

### 4.3.2 Results and analysis

Figure 4.13 shows the simulated optical spectra of the distributed CW carrier, NRZ and DPSK modulated carrier. The data rate of both NRZ and DPSK are 10Gb/s. The normalized spectrum clearly shows the spectral width of three different carriers. Where DPSK shows much wider spectrum than NRZ or CW carrier. Figure 4.14 illustrates the wavelength shifted spectrum of OFDM-QAM. The wavelength shifting parameters can be found in Table 4.1. The gross data rate of OFDM-QAM was maintaining approximately 10 Gb/s.

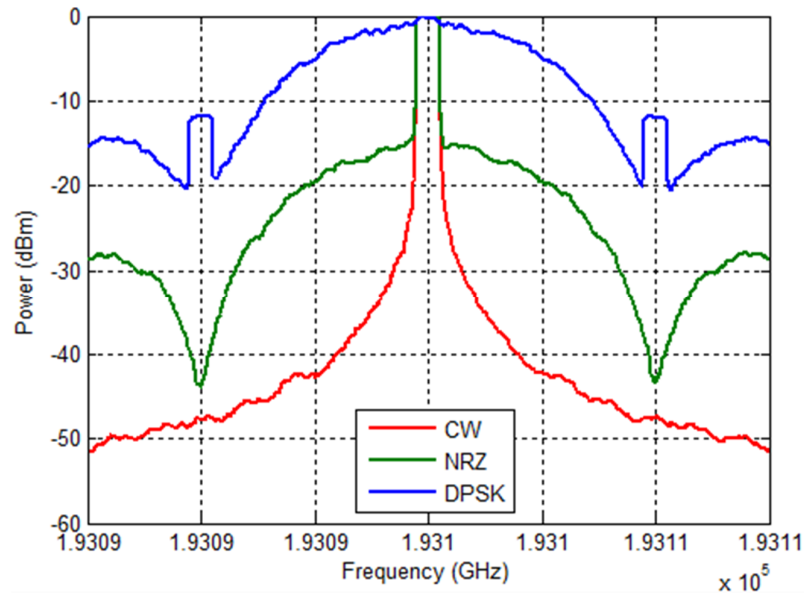


Figure 4.13: Normalized Optical spectra of CW, NRZ and DPSK modulated signal

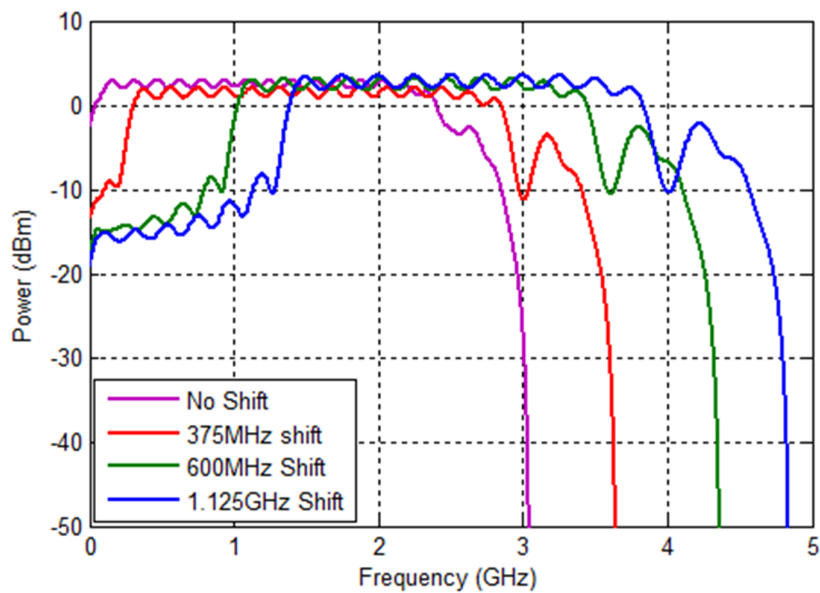


Figure 4.14: Spectrum of OFDM signal with different frequency shifting

Since the RB tolerance depends on the interferometric beat noise falling within the Rx bandwidth, the RB tolerance of the wavelength-shifted signal can be improved by reducing spectral overlap with the carrier wavelength. Inset of Figure 4.15(a) and (b) show the simulated constellation diagrams of upstream 16-QAM OFDM signal. At the same BER of  $1 \times 10^{-3}$ , there are 9-dB improvement is observed with wavelength shift of 375 MHz (see Figure 4.15), without wavelength-shifting (SCR = 46dB) and with wavelength-shifting (SCR = 37 dB) respectively. Result show that wavelength-shifting can significantly mitigate RB

generated by the CW carrier by withstanding a much higher RB noise (SCR improved by 9 dB). Similarly, RB generated by NRZ and DPSK modulated signal are also investigated. Modulated signal also shows the similar trend of SCR improvement by wavelength shifting. Figure 4.16 and 4.17 illustrate the BER performance under different SCR when RB is generated by NRZ and DPSK modulated carrier. Unlike CW, NRZ also improves a SCR of 7 dB by shifting 375 MHz. On the other hand, DPSK improves by only 1 dB. The answer could be explained by analyzing the spectrum width of the generated carrier. The CW only holds a line width of 10MHz while NRZ and DPSK has broader spectrum (see fig 4.13). At the same time, the RB spectrum is also identical with carrier spectrum. As a result, broader spectrum produces much higher interferometric beating noise. Constellation diagram, Figure 4.15 (b) is taken at SCR of 46 which shows better than the SCR of 31 (see fig 4.15 (b)).

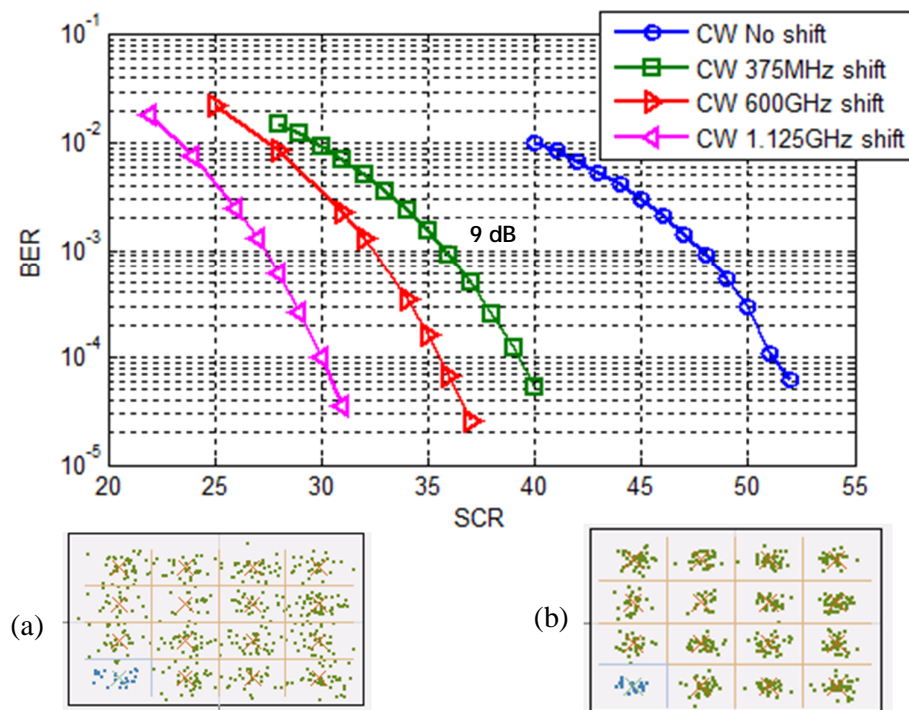


Figure 4.15: BER performance under different SCR level at different OFDM spectrum shifting while CW source generates the RB noise; constellation diagram of subcarrier 5

(a) at SCR 31 (b) at SCR 46

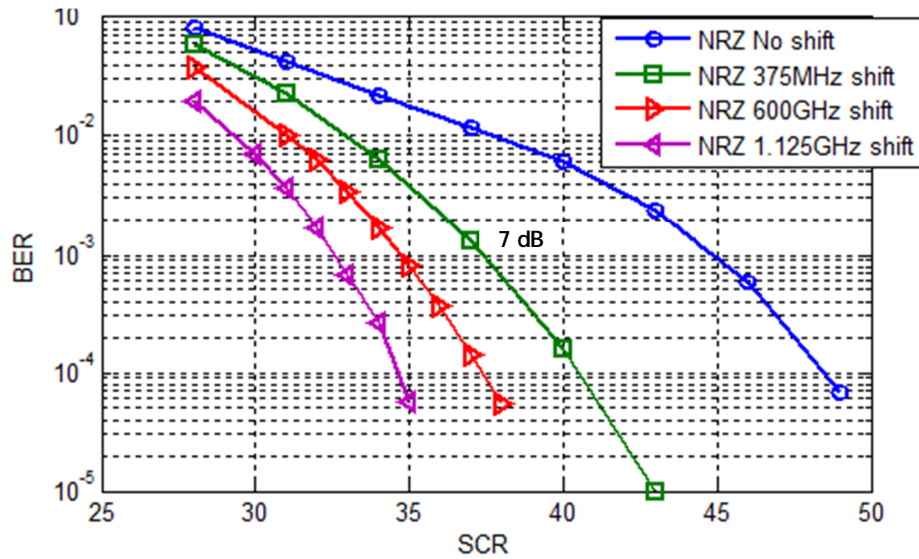


Figure 4.16: BER performance under different SCR level at different OFDM spectrum shifting when NRZ modulated signal generates the RB noise

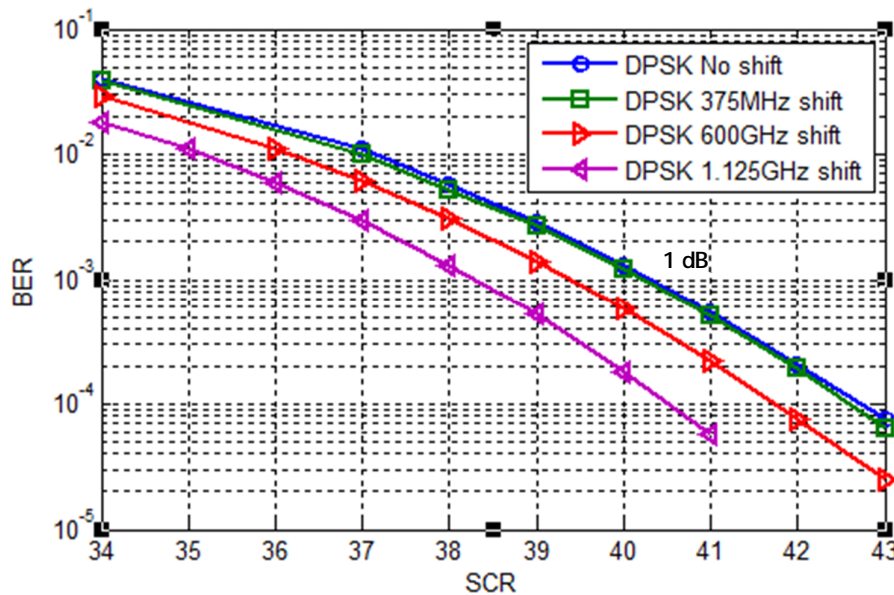


Figure 4.17: BER performance under different SCR level at different OFDM spectrum shifting while DPSK modulated signal generates the RB noise

The relative performance between three different carrier sources is presented Figure 4.18. Here we can see that, the BER curve of DPSK is higher than NRZ or CW. In addition CW performs better comparing to NRZ or DPSK. Though CW and NRZ are close together, DPSK gives less performance than CW or NRZ. CW and NRZ show almost 3 dB improvement comparing to DPSK (see fig 4.18).

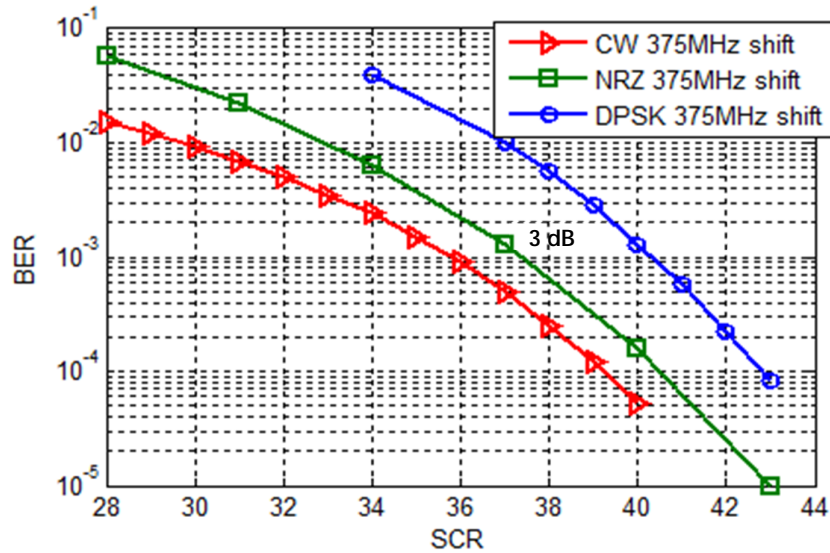


Figure 4.18: Measured BER for different sources (CW, DPSK, NRZ)

As CW generates less crosstalk noise as it has very narrow bandwidth comparing to NRZ or DPSK. Broader spectrum produces more crosstalk. DPSK shows broad spectrum comparing to NRZ signal (see fig 4.13). So, the performance of DPSK is less because broader spectrum overlaps with crosstalk region and produce more noisy signal.

#### 4.4 Single Fiber Network: Both RB and Re-modulation Noise

BSFSW transmission is the most interesting scheme mainly because of its cost-efficiency in terms of CAPEX. The use of a single fiber reduces the cost by 50% as compared to a dual fiber implementation [17]. BDFSW transmission system with detailed analysis is described in section 4.2. The remodulation noise effect was mainly studied in 4.2 sections. Finally this section will describe the single fiber setup. Single fiber system can optimize the use of optical resources and reduce the network size outside of the plant. RB represents an important limiting effect owing to signals propagating in opposite directions produce crosstalk between the signal travelling in one direction and the backscattering from the reverse directed signal. This causes both coherent and incoherent crosstalk as the signals overlap in the detection band. Note that proposed BSFSW system only considers direct-detection mechanism, that is, receivers detect only the optical power (the amplitude of the incoming signal squared). Recently several methods are studied to mitigate the RB effects by introducing additional phase modulator at ONU and optical notch filter at CO [18], wavelength offset detuning [19],

frequency dithering [20], and cross remodulation technique [21]. However, these schemes either cannot completely RB or require additional light sources for US carriers or separate fiber links for DS and US signals. This section experimentally demonstrates a simple wavelength shifting approach to mitigate RB effect on system performance. There are several ways of wavelength shifting approach have been proposed. Single Side Band modulation (SSB) with carrier suppression is a type of wavelength shifting of optical carrier presented in [22]. It requires complex setup of modulator with additional PM to produce a wavelength shifting of some GHz and generates a new wavelength. In [23], two optical interleavers are used in CO and ONU to separate odd and even part of signal. It also used an additional RF mixer to drive IM at predefined voltage which produces complexity at ONU side. This work emphasizes on simplest way of wavelength shifting to reduce spectral overlap with the carrier wavelength. The previous BDFSW experiment used RSOA for its simplicity, wavelength independency, cost effectiveness, high gain with high optical power budget and amplitude squeezing characteristics. However, the E/O modulation bandwidth of RSOA is limited to approximately 2 GHz. To reach 10 Gb/s, spectrally efficient OFDM-QAM was used in BDFSW experiment. But further wavelength shifting requires more bandwidth efficient device. MZM can be a solution to overcome this limitation.

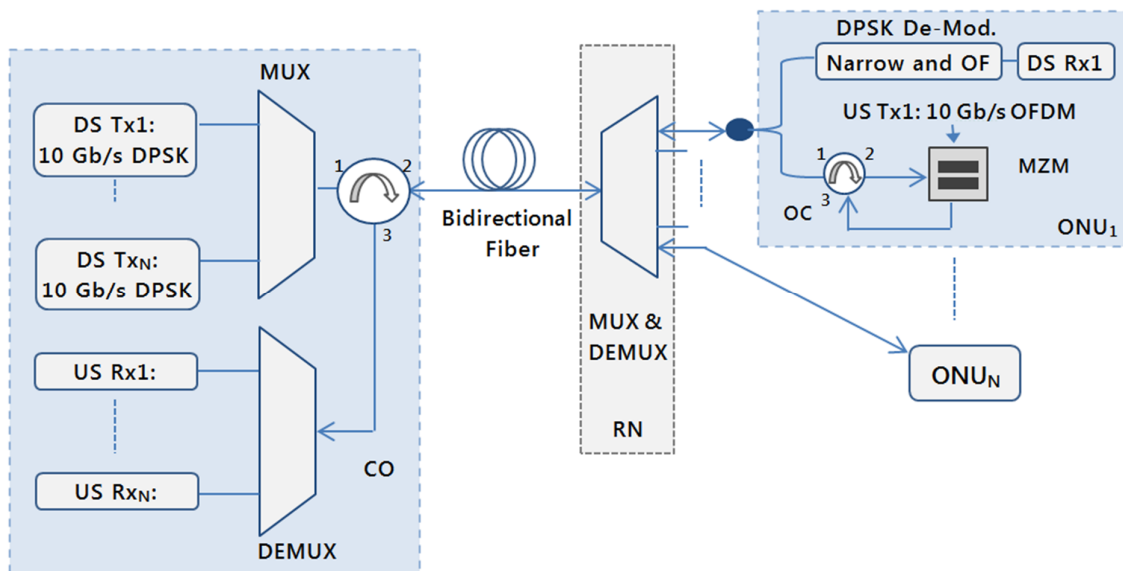


Figure 4.19: Proposed architecture for 10 Gb/s symmetric bidirectional single fiber wavelength reused WDM-PON.

Figure 4.19 shows the proposed architecture for 10 Gb/s symmetric bidirectional single fiber wavelength reused WDM-PON. This architecture is similar with previous proposed architecture except the dual fiber is replaced with single fiber and the RSOA is replaced with MZM to overcome the bandwidth limitation of RSOA. The CO consists of 10 Gb/s DPSK signal for each WDM wavelengths, which are multiplexed before transmission over the bidirectional fiber. At RN, DEMUX distributes the DS signal to ONU. The DS DPSK modulated signal is split into two portions in each ONU. One portion is used for DS receiver with narrow band optical filter as a DPSK de-modulator that converts phase information to amplitude variation and finally, reaches to conventional direct detection photodiode. . The other portion is used for generating the US modulated signal.

#### 4.4.1 Simulation Setup

Figure 4.20 shows the simulation setup to evaluate the performance of proposed bi-directional symmetrical 10 Gb/s single fiber wavelength reuse WDM-PON. The transmission system design and analysis are carried out by optical system design simulation tool VPITransmissionMaker-9.1<sup>®</sup>. At the CO, a DFB laser operating at 1550 nm is externally modulated by a phase modulator (PM) with a 10 Gb/s NRZ  $2^{31}-1$  PRBS sequence to generate the DPSK signal. The DS signal is then transmitted to the ONU over the 20 km standard SMF (chromatic dispersion  $D=16$  ps/nm/ km, 4 dB propagation loss). At the ONU, the DS DPSK signal is divided by a 50:50 optical coupler, where part of the signal is detected by a DPSK demodulator followed by direct detection optical receiver. As a DPSK demodulator, a narrow optical filter [Gaussian profile, full width half maximum (FWHM) is 60% of data rate] is used to convert phase information to intensity .Finally, the DS signal is received by a direct detection optical receiver consists of variable optical attenuator (VOA), PIN photodiode and electrical low pass Bessel filter (bandwidth is 75% of data rate).

Another part of the DPSK modulated DS optical signal is seeded to MZM for the re-modulation with 10 Gb/s OFDM signal. As the seeding power of has a significant effect on US signal to crosstalk ratio (SCR) performance, two erbium-doped fiber amplifies (EDFAs) are used to maintain the acceptable SCR label. The optical circulator (OC) is used to separate the DS seeding signal and US modulated signal of MZM.

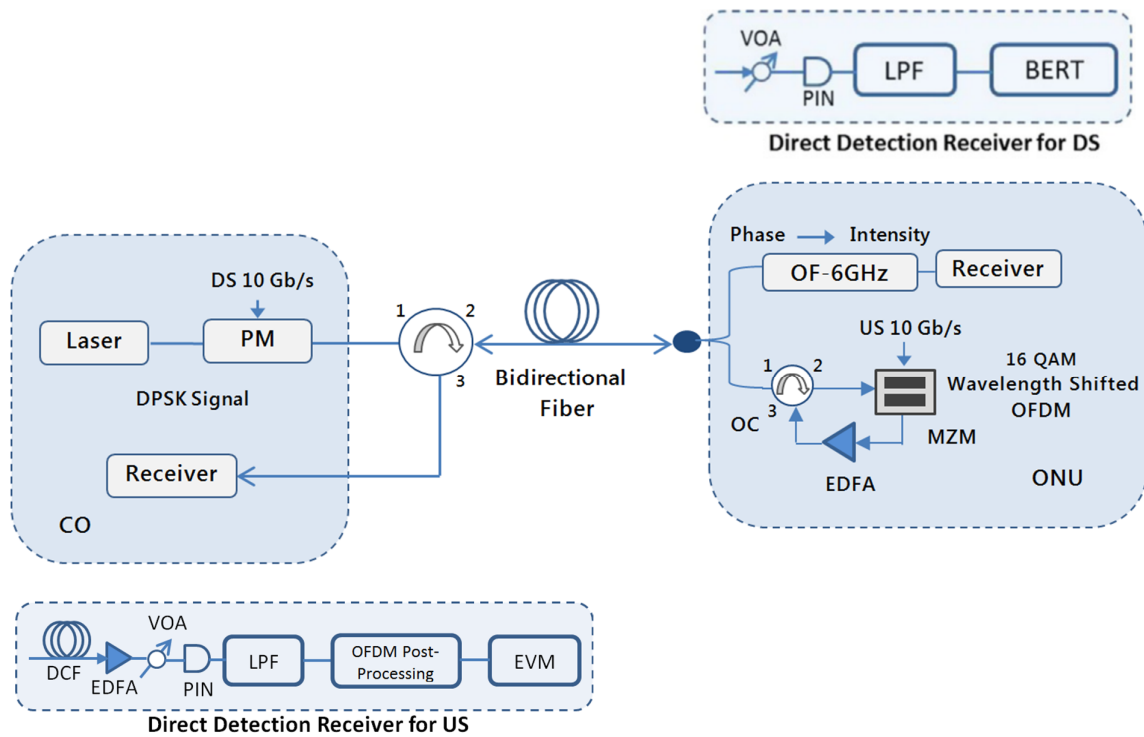


Figure 4.20: Simulation setup for single fiber 10 Gb/s DPSK in DS and MZM re-modulation with OFDM-QAM in US.

A real valued baseband OFDM is generated with the signal processing of serial-to-parallel conversion, QAM symbol encoding, mirroring, inverse Fast Fourier transform (IFFT), cyclic prefix insertion and finally parallel-to-serial (P2S) transmission. Each OFDM symbol consists of 32 subcarriers of which 15 subcarriers carry real data, and one (1) carrier has no power. The remaining 16 subcarriers are the complex conjugate of the aforementioned 16 subcarriers to maintain Hermitian symmetry in the input of IFFT processing block. The bandwidth of OFDM signal is set to 2.5 GHz, where the subcarriers are modulated with 16-QAM format and thus provides a data rate of 10 Gb/s. The modulated OFDM signal is amplified by EDFA and transmitted over the same feeder fiber. EDFA gain depends on SCR label. To reach SCR 40, a small gain of 22dB is needed. A dispersion compensation fiber (DCF) (compensating 320 ps/nm) is used to overcome the effect of chromatic dispersion in US performance. Finally, the US OFDM is received by PIN photodiode for post signal processing and EVM measurement.

The main concern of single fiber deployment is RB noise which severely degrades the upstream performance. To overcome this limitation, wavelength shifted approach is used. PSD of RB noise is identical to the source signal. Therefore, by reducing the spectral overlap

with the carrier wavelength, wavelength-shifted approach can be a mitigation technique. The effect of RB is analyzed in section 4.3 which confirms that the RB tolerance can be improved by shifting the signal wavelength because of reduced spectral overlap.

#### 4.4 Results and Analysis

The performance of DPSK modulated signal in DS is measured through bit error rate (BER) against photodiode received power as shown in Figure 4.21. Figure 4.21 represents the negligible power penalty in DPSK transmitted signal over 20 km fiber in compared to back-to-back transmission.

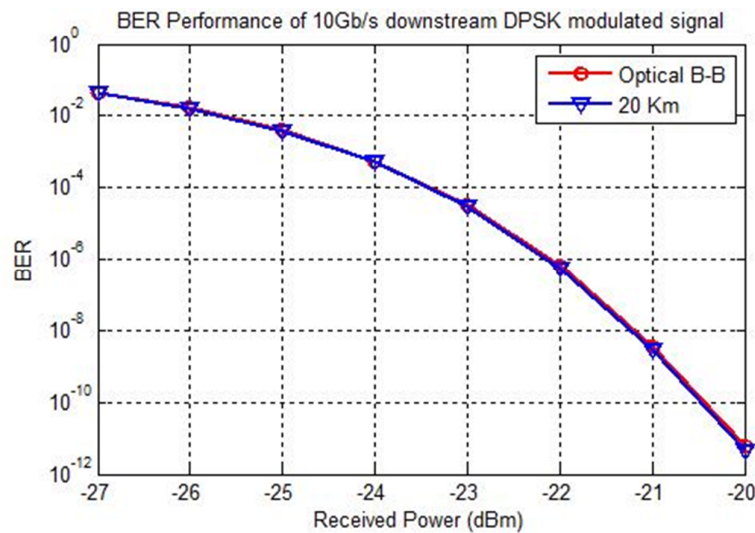


Figure 4.21 BER performance of 10 Gb/s downstream DPSK modulated signal for both B-B and over 20 km fiber transmission.

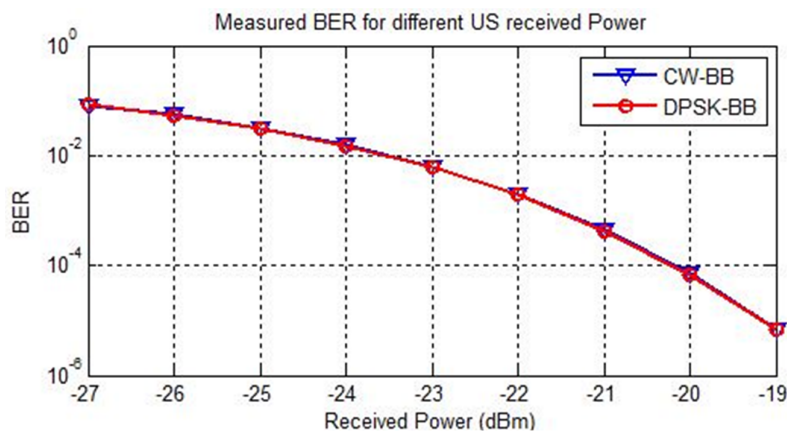


Figure 4.22 Measured BER for different US received power in the case of B-B for CW and DPSK seeded wavelength

Figure 4.22 shows the BER for different US received power in B-B for CW and DPSK seeded wavelength. Figure 4.22 shows the negligible power penalty CW and DPSK seeded wavelength with maintaining BER less than FEC threshold.

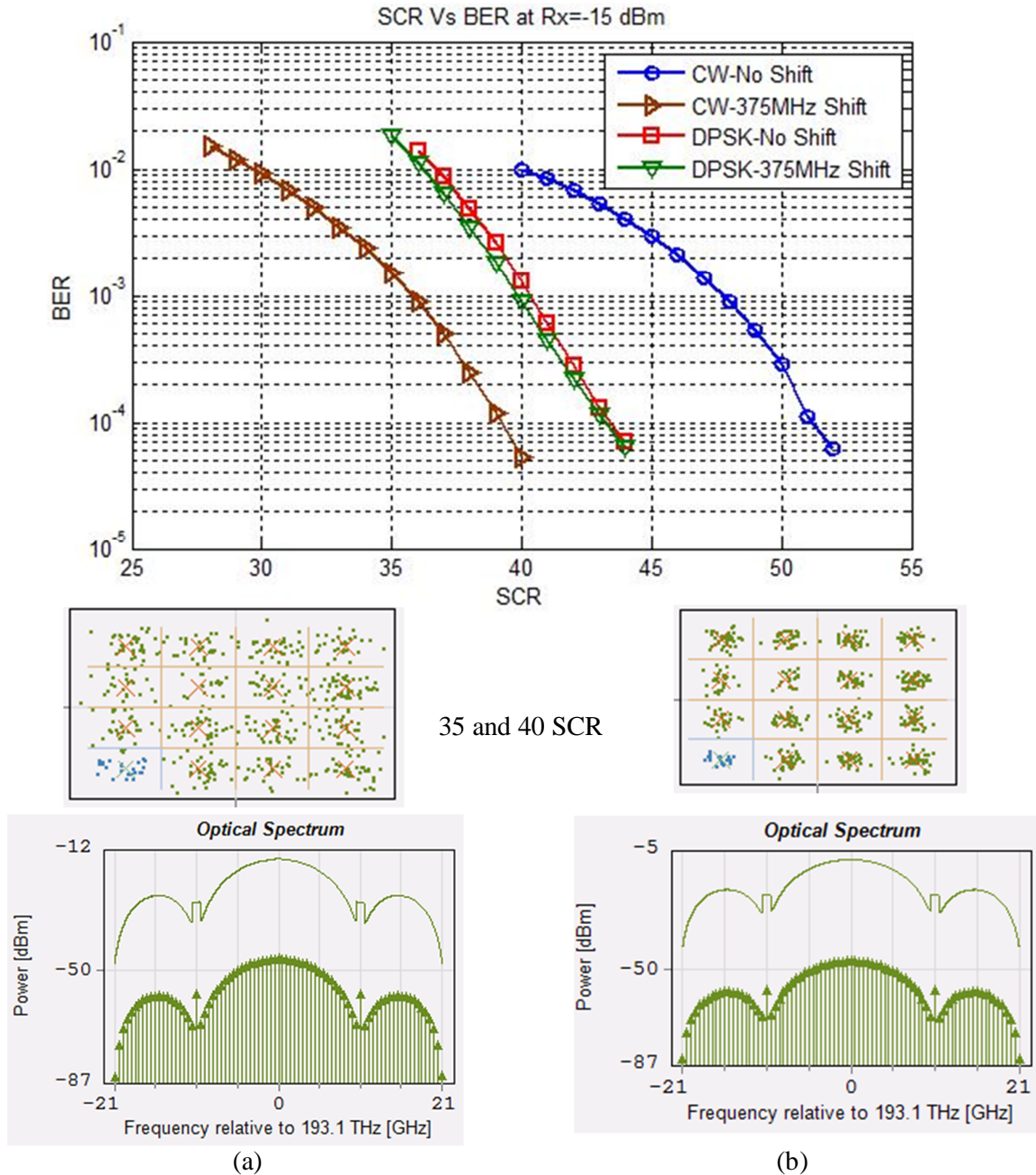


Figure 4.23 Measured BER Vs SCR for CW and DPSK seeding with shifted wavelength  
 (a) Constellation diagram at SCR 35 for DPSK seeding and corresponding signal with RB  
 (b) Constellation diagram at SCR 40 for DPSK seeding and corresponding signal with RB

Figure 4.23 shows the measured BER Vs. SCR for CW and DPSK seed with 375 MHz wavelength shift. MZM input power was fixed to  $-7$  dBm. The gain of EDFA was maintained for different SCR and BER was measured for US performance measurement.

In CW seeded wavelength, the US OFDM-QAM is only shifted to 375 MHz wavelength and a significant improvement is achieved. This improves the SCR almost 9dB that matches the previous analysis shown in Figure 4.15. On the other hand, in DPSK seeded wavelength, the improvement is not satisfying. As the spectra of RB reflection and the DPSK modulated signal are nearly the same. Moreover, higher optical spectral overlapping will produce higher electrical beat noise at the same frequency band when detected by a photo detector Insets of Figure 4.23 indicate the schematic optical spectra and constellation of received OFDM-QAM at different SCR.

## REFERENCES

- [1].N. Calabretta, M. Presi, R. Proietti, G. Contestabile, E. Ciaramella, A bidirectional WDM/TDM-PON using DPSK downstream signals and a narrowband AWG, *IEEE Photonics Technol. Lett.* 19 (16) (20 07) 1227 –1229.
- [2].C.W. Chow, Wavelength remodulation using DPSK down-and-upstream with high extinction ratio for 10-Gb/s DWDM-passive optical network s, *IEEE Photonics Technol. Lett* 20 (1) (20 08) 12 –14.
- [3].C.W. Chow, C.H. Yeh, Y.F. Wu, H.Y. Chen, Y.H. Lin, J.Y. Sung, Y. Liu, C.-L. Pan, 13-Gb/s WDM-OFDM PON using RSOA-based colorless ONU with seeding light source in the local exchange, *Electron. Lett.* 47 (22) (2011) 1235– 1236.
- [4].T. Dong, Y. Bao, Y. Ji, A . Lau, Z. Li, C. Lu, Bidirectional hybrid OFDM-WDM-PON system for 40-Gb/s downlink and 10-Gb/s uplink transmission using RSOA remodulation, *IEEE Photonics Technol. Lett.* 24 (22) (2012) 2024 – 2026.
- [5].C. Chen, C.F. Zhang, F. Yuan, K. Qiu, Bidirectional RF up-converted OFDMA-PON with novel source-free ONUs using FWM in SOA, *IEEE Photonics Technol. Lett.* 24 (24) (2012) 2206–2209.
- [6].C. Zhang, C. Chen, Y. Feng, K. Qiu, Experimental demonstration of novel source-free ONUs in bidirectional RF up-converted optical OFDM-PON utiliz-ing polarization multiplexing, *Opt. Express* 20 (6) (2012) 6230 – 6235.
- [7].C. Chen, C. Zhang, D. Liu, K. Qiu, S. Liu, Tunable optical frequency comb enabled scalable and cost-effective m ultiuser orthogonal frequency-division multiple access passive optical network with source-free optical network units, *Opt. Lett.* 37 (19) (2012)
- [8].A. D 'Errico, R. Proietti, L. Giorgi, G. Contestabile, E. Ciaramella, WDM-DPS detection by means of frequency-periodic Gaussian fi ltering, *Electron. Lett.* 42 (2) (20)
- [9].L. Mehedy, M. bakaul, A . Nirmalathas, E. Skafi das, OFDM versus single carrier towards spectrally ef fi cient 10 0 Gb/s transmission with direct detection, *J. Opt. Commun. Netw.* 4 (10) (2012) 779 – 789 .
- [10]. P.K. Choudhury, Adaptive OFDM for chirped reflective ONU based high speed passive optical network s, *Springer J. Opt.* 43 (3) (2014) 239– 24 6
- [11]. P. Choudhury, M. Presi, G. Cossu, A . Chiuchiarelli, E. Ciaramella, Chirped RSOA modulation by using adaptive OFDM for long reach WDM-PONs, *IEEE Photo-nics Switch.* (2012) 1 –3.

- [12]. P. Gysel, R.K. Staubli, Statistical properties of Rayleigh backscattering in single-mode fibers, *J. Lightwave Technol.* 8 (1990) 561–567
- [13]. C. W. Chow, C. H. Yeh, C. H. Wang, F. Y. Shih and S. Chi, “Signal remodulation of OFDM-QAM for long reach carrier distributed passive optical networks,” *IEEE Photon. Technol. Lett.*, vol. 21, pp. 715-717, 2009.
- [14]. C. W. Chow, C. H. Yeh, Y. T. Li, C. H. Wang, F. Y. Shih, Y. M. Lin, C. L. Pan and S. Chi, “Demonstration of High Spectral Efficient Long Reach Passive Optical Networks using OFDM-QAM,” *Proc. CLEO’08*, San Jose, USA, CPDB7.
- [15]. T. Duong, N. Genay, A. Pizzinat, B. Charbonnier, P. Chanclou, C. Kazmierski, “Low cost multi band-OFDM for remote modulation of colourless ONU in hybrid WDM/TDM-PON architecture,” *Proc. Of ECOC*, 2007, Berlin, Germany, Paper 5.4.2
- [16]. C. W. Chow, C. H. Yeh, C. H. Wang, F. Y. Shih, and S. Chi “Rayleigh Backscattering Performance of OFDM-QAM in Carrier Distributed Passive Optical Networks,” *IEEE Photon. Technol. Lett.*, vol. 20, pp. 1848-1850, 2008.
- [17]. K. Iwatsuki, J. Kani, H. Suyuki, M. Fujiwara, “Access and Metro Networks Based on WDM technologies”, *IEEE J. Lightwave Technol.*, vol.22, no.11, pp.2623-2630, Nov
- [18]. T.Yoshida, S. Kimura, H. Kimura, K. Kumozaki, and T. Imai, “A new single-fiber 10-Gb/s optical loopback method using phase modulation for WDM optical access network,” *J. Lightw. Technol.*, vol. 24, no. 2, pp. 786–796, 2006.
- [19]. C. W. Chow, G. Talli, and P. D. Townsend, “Rayleigh noise reduction in 10-Gb/s DWDM-PONs by wavelength detuning and phase-modulation-induced spectral broadening,” *IEEE Photon. Technol. Lett.*, vol. 19, no. 6, pp. 423–425, Mar. 15, 2007.
- [20]. J. A. Lazaro, C. Arellano, V. Polo, and J. Prat, “Rayleigh scattering reduction by means of optical frequency dithering in passive optical networks with remotely seeded ONUs,” *IEEE Photon. Technol. Lett.*, vol. 19, no. 2, pp. 64–66, Jan. 15, 2007.
- [21]. H.H. Lin, C.Y. Lee, S.C. Lin, S.L. Lee, and G. Keuser, “WDM-PON systems using cross-remodulation to double network capacity with reduced Rayleigh scattering effects,” presented at the OFC 2008
- [22]. J. Prat, M. Omella, V. Polo, “Wavelength shifting for colorless ONUs in single-fiber WDM-PONs”, *Proc. OFC/NFOFC’07*, OTuG6, Anaheim (CA), March 2007
- [23]. A. Chowdhury, Hung-Chang Chien, Ming-Fang Huang, Jianjun Yu, Gee-Kung Chang “Rayleigh backscattering noise-eliminated 115-km long-reach bidirectional centralized WDM-PON with 10-Gb/s DPSK downstream and remodulated 2.5-Gb/s OCS-SCM upstream signal,” *IEEE Photon. Technol. Lett.*, vol. 20, no. 24, pp. 2081-2083, 2008.

## CHAPTER V

### Conclusion and Future Work

#### 5.1 Conclusions

WDM-PONs encompasses promising approaches to realize fiber optic access networks with wavelength-agnostic ONUs, so called colorless ONUs. However, further R&D has to be conducted with respect to network architectures, key components and cost reduction.

Up to now, several CWDM and DWDM-PON architectures have been reported based on colorless ONUs with uniform designs using RSOAs.

This thesis work studied the two major problems occur in bidirectional wavelength reuse system i.e. remodulation noise and Rayleigh backscattering (RB). It is found that these problems cannot be totally removed but some techniques and novel system design can mitigate the problem. We analyzed two different modulation formats in DS and US so that the residue of DS signal can be minimized in US seeding. This can improve the system performance.

A symmetric 10Gb/s bidirectional wavelength reused WDM- PON is proposed with RSOA remodulation in colorless ONU. The remodulation noise in US receiver is effectively minimized by employing the constant envelope DPSK modulated signal in DS transmission. A narrowband filter is utilized for phase to intensity conversion that makes the DS receiver with a simple photodiode. Moreover, spectrally efficient OFDM modulation with 16-QAM data is used for RSOA remodulation to overcome the limited bandwidth response of this device. The results show that the BER performance of DS DPSK signal over 25km feeder fiber is very close to back to back transmission. On the contrary, there- modulated uplink SNR performance of OFDM transmission over the fiber is significantly affected by chromatic dispersion in the presence of residual phase modulation of seeding signal. By applying the dispersion compensation technique in US receiver, the subcarrier SNRs are effectively improved to achieve the BER below the FEC threshold.

Further investigation is carried out to analyze the impact of RB noise on system performance. It is found that the interference between upstream data signal and RB components produce the optical beating noise in CO which is highly coherent near the DC frequency. This in-band

coherent noise severely degrades the system performance. To overcome this limitation, effective frequency shifting is considered as a mitigation technique because RB tolerance of the wavelength-shifted signal improves due to the reduced spectral overlap with the carrier wavelength. By shifting the signal frequency, system performance is measured. Finally, a significant improvement is observed for all the cases.

## 5.2 Future Work

As future lines, the work carried out in this thesis work can be continued by applying more robust design based on RSOA, R-EAM/MZM WDM PON where Rayleigh backscattering effect will be major concern. Several studies have found that RB cannot be totally minimized as it generates by the imperfection of fiber. As a result, researchers are investigating more and more techniques to mitigate the crosstalk effect. There are several research work can be considered as a future work.

- New OFDM Access Network Topology (OTONES).
- More robust Reflective ONU based centralized CW seeding system design.
- The effect of RB on advanced modulation format.

## Appendix

### Research Publication

#### **Journal:**

Pallab K. Choudhury, Tanvir Zaman Khan, "Symmetric 10 Gb/s wavelength reused bidirectional RSOA based WDM-PON with DPSK modulated downstream and OFDM modulated upstream signals", Optics Communications, by ELSEVIER, Volume: 372, pp.180-184, 08/2016